Coherent and correlated transport in mesoscopic structures

Cand.scient thesis

Jonas Nyvold Pedersen

rsted Laboratory
Niels Bohr Institute fAPG
University of Copenhagen

Supervisor: Karsten Flensberg

Copenhagen, June 21st 2004

Preface:

When this project started in the spring of 2003, the plan was to study the influence of phonons on the current in tunnelling devices consisting of e.g. a double quantum dot. Calculations which took the filled Fermi seas in the leads into account had already been published for a single quantum dot, but including an extra dot turned out to be surprisingly complicated.
Instead I ended up writing a project about coherent and correlated transport in a nanomagnetic device.

I appreciate very much the help and many hours of support I have received from my supervisor when writing this thesis. Always helpful even when it came to the small details. Thanks a lot, Karsten.
I am also very thankful for the help I got from Antti-Pekka Jauho (MIC, DTU) in the beginning of the project. First and foremost the introduction to nonequilibrium Green's function theory which forms a large part of the theoretical background for this thesis.

Thanks to Mai, family and friends (in the physics world and outside) for kind support throughout the project period.

Jonas Nyvold Pedersen
pedjo@fys.ku.dk/jonasnyvold@hotmail.com

Contents

1 Introduction **1**

2 The FAB model **3**
2.1 Introducing the FAB model 4
2.2 Motivation for studying the FAB model 7
2.3 Diagonalizing the Hamiltonian 8

3 The nonequilibrium Green's function formalism **11**
3.1 Pictures in quantum mechanics 11
3.2 Equilibrium Green's functions 14
3.3 Nonequilibrium Green's functions 16
3.4 Analytic continuation in Keldysh space 19
3.5 Derivation of the current formula 22

4 The FAB model without interactions (parallel) **27**
4.1 Calculation of the current in linear response 30

5 The FAB model without interactions (antiparallel) **35**
5.1 Current formula 35
5.2 Calculation of the current in linear response 37

6 Unified description of tunnelling through QDs **41**
6.1 Derivation of the retarded Green's function 42
6.2 Equation of motion for $G^R_{\alpha\beta,\alpha'\beta'}$ 43
6.2.1 Equation of motion for D^R and E^R 44
6.3 Unified expression for $G^R_{\alpha\beta,\alpha'\beta'}$ 47
6.4 Discussion of the unified description 48

7 Green's function approach to the FAB model **49**
7.1 The FAB model in the unified description 49
7.2 Numerical solution of the FAB model 53
7.2.1 Expressions for K and Λ 53
7.2.2 Condition for $\mathbf{M}^R$ 54
7.2.3 Calculation of the occupations 56

7.3 Calculation of the current . . . 58
7.4 Results . . . 60
7.4.1 No Coulomb repulsion on the dot . . . 60
7.4.2 Interacting electrons on the dot . . . 62
7.5 Discussion of the results . . . 63

8 Rate equation approach to a single level with spin 67
8.1 Density matrix and rate equations . . . 68
8.2 The idea behind the derivation of the rate equations . . . 69
8.3 Derivation of the rate equations . . . 74
8.4 Range of validity for the rate equations . . . 78

9 Scattering formalism 81
9.1 The transition operator $\hat{T}$ . . . 81
9.2 Applied to the FAB model (parallel geometry) . . . 82
9.2.1 Comparison with Green's function approach . . . 88
9.3 Applied to the FAB model (antiparallel geometry) . . . 90
9.4 Final remarks . . . 91

10 Summary and outlook 93

Appendices 96

A Details 97
A.1 Nonequilibrium Green's functions . . . 97
A.1.1 Heisenberg operators as time-ordered exponentials . . . 97
A.1.2 Composition of operators . . . 100
A.1.3 Partial integration for current Green's functions . . . 101
A.1.4 Convolution theorem for Fourier transforms . . . 101
A.1.5 Current formula . . . 102
A.2 The FAB model for U=0 (parallel geometry) . . . 103
A.3 Unified description (derivation of EOM for E^R) . . . 104
A.4 Solving the FAB model with interactions . . . 105
A.4.1 Fermi function integral . . . 105
A.4.2 Residues . . . 106
A.4.3 Explicit form of $[\mathbf{M}_0^R]^{-1}$ . . . 107
A.4.4 Occupancies . . . 107
A.4.5 Interacting electrons, more results . . . 108
A.5 Current Green's functions for the rate equations . . . 109

B List of abbreviations and symbols 111

Chapter 1

Introduction

In the last few years an enormous attention has been drawn to a new emerging research field, which has been named after the characteristic length scale: nanoscience. It deals with fabrication and characterization of devices of the size of an atom, and the field involves chemistry, biology, physics and the applied sciences. Electronic devices made of single molecules have been produced and new revolutionary devices have been suggested, but so far much is still on the level of fundamental research. Moreover, many of the effects on the nanometer scale are still not well understood.

On the sub-micron scale a wealth of interesting phenomena exist. Many of them appear in 2-dimensional electron gasses which arise on the interface between layers in semiconductor structures, e.g. in GaAs-AlGaAs devices.
An example is the Aharanov-Bohm effect where a ring-shaped geometry lets the electrons pass by on both sides of an enclosed magnetic flux. The electronic wave function get a phase shift due to the magnetic flux, which depend on the size of the magnetic field and even more important, it is different for the two paths. Therefore the interference between wave functions from the two paths depend on the magnetic field, and oscillations in the conductance occur when it is varied.
Another effect is seen in wave guide geometries in 2-dimensional electron gasses, where the conductance is quantized in units of e^2/h due to the finite size in one direction.[i]
Both effects belong to the field known as mesoscopic physics, where the size of the structures are comparable with the coherence length of the electrons. Mesoscopic physics is the border between the classical physics and the true quantum world, and the analytic tools are often taken from both classical and quantum mechanics.

The phenomena mentioned above can be described within a single-electron picture, i.e. the electrons are considered as independent particles with no mutual interactions. For structures on the nanometer scale this description is sometimes valid, e.g. for a chain of a few gold atoms where the quantized conductance can be explained without treating the electrons as interacting. But in some systems the picture becomes insufficient when the

[i] See e.g. [1].

electrons are confined on the nanometer scale due to the small distances between electrons. New effects occur because of the interactions and they are named many-body effects.
An example is seen in quantum dot structures. When the gate voltage is shifted, so-called Coulomb blockade oscillations appear in the conductance due to the filling of the quantum dot. To complicate the picture even more there are systems were both coherence and interactions have to be taken into account, for instance in a molecular electronic device consisting of a single molecule, e.g. a benzene ring, contacted to metallic leads.
Another feature of nanodevices are the pronounced quantization of the energy levels, which give rise to a step-like current as a function of bias voltage, e.g. in resonant tunnelling devices.

The transport properties can also be strongly influenced by the spin of the electrons. The study of spin-dependent transport forms a research field called spintronics, which has both academic and technologic interest. A well described effect is seen in multilayer structures of ferromagnetic metals, where a Giant Magnetoresistance (GMR) occurs due to the different magnetizations of the layers.
So a natural question is: What happen when the Coulomb interaction and the spin-dependent transport mechanisms are joined in a nanodevice? This question has gained a great interest since it has been made possible to make such (nontrivial) structures, e.g. a carbon nanotube contacted to ferromagnetic leads. Examples of possible effects are spin pile-up on the dot and Kondo effect, which complicate the predictions of the transport properties.[ii]

In this thesis we investigate the electron transport through a small nanomagnetic system. It includes an interesting interplay between energy quantization, magnetism, coherence and interactions. Moreover, we present a way to experimentally determine whether the interactions can be negleted or not.
Three different analytical tools are applied to give an understanding of the basic mechanisms behind the quantum transport and illustrate the difficulties.

The thesis is organized as follows: In Chap. 2 the model we wish to study is introduced. Chap. 3 gives an introduction to the nonequilibrium Green's function formalism, which forms a large part of the theoretical background for this thesis and is one of the applied tools. In the following two chapters, it is applied to the model in two different cases where the electrons are considered as noninteracting. Still within the Green's function formalism, we present an approximation scheme which makes it possible to deal with interacting electrons (Chap. 6), and in Chap. 7 the approximation scheme is applied to our model. Then we present another way of dealing with quantum transport and introduce a method to derive a set of quantum rate equations for the model, see Chap. 8.
Finally, the model is solved using a scattering formalism (Chap. 9), and in Chap. 10 the summary and the conclusion are found.[iii]

[ii] For an introduction to spin-dependent transport in nanostructures, see [22].
[iii] In App. B a list of symbols and abbreviations are found.

Chapter 2

The FAB model

Tunnelling junctions are very well studied nanodevices. These structures consist for instance of a semiconductor quantum dot, a carbon nanotube or a single molecule contacted to metallic leads. As mentioned in the introduction, the transport properties get even more delicate in case of ferromagnetic leads, e.g. in a carbon nanotube suspended between two ferromagnetic contacts [2].
Another example of a spin dependent junction is presented in [3], where they fabricate a tunnelling junction consisting of two ferromagnetic leads (Ni) and a barrier made of a self-assembled-monolayer of the organic molecule octanethiol. The magnetizations of the leads can be changed with an applied magnetic field, and the resistance of the junction is measured when the magnetic field is swept from -0.6 T to 0.6 T at constant bias voltage, see Fig. 2.1(a). A sketch of the qualitative behaviour is shown in Fig. 2.1(b) and is explained as follows:
For the full curve, where B is swept from negative to positive values, three phases are encountered. For large negative values of B the magnetizations of both leads are parallel to the field, and the magnetizations are kept when the applied field drop to zero. This phase is P_1 on Fig. 2.1(b). When B is increased above zero, small domains in the leads will start to align along the field. If the domains closest to the molecule on each side of the junction are antiparallel we have an effective antiparallel configuration of the leads, resulting in a higher resistance due to spin blockade. This corresponds to the phase AP on Fig. 2.1(b). For even larger values of B the domains in both leads are aligned along the field, and we end up in the parallel configuration P_2. When B is swept in the opposite direction the same phases are seen, shown as the dashed curve in Fig. 2.1(b).
In the experiment they find a change in resistance up to 16% between the parallel and antiparallel configuration, so some knowledge about the configuration of the leads can be achieved by measuring the resistance.[i]

The idea we present here is to study a single molecule (or a quantum dot) contacted to two ferromagnetic leads.[ii] If the latter are very thin films the magnetizations will tend to align in the plane of the leads, and with an applied in-plane magnetic field the configura-

[i] A schematic drawing of the different configurations is shown in Fig. 2.2(a).
[ii] See also [20], [21] and [22] and references therein.

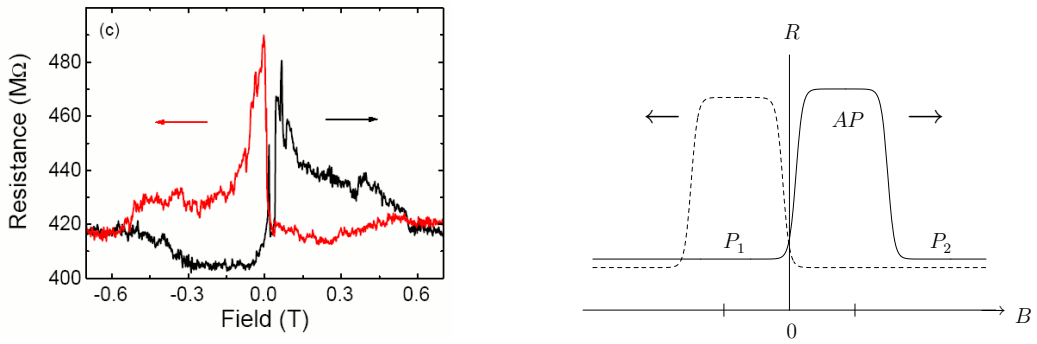

(a) (b)

Figure 2.1: Fig. 2.1(a) shows the resistance versus magnetic field B for the tunnelling junction described in the text. The bias voltage is 5 mV and the temperature 4.2 K [3]. The black curve is for increasing magnetic field and the other is for decreasing field. Fig. 2.1(b) is a schematic drawing of the curves from Fig. 2.1(a) where the full curve is for increasing magnetic field.

tion of the leads can be controlled.
Now a second magnetic field is applied out of the plane spanned by the leads, see Fig. 2.2(b). Due to the strongly anisotropic magnetic susceptibility of the magnetic thin film this field will not significantly change the magnetizations of the leads, but it will give rise to a Zeeman splitting of the dot energy levels. How the conductance depends on the angle θ between the magnetizations of the leads and the magnetic field is the subject for the rest of this thesis.

2.1 Introducing the FAB model

To formalize the idea described above, we consider a quantum dot with an applied magnetic field contacted to two ferromagnetic leads, as shown schematically in Fig. 2.3(a).
The leads are assumed to be polarized, which means that the density of states for spin-$\uparrow'$ electrons[iii] $\rho_{\uparrow'}(\varepsilon)$ is different from the density of states for the spin-$\downarrow'$ electrons $\rho_{\downarrow'}(\varepsilon)$. If there is only one kind of spin present the leads will be called fully polarized. In the rest of this thesis, except Chap. 5 and Sec. 9.3, it will be assumed that the magnetizations of the leads are parallel. This configuration is called the parallel geometry.
In equilibrium the chemical potentials of the leads are identical and equal to μ, which is set as the zero point of the energy scale. In case of an applied bias eV, it is assumed to be symmetric around $\mu = 0$, so the chemical potentials of the left and right lead are $\mu_L = \frac{eV}{2}$ and $\mu_R = -\frac{eV}{2}$, respectively.

[iii] The prime on the spin is because we later on will introduce another spin basis.

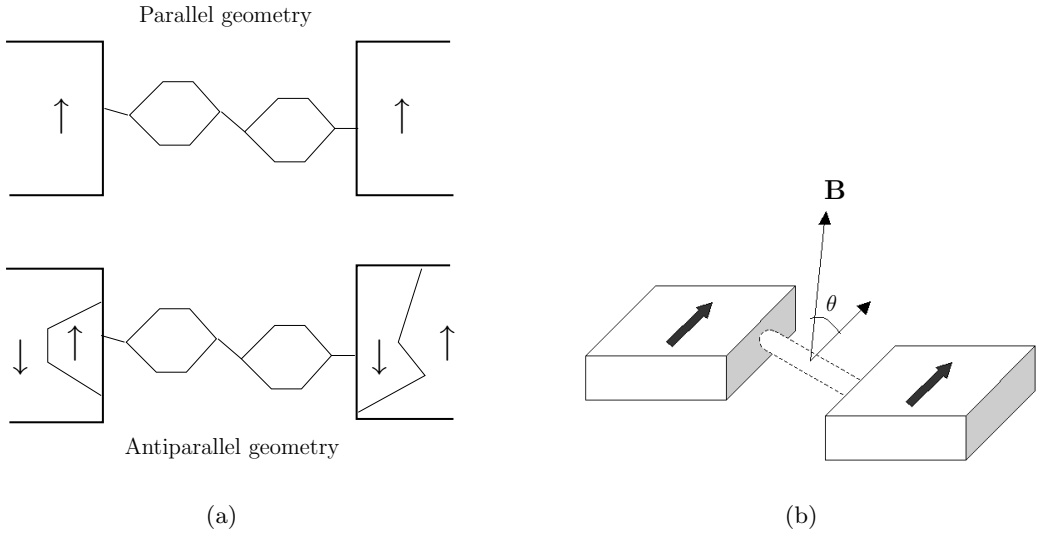

(a) (b)

Figure 2.2: Fig. 2.2(a) shows two ferromagnetic films with a molecule between them. On the upper figure the magnetizations of the films are identical, but in the lower figure different domains occur. The domains closest to the molecule have opposite magnetizations, so we have an effective antiparallel geometry. Fig. 2.2(b) shows a drawing of a molecule, e.g. a carbon nanotube, between two thin films with in-plane magnetizations. A magnetic field is applied out of the plane of the films.

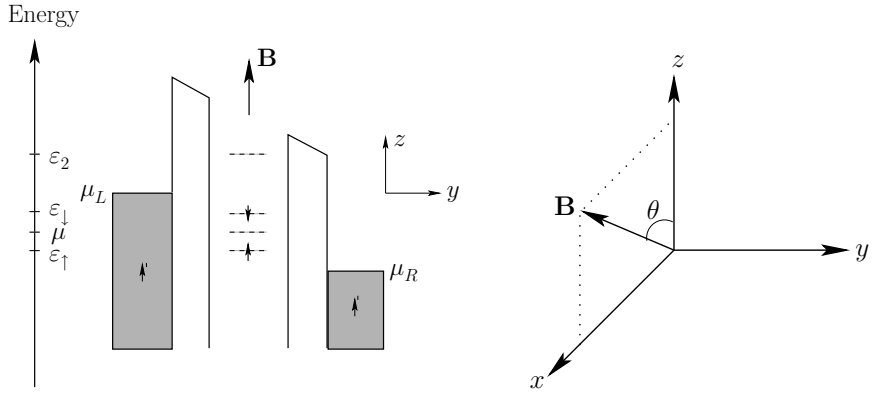

(a) (b)

Figure 2.3: In 2.3(a) is shown a schematic drawing of a system with two ferromagnetic leads coupled to a quantum dot with an applied magnetic field. Notice the different spin bases for the leads and the dot. In 2.3(b) the definition of the angle θ is shown.

In absence of the applied magnetic field the quantum dot is assumed to have only a single spin-degenerate level with energy ε_d, which can be changed by a nearby gate. That the quantum dot contains only a single level is an approximation which is reasonable when only a single electronic state takes part in the electron transport, meaning that the other energy levels are far above or far below the chemical potentials of the contacts.
Due to the small size of the quantum dot, the dot electrons will interact through a Coulomb potential which increases the energy of the double occupied state, so $\varepsilon_2 = 2\varepsilon_d + U$.
The splitting of the energy levels are important for the effects we are interested in, so we consider the regime where the splitting of the energy levels, Δ, is much larger than the temperature and the applied bias. In the opposite limit ($\Delta \ll k_b T, eV$) the effects we discuss in this thesis are not important.

The applied magnetic field is assumed to interact only with the spin of the dot electrons, leaving the leads unaffected as explained above. Choosing a coordinate system were the magnetization of the leads is along the z-axis we let the magnetic field lie in the xz-plane, as shown in Fig. 2.3(b). If θ is the polar angle the magnetic field can now be written as $\overline{B} = B\,(\sin\theta, 0, \cos\theta)$.

To model system we apply the famous Anderson Hamiltonian with an extra term due to the magnetic field. The Anderson Hamiltonian was first introduced to describe a magnetic impurities embedded in a sea of conducting electrons. Now it is also widely used to study transport through quantum dots.
Our Hamiltonian reads

$$\begin{aligned} H = &\sum_{k\eta\sigma} \varepsilon_{k\eta\sigma} c^\dagger_{k\eta\sigma} c_{k\eta\sigma} + \sum_{k\eta\sigma} \left(t_{k\eta\sigma} c^\dagger_{k\eta\sigma} c_{d\sigma} + h.c. \right) \\ &+ \sum_{\sigma} \varepsilon_d c^\dagger_{d\sigma} c_{d\sigma} + U n_{\uparrow'} n_{\downarrow'} - \frac{e}{m} \bar{S} \cdot \bar{B}. \end{aligned} \tag{2.1}$$

where the first four terms are the original Anderson Hamiltonian in case of spin-independent leads.
We will name our model the "**F**erromagnetic **A**nderson model with an applied magnetic field **B**"[iv], and we will use the abbreviation the FAB model.

The first term in Eq. (2.1) is the Hamiltonian for the leads ($\eta = L, R$) and the second describes tunnelling between the dot and leads, H_T. It should be emphasized that the tunnelling does not change the spin of the electrons, meaning that no spin-flip occurs in the tunnelling process. The next two terms are the for the isolated dot, where the latter stems from the on-site Coulomb repulsion. The last term is due to the interaction between the magnetic moment of the electrons and the magnetic field. $\bar{S}$ is the spin (angular momentum) operator which in first quantization is given as[1] $\bar{S} = \frac{\hbar}{2}\bar{\tau}$ where $\bar{\tau}$

[iv] Ferromagnetic stems from the ferromagnetic leads.

is the vector containing the Pauli spin matrices

$$\bar{\tau} = \left\{ \begin{pmatrix} 0 & 1 \\ 1 & 0 \end{pmatrix}, \begin{pmatrix} 0 & -i \\ i & 0 \end{pmatrix}, \begin{pmatrix} 1 & 0 \\ 0 & -1 \end{pmatrix} \right\}. \tag{2.2}$$

In second quantization $\bar{S}$ becomes

$$S_x = \frac{\hbar}{2}\left(c^\dagger_{d\downarrow'}c_{d\uparrow'} + c^\dagger_{d\uparrow'}c_{d\downarrow'}\right), \quad S_y = \frac{i\hbar}{2}\left(c^\dagger_{d\downarrow'}c_{d\uparrow'} - c^\dagger_{d\uparrow'}c_{d\downarrow'}\right), \quad S_z = \frac{\hbar}{2}\left(c^\dagger_{d\uparrow'}c_{d\uparrow'} - c^\dagger_{d\downarrow'}c_{d\downarrow'}\right). \tag{2.3}$$

With our choice of coordinate system the Hamiltonian is[v]

$$\begin{aligned} H = &\sum_{k\eta\sigma} \varepsilon_{k\eta\sigma} c^\dagger_{k\eta\sigma} c_{k\eta\sigma} + \sum_{k\eta\sigma}\left(t_{k\eta\sigma} c^\dagger_{k\eta\sigma} c_{d\sigma} + h.c.\right) \\ &+ \sum_{\sigma}\left(\varepsilon_d - \sigma B\cos\theta\right) c^\dagger_{d\sigma} c_{d\sigma} + U n_{\uparrow'} n_{\downarrow'} - B\sin\theta\left(c^\dagger_{d\uparrow'}c_{d\downarrow'} + c^\dagger_{d\downarrow'}c_{d\uparrow'}\right) \end{aligned} \tag{2.4}$$

with $\sigma = 1(-1)$ for spin-$\uparrow'(\downarrow')$.

2.2 Motivation for studying the FAB model

One source of inspiration for studying this system is that Jesper Q. Thomassen in his master thesis [5] found an interesting behavior for the conductance G as a function of the angle θ under certain restrictions. First it is assumed that the leads are fully polarized with only spin-$\uparrow'$ electrons and that the bare dot energy is situated at the equilibrium chemical potential, $\varepsilon_d = \mu = 0$. For low temperatures and in linear response an exact analytic expression can be found for $U = 0$ in case of fully polarized leads, and the result is[vi]

$$G(\theta) \propto \Gamma^L_{\uparrow'}\Gamma^R_{\uparrow'}\frac{4\cos^2\theta}{4B^2 + \Gamma^2_{\uparrow'}\cos^2\theta}, \qquad \Gamma_{\uparrow'} = \Gamma^L_{\uparrow'} + \Gamma^R_{\uparrow'} \tag{2.5}$$

where $\Gamma^\eta_{\uparrow'}$ is the coupling between the lead η and the dot.
The model is solved using nonequilibrium Green's functions and the so-called equation of motion technique. For $U \neq 0$ the equations of motion get very complicated. However, in the limit $U \approx \infty$, meaning that U is by far the biggest energy in the problem, the equations cannot be solved exactly but simplified and solved numerically. In this limit the conductance resembles $G(\theta) \propto \cos^4\frac{\theta}{2}$. A sketch of the behavior in the two limiting cases can be seen in Fig. 2.4.
For $U = 0$ the conductance vanishes for $\theta = \frac{\pi}{2}$ and $\theta = \frac{3\pi}{2}$, which is explained as a interference phenomenon.[vii] For $U \approx \infty$ this feature has disappeared so the interactions has enhanced the conductance. However, it would be interesting to explore how the interactions influence the conductance for $0 < U < \infty$, which is the aim in this thesis.

[v] We have redefined B, so $\frac{e\hbar}{m}B \to B$ which is an energy.
[vi] The result will be derived in Sec. 4.1.
[vii] A more through discussion we be left to Chap. 4

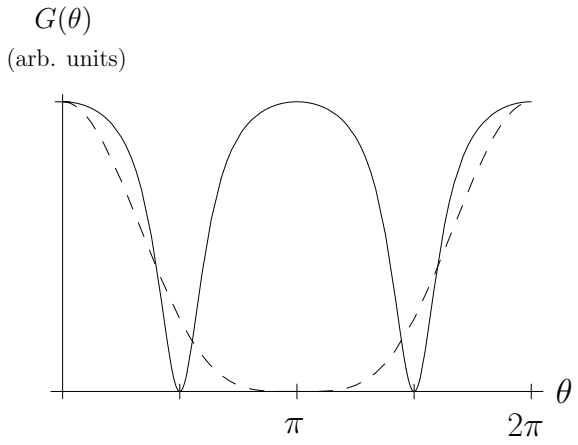

Figure 2.4: Sketch of the conductance G for $U = 0$ (full line) and $U \approx \infty$ (dashed line) for $B = 0.2$ and $\Gamma_{\uparrow'} = 1$. Both curves are normalized to unity in the endpoints.

2.3 Diagonalizing the Hamiltonian

One of the attempts to solve the system described in the previous section is done by using the nonequilibrium Green's function approach presented in Chap. 3. For $U \neq 0$ the retarded Green's function is found using a method introduced in Chap. 6. The latter requires that the eigenstates and eigenvalues of the central region are known, which in this case is the dot with the applied magnetic field, so the last three terms in Eq. (2.4) are named the dot Hamiltonian:

$$H_{\text{dot}} = \sum_{\sigma} \left(\varepsilon_d - \sigma B \cos\theta\right) c^{\dagger}_{d\sigma} c_{d\sigma} - B \sin\theta \left(c^{\dagger}_{d\uparrow'} c_{d\downarrow'} + c^{\dagger}_{d\downarrow'} c_{d\uparrow'}\right) + U n_{\uparrow'} n_{\downarrow'}. \tag{2.6}$$

It is simple to write down the matrix for the first two terms in Eq. (2.6). The eigenvectors form a new (unprimed) spin basis, denoted the dot basis, where the spin-$\uparrow$ state is parallel to the magnetic field and has the energy $\varepsilon_{\uparrow} = \varepsilon_d - B$. The other spin state is antiparallel to the magnetic field and has the energy $\varepsilon_{\downarrow} = \varepsilon_d + B$.

The four eigenstates of the dot Hamiltonian are now identified as $|0\rangle$, $|\uparrow\rangle = c^{\dagger}_{d\uparrow}|0\rangle$, $|\downarrow\rangle = c^{\dagger}_{d\downarrow}|0\rangle$ and $|2\rangle = c^{\dagger}_{d\downarrow} c^{\dagger}_{d\uparrow}|0\rangle$ corresponding to the empty state, a single electron with spin up, a single electron with spin down and the doubled occupied state. The eigenenergies are 0, $\varepsilon_{\uparrow}$, $\varepsilon_{\downarrow}$ and $\varepsilon_2 = \varepsilon_{\uparrow} + \varepsilon_{\downarrow} + U$.

A cautionary note: From now on there will be two different spin bases. The primed spin basis is used for the leads and is defined by their magnetizations. The unprimed spin basis is used for the dot electrons because the dot Hamiltonian is diagonal in this basis. The direction is along the magnetic field.
In summations the indices referring to the primed (unprimed) basis will be labelled with σ (μ).

The matrix for changing from the primed to the unprimed basis is a standard change-of-basis matrix $\mathbf{R}(\theta)$ for spin-$\frac{1}{2}$ systems, and with our choice of coordinate system it is

$$\mathbf{R}(\theta) = \begin{pmatrix} \langle\uparrow' \mid \uparrow\rangle & \langle\uparrow' \mid \downarrow\rangle \\ \langle\downarrow' \mid \uparrow\rangle & \langle\downarrow' \mid \downarrow\rangle \end{pmatrix} = \begin{pmatrix} \cos\frac{\theta}{2} & \sin\frac{\theta}{2} \\ -\sin\frac{\theta}{2} & \cos\frac{\theta}{2} \end{pmatrix}. \tag{2.7}$$

Using the normal transformation rule for operators in second quantization we write $c_{d\sigma} = \sum_\mu \langle\sigma|\mu\rangle\, c_{d\mu} = \sum_\mu R_{\sigma\mu} c_{d\mu}$. This is inserted in the tunnelling part of the Hamiltonian giving

$$H_T = \sum_{k\eta\sigma\mu} \left(t_{k\eta\sigma} R_{\sigma\mu} c^\dagger_{k\eta\sigma} c_{d\mu} + h.c. \right). \tag{2.8}$$

Now the full Hamiltonian is

$$\begin{aligned} H = &\sum_{k\eta\sigma} \varepsilon_{k\eta\sigma} c^\dagger_{k\eta\sigma} c_{k\eta\sigma} + \sum_{k\eta\sigma\mu} \left(V_{k\eta\sigma,\mu} c^\dagger_{k\eta\sigma} c_{d\mu} + h.c. \right) \\ &+ \sum_\mu \varepsilon_\mu c^\dagger_{d\mu} c_{d\mu} + U n_\uparrow n_\downarrow \end{aligned} \tag{2.9}$$

with $V_{k\eta\sigma,\mu} = t_{k\eta\sigma} R_{\sigma\mu}$.

Finally, it should be noted that all the dependence of the magnetic field (except for the shift of the dot energies) is now put into the tunnelling Hamiltonian. This is found to be useful when we consider a scattering formalism where the tunnelling Hamiltonian is treated as a perturbation (see Chap. 9).

Chapter 3

The nonequilibrium Green's function formalism

The Green's function method is originally a way to solve differential equations by transforming them to related solvable problems. In many-particle physics objects are introduced which are related to physical quantities such as density of states, particle density, current etc. They are solutions to a differential equation called the equation of motion and therefore named Green's functions. Green's functions are very studied objects because they allow for applying perturbation theory even to infinite order.

We will distinguish between two different situations: equilibrium and nonequilibrium. Within an equilibrium theory phenomena like impurity scattering in metals, pair interaction in electron gasses and electron-phonon interactions can be studied, just to mention a few. However, transport properties cannot be included in an equilibrium theory because it is the nonequilibrium which drives the current in the system, e.g. due to an applied bias. Dealing properly with transport requires a true nonequilibrium description.

First a short description of the different pictures in quantum mechanics is given. Afterwards a brief sketch of the equilibrium Green function formalism is presented because some of the properties are needed later on. The nonequilibrium formalism is introduced and the focus will be on the issues necessary in this thesis. It will be shown that the structural form of the nonequilibrium Green's functions are similar to those in equilibrium, but with more complicated integrals. Then a way of transforming the complicated integrals are presented, and finally a current formula in terms of the nonequilibrium Green's functions will be derived.

3.1 Pictures in quantum mechanics

When showing that the nonequilibrium and the equilibrium description are equivalent we need to transform the operators between the different pictures in quantum mechanics.[i]

[i] This chapter is inspired by [13] and [1].

In the following we consider a general Hamiltonian of the form

$$\mathcal{H}(t) = H + V(t) \tag{3.1}$$

where H is time-independent. $V(t)$ may or may not be time-dependent and both cases will be treated.

The Schrdinger picture
In the Schrdinger picture operators A, which can be time-dependent, are unchanged while the states $|\psi\rangle$ bear the time-dependence and evolve under the time-dependent Schrdinger equation[ii]

$$i\partial_t|\psi(t)\rangle = \mathcal{H}(t)|\psi(t)\rangle. \tag{3.2}$$

Performing the time-integral from t_0 to t gives the iterative solution

$$|\psi(t)\rangle = \left[\sum_n \frac{(-i)^n}{n!}\int_{t_0}^{t} dt_1 \cdots \int_{t_0}^{t} dt_n T_t\left\{\mathcal{H}(t_1)\cdots\mathcal{H}(t_n)\right\}\right]|\psi(t_0)\rangle, \tag{3.3}$$

where the time-ordering operator has been introduced. It orders the product of operators according to their time argument with the later times to the left, e.g.[iii]

$$T_t\left\{V(t_1)V(t_2)V(t_3)\right\} = V(t_3)V(t_2)V(t_1), \qquad t_1 < t_2 < t_3. \tag{3.4}$$

We now define the time-evolution operator $U(t,t_0)$ and write $|\psi(t)\rangle$ as

$$|\psi(t)\rangle = U(t,t_0)|\psi(t_0)\rangle, \tag{3.5}$$

where

$$U(t,t_0) = \sum_n \frac{(-i)^n}{n!}\int_{t_0}^{t} dt_1 \cdots \int_{t_0}^{t} dt_n T_t\left\{\mathcal{H}(t_1)\cdots\mathcal{H}(t_n)\right\} \equiv T_t e^{-i\int_{t_0}^{t} dt'\mathcal{H}(t')}. \tag{3.6}$$

Because $\mathcal{H}(t)$ is a hermitian operator one has $U^\dagger U = UU^\dagger = 1$.
It is easily seen that $U(t,t_0)$ is a solution to the Schrdinger equation and in case of a time-independent Hamiltonian we obtain $U(t,t_0) = e^{-i\mathcal{H}(t-t_0)}$.

The Heisenberg picture
In the Heisenberg picture all states are time-independent, so the states are defined as

$$|\psi_{\mathcal{H}}\rangle = U_{\mathcal{H}}(t,t_0)|\psi(t)\rangle, \tag{3.7}$$

where $U_{\mathcal{H}}(t,t_0) = U^\dagger(t,t_0)$, with $U^\dagger(t,t_0)$ defined through Eq. (3.6).
For a given operator the expectation value should be independent of the chosen picture, so the operators in the Heisenberg picture fulfill

$$\langle\psi(t)|A|\psi(t)\rangle = \langle\psi_{\mathcal{H}}|A_{\mathcal{H}}(t)|\psi_{\mathcal{H}}\rangle, \tag{3.8}$$

[ii] In [25] the Schdinger equation is derived in analogy with classical mechanics.
[iii] To familiarize with the time-ordering operator see e.g. [1].

which gives the definition of the Heisenberg operators

$$A_{\mathcal{H}}(t) \equiv U_{\mathcal{H}}(t,t_0)AU^{\dagger}_{\mathcal{H}}(t,t_0). \tag{3.9}$$

Exploiting that the time-evolution operator $U_{\mathcal{H}}$ satisfies the Schrdinger equation and consequently that $U^{\dagger}_{\mathcal{H}}$ fulfills $-i\partial_t U^{\dagger}_{\mathcal{H}}(t,t_0) = U^{\dagger}_{\mathcal{H}}(t,t_0)\mathcal{H}(t)$ we obtain the important equation of motion for the operators in the Heisenberg picture[iv]

$$i\partial_t A_{\mathcal{H}}(t) = [A_{\mathcal{H}}(t), H(t)] + i(\partial_t A)(t). \tag{3.10}$$

The interaction picture

In the Heisenberg picture time-evolution of states and operators is controlled by the complicated Hamiltonian $\mathcal{H}$. In the interaction (or Dirac) picture states and operators are defined as

$$|\psi_H(t)\rangle \equiv e^{iH(t-t_0)}|\psi(t)\rangle, \tag{3.11}$$

and

$$A_H(t) \equiv e^{iH(t-t_0)}Ae^{-iH(t-t_0)}, \tag{3.12}$$

so the time-dependence is with respect to the time-independent part of the Hamiltonian, H. Taking the derivative in Eq. (3.11) and using the Schrdinger equation (3.2) we obtain

$$i\partial_t|\psi_H(t)\rangle = V_H(t)|\psi_H(t)\rangle, \tag{3.13}$$

so the time-evolution of the states in the interaction picture is controlled solely by $V(t)$. From the definition of the operators in the Heisenberg and the interaction picture it is seen that they are related through

$$A_{\mathcal{H}}(t) = v^{\dagger}_H(t,t_0)A_H(t)v_H(t,t_0), \tag{3.14}$$

with

$$v_H(t,t_0) = e^{iH(t-t_0)}U^{\dagger}_{\mathcal{H}}(t,t_0). \tag{3.15}$$

When the relation between equilibrium and nonequilibrium is establish this relation will become useful. Using the Schrdinger equation Eq. (3.2) it is seen that the derivative of $v_H(t,t_0)$ is

$$i\partial_t v_H(t,t_0) = V_H(t)v_H(t,t_0), \tag{3.16}$$

with the solution

$$v_H(t,t_0) = T_t e^{-i\int_{t_0}^{t} dt' V_H(t')}. \tag{3.17}$$

Writing out the expression for $v_H(t,t_0)$ gives the famous Dyson series, which is used in time-dependent perturbation theory [25].

[iv] The commutator is defined as $[A,B] = AB - BA$.

3.2 Equilibrium Green's functions

In this section some of the basic relations in equlibrium Green's functions theory are stated and it is not meant as a general introduction to Green's functions. The focus will be on the aspects needed in the nonequlibrium Green's functions theory and no proofs are included. It is emphasized that in equilibrium is $V(t) = V$ and therefore is $\mathcal{H}$ time-independent.[v]

We define the following Green's functions[vi]

$$G^<(\mathbf{r}\sigma t, \mathbf{r}'\sigma' t') = i \left\langle \Psi^\dagger_{\sigma'}(\mathbf{r}'t')\Psi_\sigma(\mathbf{r}t) \right\rangle_\mathcal{H} \qquad \text{(lesser)}, \tag{3.18}$$

$$G^>(\mathbf{r}\sigma t, \mathbf{r}'\sigma' t') = -i \left\langle \Psi_\sigma(\mathbf{r}t)\Psi^\dagger_{\sigma'}(\mathbf{r}'t') \right\rangle_\mathcal{H} \qquad \text{(greater)}, \tag{3.19}$$

$$G^t(\mathbf{r}\sigma t, \mathbf{r}'\sigma' t') = -i \left\langle T_t \left[\Psi_\sigma(\mathbf{r}t)\Psi^\dagger_{\sigma'}(\mathbf{r}'t') \right] \right\rangle_\mathcal{H} \qquad \text{(time}-\text{ordered)}, \tag{3.20}$$

$$G^R(\mathbf{r}\sigma t, \mathbf{r}'\sigma' t') = -i\theta(t-t') \left\langle \left\{ \Psi_\sigma(\mathbf{r}t), \Psi^\dagger_{\sigma'}(\mathbf{r}'t') \right\} \right\rangle_\mathcal{H} \qquad \text{(retarded)}, \tag{3.21}$$

$$G^A(\mathbf{r}\sigma t, \mathbf{r}'\sigma' t') = i\theta(t'-t) \left\langle \left\{ \Psi_\sigma(\mathbf{r}t), \Psi^\dagger_{\sigma'}(\mathbf{r}'t') \right\} \right\rangle_\mathcal{H} \qquad \text{(advanced)}. \tag{3.22}$$

The operators $\Psi^\dagger_{\sigma'}(\mathbf{r}t)[\Psi_{\sigma'}(\mathbf{r}t)]$ are the field operators for creating [annihilating] an electron with spin σ at the point $\mathbf{r}$. Both operators are written in the Heisenberg picture. The average values are defined as a thermal average[vii]

$$\langle A \rangle_\mathcal{H} \equiv \langle \rho_\mathcal{H} A \rangle = \frac{1}{Z_\mathcal{H}} \mathrm{Tr}[e^{-\beta\mathcal{H}}A], \qquad Z_\mathcal{H} = \mathrm{Tr}[e^{-\beta\mathcal{H}}], \tag{3.23}$$

with $\rho_\mathcal{H}$ being the density operator with respect to $\mathcal{H}$.
The Green's functions are not independent and we note in particular the important relation

$$G^R - G^A = G^> - G^<. \tag{3.24}$$

Using the general rule for changing basis in second quantization we can write the field operator as $\Psi_\sigma(\mathbf{r}t) = \sum_\nu \psi_\nu(\sigma\mathbf{r})c_\nu(t)$, where $\{|\psi_\nu\rangle\}$ are a complete set of wave functions satisfying the Schrdinger equation and $c_\nu(t)$ is the operator for annihilating an electron in the state ν, written in the Heisenberg picture. Consequently, the Green's functions can be expressed in an arbitrary basis.

Consider the Green's functions written in the basis $\{|\psi_\nu\rangle\}$, e.g. the retarded Green's function[viii]

$$G^R_{\nu\nu'}(t,t') = -i\theta(t-t') \left\langle \left\{ c_\nu(t), c^\dagger_\nu(t') \right\} \right\rangle, \tag{3.25}$$

[v] For a general introduction to equilibrium Green's functions, see [1], which is also the basis for this chapter.

[vi] The anti-commutator is $\{A, B\} = AB + BA$.

[vii] $\beta = \frac{1}{k_B T}$, with T being the temperature.

[viii] The spin label has been suppressed.

and similarly for the other Green's functions.
In equilibrium no reference is given to an initial time t_0, so the Green's functions depend only on the difference between the time arguments, $t - t'$, so it is natural to perform a Fourier transformation with respect to time.
In Fourier space holds the important fluctuation-dissipation theorem which relates the occupation of the state ν to the retarded Green's function

$$\left\langle c_\nu^\dagger c_{\nu'} \right\rangle = i \int \frac{d\omega}{2\pi} \left[G^R_{\nu'\nu}(\omega) - \left(G^R_{\nu\nu'}(\omega) \right)^* \right] f(\omega), \tag{3.26}$$

and it is proven in Sec. A.4.4. The proof requires a time-independent Hamiltonian and is therefore only valid in equilibrium.

Perturbation series in equilibrium
When calculating the Green's function we need to evaluate average values like $\left\langle A_{\mathcal{H}}(t) B_{\mathcal{H}}(t') \right\rangle_{\mathcal{H}}$, where the operators are written in the Heisenberg picture. The trick used to calculate these expectation values is to introduce the complex time $\tau = it$, and after the change of variable can the time-evolution operator in the interaction picture be written as[ix]

$$\begin{aligned} U_H(\tau, \tau') &= \sum_{n=0}^{\infty} \frac{(-1)^n}{n!} \int_{\tau'}^{\tau} d\tau_1 \cdots \int_{\tau'}^{\tau} d\tau_n T_\tau [V_H(\tau_1) \cdots V_H(\tau_n)] \\ &= T_\tau e^{-\int_{\tau'}^{\tau} d\tau' V_H(\tau')}. \end{aligned} \tag{3.27}$$

Instead of using the Green's functions introduced in Eq. (3.18)-(3.22), we introduce the imaginary time Green's function, also known as the Matsubara Green's function,

$$\mathcal{G}(\sigma \mathbf{r} \tau, \sigma' \mathbf{r}' \tau') \equiv - \left\langle T_\tau [\Psi_{\mathcal{H}}(\sigma \mathbf{r} \tau) \Psi^\dagger_{\mathcal{H}}(\sigma' \mathbf{r}' \tau')] \right\rangle_{\mathcal{H}}. \tag{3.28}$$

With the definition of the complex time-evolution operator it can be written as

$$\mathcal{G}(\sigma \mathbf{r} \tau, \sigma' \mathbf{r}' \tau') = - \frac{\mathrm{Tr}[e^{-\beta H} T_\tau \{ U_H(\beta, 0) \Psi_H(\tau) \Psi'_H(\tau') \}]}{\mathrm{Tr}[e^{-\beta H} U_H(\beta, 0)]}, \tag{3.29}$$

where we notice that the average value and time-evolution is with respect to H.
To proceed we need a tool for calculating expectation values of products of time ordered operators like $\langle T_\tau [A_1(\tau_1) \cdots A_n(\tau_n)] \rangle_H$. For a quadratic H Wick's theorem can be applied (see [1]). The resulting terms can be written on a diagrammatic form with the so-called Feynman diagrams, see e.g. [1], which allows for simplifications of the infinite sums in Eq. (3.29).
Finally, it can be shown that the retarded real-time Green's function can be deduced from the Matsubara Green's function by analytic continuation.

[ix] The time-ordering operator on the complex axis is $T_\tau [A(\tau) B(\tau')] = \theta(\tau - \tau') A(\tau) B(\tau') - \theta(\tau' - \tau) B(\tau') A(\tau)$.

Eventually we stress the importance of the relation between the occupancies and the retarded Green's functions in Eq. (3.26). The relation will be widely used when applying the Green's function technique in later chapters. Moreover, Eq. (3.29) should be noticed because it serves as the link between the equilibrium an nonequilibrium theories as it will be shown in the following section.

3.3 Nonequilibrium Green's functions

[x]In nonequilibrium the Hamiltonian $\mathcal{H}$ is time-dependent and we write it as in Eq. (3.1) with H being time-independent and $V(t)$ carrying the time-dependence. As in the previous section, we will need to calculate average values of time-ordered operators using Wick's theorem, so we assume that the Hamiltonian H can be split into two parts, where H^0 is quadratic and H^i accounts for the (complicated) interactions between the electrons.
The Hamiltonian $\mathcal{H}$ reads

$$\mathcal{H}(t) = H + V(t) = H^0 + H^i + V(t). \tag{3.30}$$

As the nonequilibrium counterpart of the equilibrium time-ordered Green's function in Eq. (3.28) we introduce the contour-ordered Green's function[xi]

$$G^C(1,1') \equiv -i \left\langle T_C[\Psi_{\mathcal{H}}(1)\Psi^\dagger_{\mathcal{H}}(1')] \right\rangle_H, \tag{3.31}$$

where C is a contour along the real axis visiting t and t' once, see Fig. 3.1. T_C is the contour-ordering operator placing later times to the left, where "later" is in the contour sense,

$$T_C[\Psi_{\mathcal{H}}(1)\Psi^\dagger_{\mathcal{H}}(1')] = \begin{cases} \Psi_{\mathcal{H}}(1)\Psi^\dagger_{\mathcal{H}}(1') & \text{for } t_1 >_C t_{1'}, \\ -\Psi^\dagger_{\mathcal{H}}(1')\Psi_{\mathcal{H}}(1) & \text{for } t_1 <_C t_{1'}. \end{cases} \tag{3.32}$$

Note that the average value is with respect to the density operator ρ_H and not some time-dependent operator. This allows us to calculate the average values with respect to the eigenstates before the onset of $V(t)$, but the approach is only reasonable when the applied perturbation $V(t)$ does not completely change the system e.g. by heating it up.[xii]

As in equilibrium we define lesser and greater correlation functions

$$G^<(1,1') = i \left\langle \Psi^\dagger_{\mathcal{H}}(1')\Psi_{\mathcal{H}}(1) \right\rangle_H, \tag{3.33}$$

$$G^>(1,1') = -i \left\langle \Psi_{\mathcal{H}}(1)\Psi^\dagger_{\mathcal{H}}(1') \right\rangle_H, \tag{3.34}$$

and they are linked to the contour-ordered Green's function by

$$G^C(1,1') = \begin{cases} G^>(1,1') & \text{for } t_1 >_C t_{1'}, \\ G^<(1,1') & \text{for } t_1 <_C t_{1'}. \end{cases} \tag{3.35}$$

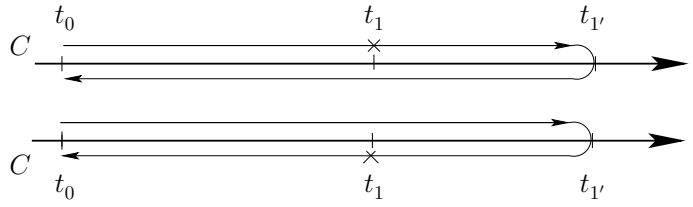

Figure 3.1: The contour C used when defining the contour-ordered Green's function, G^C. On the uppermost contour is $t_1 <_C t_{1'}$ and $t_1 < t_{1'}$. On the lower is $t_1 >_C t_{1'}$, but $t_1 < t_{1'}$

Before getting lost in technical details, we should be aware of the goal, which is to write the contour-ordered nonequilibrium Green's function on a form structurally equivalent to the equilibrium expression Eq. (3.29). To do so, we proceed in two steps. First we transform the operators from the Heisenberg picture where they evolve under the full time-dependent Hamiltonian $\mathcal{H}$, to the H^0-interaction picture where time-evolution is governed by the time-independent and quadratic part of the Hamiltonian, H^0. This is done because we, as in equilibrium, want to use Wick's theorem which requires a quadratic Hamiltonian. Afterwards, the density operator ρ_H is written as ρ_{H^0} times a contour-ordered exponential. Eventually, the Green's function in Eq. (3.31) is on the desired form, but the integrals from 0 to β in Eq. (3.29) has been replaced by contour integrals.[xiii]

In Eq. (3.14) it was shown how the operators could be transformed from the Heisenberg picture to the interaction picture. We want to apply Wick's theorem, so we write the operators in the H^0-interaction picture and by careful inspection of the contour C_t, shown in Fig. 3.2, it can be proven that[xiv]

$$A_{\mathcal{H}}(t) = T_{C_t}[e^{-i\int_{C_t} d\tau[H^i_{H^0}(\tau)+V_{H^0}(\tau)]} A_{H^0}(t)]. \tag{3.36}$$

Now consider the situation where $t_1 <_C t_{1'}$ (shown at the upper figure in Fig. 3.1). According to Eq. (3.35) $G^C(1,1')$ is equal to $G^<(1,1')$, so applying Eq. (3.36) on each operator gives

$$G^C(1,1') = i\left\langle T_{C_{t_{1'}}}[e^{-i\int_{C_{t_{1'}}} d\tau[H^i_{H^0}(\tau)+V_{H^0}(\tau)]}\Psi^\dagger_{H^0}(1')]T_{C_{t_1}}[e^{-i\int_{C_{t_1}} d\tau[H^i_{H^0}(\tau)+V_{H^0}(\tau)]}\Psi^\dagger_{H^0}(1)]\right\rangle_H . \tag{3.37}$$

A rearranging of the contours can be performed and the two exponentials can be gathered in a single time-ordered exponential, where the ordering and the integral are with respect to the contour C shown in Fig. 3.1. Doing the same analysis for $t_1 >_C t_{1'}$ leads to the

[x] This section is based on [13] and [7].
[xi] All the labels have been gathered in a single index $1 = (\sigma \mathbf{r} t)$.
[xii] See [7] and references therein.
[xiii] This section is mainly inspired by [13], but also by [7].
[xiv] The proof is found in Sec. A.1.1.

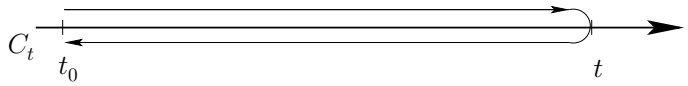

Figure 3.2: The contour C_t applied for changing from the Heisenberg picture to the H^0-interaction picture. The contour runs on the real axis but is for clarity drawn away from it.

result[xv]

$$G^C(1,1') = -i\left\langle T_C[e^{-i\int_C d\tau[H^i_{H^0}(\tau)+V_{H^0}(\tau)]}\Psi_{H^0}(1)\Psi^\dagger_{H^0}(1')]\right\rangle_H. \tag{3.38}$$

Finally we rewrite the density operator ρ_H by introducing the operator

$$v(t,t_0) = e^{iH^0(t-t_0)}e^{i(H^0+H^i)(t-t_0)}. \tag{3.39}$$

Proceeding as when deriving the time-evolution operator in the interaction picture (see Eqs. (3.16) and (3.17)) we take the derivative of Eq. (3.39) and solve the resulting differential equation with the boundary condition $v(t_0,t_0)=1$. The solution is

$$v(t,t_0) = T_t e^{-i\int_{t_0}^t dt' H^i_{H^0}(t')}. \tag{3.40}$$

Using the property $e^{-\beta H} = e^{-\beta H^0}v(t_0-i\beta,t_0)$ the density operator becomes

$$\rho_H = \frac{e^{-\beta H^0}T_t e^{-i\int_{t_0}^{t_0-i\beta} dt' H^i_{H^0}(t')}}{\mathrm{Tr}\left[e^{-\beta H^0}T_t e^{-i\int_{t_0}^{t_0-i\beta} dt' H^i_{H^0}(t')}\right]}. \tag{3.41}$$

The curve C is closed, so the integral $\int_C d\tau[H^i_{H^0}(\tau)+V_{H^0}(\tau)]=0$ because the integrand is analytic. The denominator in Eq. (3.41) can then be transformed into

$$e^{-\beta H^0}T_t e^{-i\int_{t_0}^{t_0-i\beta} dt' H^i_{H^0}(t')} = e^{-\beta H^0}T_{C_V}\left[T_t e^{-i\int_{C_V} dt' H^i_{H^0}(t')}e^{-i\int_C dt' V_{H^0}(t')}\right], \tag{3.42}$$

where the contour C_V shown in Fig. 3.3 has been introduced. The exponentials have been gathered in one single time-ordering operator because time-ordering on C_V and C is identical on the common part, and we also use that the part from t_0 to $t_0-i\beta$ is later on the contour than the C-part.

Eventually, G^C can be written as

$$G^C(1,1') = -i\frac{\mathrm{Tr}\left\{e^{-\beta H^0}T_{C_V}[e^{-i\int_{C_V} d\tau H^i_{H^0}(\tau)}e^{-i\int_C d\tau V_{H^0}(\tau)}\Psi_{H^0}(1)\Psi^\dagger_{H^0}(1')]\right\}}{\mathrm{Tr}\left\{e^{-\beta H^0}T_{C_V}\left[e^{-i\int_{C_V} d\tau H^i_{H^0}(\tau)}e^{-i\int_C d\tau V_{H^0}(\tau)}\right]\right\}}. \tag{3.43}$$

[xv] See Sec. A.1.2.

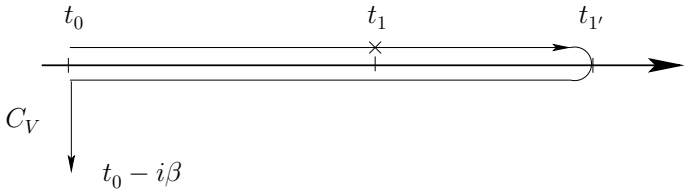

Figure 3.3: The contour C_V.

The time-dependence of the operators and the average value are with respect to the quadratic and time-independent part of the Hamiltonian. This allows us to use Wick's theorem just like in equilibrium. Moreover, if Eq. (3.43) is compared to the expression for the equilibrium time-ordered Green's functions in Eq. (3.29) it is seen that they have the same structure, the only difference being

$$\begin{aligned} U_H(\beta,0) = T_\tau e^{-\int_0^\beta d\tau' V_H(\tau')} &\longrightarrow T_{C_V}\left[e^{-i\int_{C_V} d\tau H^i_{H^0}(\tau)} e^{-i\int_C d\tau V_{H^0}(\tau)}\right] \\ &= T_{C_V}\left[e^{-i\int_{C_V} d\tau \left\{H^i_{H^0}(\tau)+\theta_C(\tau)V_{H^0}(\tau)\right\}}\right], \end{aligned} \tag{3.44}$$

where we in the last line have collected the exponentials and introduced the unit step function $\theta_C(\tau)$, which is 1 for τ on the contour C and 0 elsewhere.

From Eqs. (3.43) and (3.44) it is clear the nonequilibrium Green's function have the same perturbation expansion as the equilibrium Green's functions, so the nonequilibrium Feynman diagrams are mapped onto their equilibrium counterparts, see Eq. (3.29). The only difference is when evaluating the diagrams, because the equilibrium integrals from 0 to β have been replaced by contour integrals along the curve C_V. Transforming them to integrals on the real axis is done in the following section.

3.4 Analytic continuation in Keldysh space

We want to derive a way to change the integrals from contour integrals to real time integral. The process is called analytic continuation and an often used technique is due to Langreth (see [15]), where a deformation of the contour is performed. However, we those an approach due to Keldysh because in this framework the rules can be derived by simple bookkeeping.[xvi]

We start with changing the contour C_V from Fig. 3.3. If we let $t_0 \to -\infty$ and turn on the time-dependent part $V(t)$ very slowly (adiabatically), it can be shown that the integral from t_0 to $t_0 - i\beta$ vanishes and that the information lost by doing so is the correlations between the electrons before the onset of $V(t)$. When calculating transport, we are most often interested in the steady state behaviour, where the initial conditions are no longer

[xvi] The derivation in this section is based on [13] and [14], but also [7].

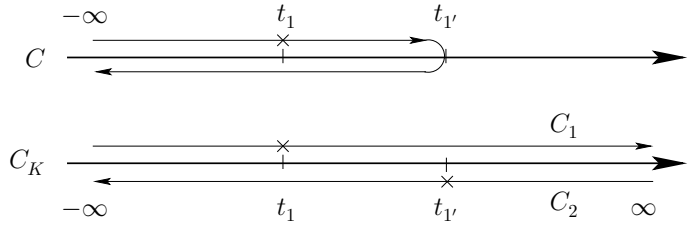

Figure 3.4: The contour C is changed to the Keldysh contour C_K consisting of the two branches, C_1 and C_2. The contours run on the real axis but are for clarity drawn away from it.

important. Without further arguments we will set $t_0 = -\infty$ and neglect the part from t_0 to $t_0 - i\beta$, so in the rest of this section $C = C_V$.[xvii]
Moreover, we extend the curve C from the outermost point to infinity and back again. The integral along the added piece vanishes because the extension forms a closed curve. The resulting curve contains two branches where C_1 runs from $-\infty$ to ∞ on the real axis, and C_2 runs in the opposite direction. This is the Keldysh contour C_K shown in Fig. 3.4.

In the Keldysh formalism the contour-ordered Green's function $G^C(1,1')$ is replaced by the Keldysh contour-ordered Green's function $G^{C_K}(1,1')$, which is a 2×2 matrix. The link between the contour-ordered Green's function and the Keldysh Green's function is [13]

$$G^{C_K}(1,1') \mapsto \hat{G}(1,1') \equiv \begin{pmatrix} G_{11}(1,1') & G_{12}(1,1') \\ G_{21}(1,1') & G_{22}(1,1') \end{pmatrix}. \tag{3.45}$$

The indices on the matrix elements refer to which branch of the contour the time-arguments belong to, i.e. $G_{ij}(1,1')$ means $t_1 \in C_i$ and $t_{1'} \in C_j$. If we compare with the Green's functions defined in the previous section, we can write

$$G_{11}(1,1') = -i\left\langle T_t[\Psi_{\mathcal{H}}(1)\Psi^\dagger_{\mathcal{H}}(1')]\right\rangle_{\mathcal{H}}, \tag{3.46}$$
$$G_{12}(1,1') = G^<(1,1'), \tag{3.47}$$
$$G_{21}(1,1') = G^>(1,1'), \tag{3.48}$$
$$G_{22}(1,1') = -i\left\langle \tilde{T}_t[\Psi_{\mathcal{H}}(1)\Psi^\dagger_{\mathcal{H}}(1')]\right\rangle_{\mathcal{H}}, \tag{3.49}$$

where $\tilde{T}_t$ is the anti-time-ordering operator.[xviii]
We also define the retarded and advanced Green's functions like in Eqs. (3.21) and (3.22), and write them in terms of the lesser and greater Green's functions

$$G^R(1,1') = \theta(t_1 - t_{1'})[G^>(1,1') - G^<(1,1')], \tag{3.50}$$
$$G^A(1,1') = \theta(t_{1'} - t_1)[G^<(1,1') - G^>(1,1')]. \tag{3.51}$$

[xvii] For a further discussion of the validity of the approach, see [14] and references therein.
[xviii] Notice that when transforming the contour from $C \to C_K$ the Green's functions are unchanged whether we choose the outermost point to be on C_1 or C_2.

They are all related to the elements of $\hat{G}$, e.g. if both time labels are on the contour C_1 then $G^R(1,1') = G_{11}(1,1') - G_{12}(1,1')$ holds, and if both time labels are on C_2 one has $G^R(1,1') = G_{21}(1,1') - G_{22}(1,1')$. Similar relations are derived for $G^A(1,1')$,

$$G^R(1,1') = G_{11}(1,1') - G_{12}(1,1') = G_{21}(1,1') - G_{22}(1,1'), \tag{3.52}$$
$$G^A(1,1') = G_{11}(1,1') - G_{21}(1,1') = G_{12}(1,1') - G_{22}(1,1'). \tag{3.53}$$

In the nonequilibrium formalism it is often necessary to evaluate a product of operators on the form

$$D^{C_K}(1,1') = \int_{C_K} d\tau \; A^{C_K}(1,\tau)B^{C_K}(\tau,1'), \tag{3.54}$$

for instance when having derived a Dyson equation. The integration is along the contour C_K, but instead we want to write it as a standard integral along the real axis.
We start by writing the (11)-element as

$$\begin{aligned} D_{11}(1,1') &= \int_{C_1} dt A_{11}(1,t)B_{11}(t,1') + \int_{C_2} dt A_{12}(1,t)B_{21}(t,1') \\ &= \int_{-\infty}^{\infty} dt \left[A_{11}(1,t)B_{11}(t,1') - A_{12}(1,t)B_{21}(t,1')\right]. \end{aligned} \tag{3.55}$$

Relations for the other elements are derived in the same way and we obtain

$$D_{11} = A_{11}B_{11} - A_{12}B_{21}, \qquad D_{12} = A_{11}B_{12} - A_{12}B_{22}, \tag{3.56}$$
$$D_{21} = A_{21}B_{11} - A_{22}B_{21}, \qquad D_{22} = A_{21}B_{12} - A_{22}B_{22}, \tag{3.57}$$

where the integration over the internal variable has been suppressed.
Using the relations in Eqs. (3.52) and (3.53) the rules for analytic continuation of the function $\hat{D}^{C_K}$ can be written as

$$D^R(1,1') = \int dt A^R(1,t)B^R(t,1'), \tag{3.58}$$
$$D^A(1,1') = \int dt A^A(1,t)B^A(t,1'), \tag{3.59}$$
$$D^<(1,1') = \int dt A^<(1,t)B^A(t,1') + A^R(1,t)B^<(t,1'), \tag{3.60}$$
$$D^>(1,1') = \int dt A^>(1,t)B^A(t,1') + A^R(1,t)B^>(t,1'), \tag{3.61}$$

where also $G_{12} = G^<$ and $G_{21} = G^>$ have been applied.
The rules are central in the nonequilibrium formalism because they relate the complicated contour integrals to integrals on the real axis, and they can easily be generalized to multiple products of Green's functions. The usefulness of the rules will come clear in the next section when we derive the current formula.
Similar relations can be derived for functions of the type $D^{C_K}(1,1') = A^{C_K}(1,1')B^{C_K}(1,1')$ and $D^{C_K}(1,1') = A^{C_K}(1,1')B^{C_K}(1',1)$, but they are not needed in this thesis.[xix]

[xix] The other rules for analytic continuation can be found in [7].

3.5 Derivation of the current formula

It might not seem obvious how the formalism presented in the previous section can be related to a tunnelling setup. In this section, we derive the famous current formula due to Meir and Wingreen [16], but the derivation in [7] is used. Only a few proofs in the derivation will be found here while the details are given in Sec. A.1.

As a starting point we consider three disconnected regions: two metallic leads and a central region, each having its own chemical potential. At $t = -\infty$ a coupling between them onsets and the coupling is treated as a perturbation. No assumptions concerning the size of the perturbation is done, so it has to be treated to all orders.
After some time the system reaches steady state, and we make the assumption that the leads are sufficiently large such that they maintain their chemical potentials.

The aim is to write the current in terms of a nonequilibrium Green's function for an interacting central region contacted to two leads, and we consider the model Hamiltonian

$$\begin{aligned} H &= \sum_{k,\eta=L,R} \varepsilon_{k\eta} c_{k\eta}^\dagger c_{k\eta} + \sum_n \varepsilon_n d_n^\dagger d_n + \sum_{k\eta n} (V_{k\eta,n} c_{k\eta}^\dagger d_n + h.c.) \\ &= H_C + H_{\text{dot}} + H_T. \end{aligned} \tag{3.62}$$

The first term is for the leads which are assumed noninteracting and k is a collection of quantum numbers. The next term is for the central region (the quantum dot) where the states $\{|n\rangle\}$ form a complete orthonormal basis. The last term is the tunnelling term with $V_{k\eta,n}$ being the tunnelling amplitude for an electron leaving the quantum dot in the state n and entering the lead η in state k.

Using the continuity equation, we obtain that the number of electrons leaving (or entering) the left lead L plus the current flowing out from (into) it per unit time is equal to zero. This gives

$$J_L = -e \left\langle \dot{N}_L \right\rangle = -\frac{ie}{\hbar} \left\langle [H, N_L] \right\rangle, \tag{3.63}$$

where $N_L = \sum_k c_{kL}^\dagger c_{kL}$ is the operator which counts the number of electrons in the lead L. Unless explicitly otherwise stated, all operators in this section are written in the Heisenberg picture and the average value is with respect to the full Hamiltonian H from Eq. (3.62).
Calculating the commutator gives

$$\begin{aligned} J_L &= \frac{e}{\hbar} \sum_{kn} \left[V_{kL,n} (G^<_{n,kL}(t,t)) - V^*_{kL,n} (-iG^<_{kL,n}(t,t)) \right] \\ &= \frac{2e}{\hbar} \text{Re} \left\{ \sum_{kn} V_{kL,n} G^<_{n,kL}(t,t) \right\}, \end{aligned} \tag{3.64}$$

where we have introduced the new Green's functions

$$G^<_{k\eta,n}(t,t') = i \left\langle c_{k\eta}^\dagger(t') d_n(t) \right\rangle, \qquad G^<_{n,k\eta}(t,t') = i \left\langle d_n^\dagger(t') c_{k\eta}(t) \right\rangle \tag{3.65}$$

and used the property $[G^<_{n,k\eta}(t,t')]^* = -G^<_{k\eta,n}(t,t')$.

It is clear that we need an expression for the lesser current Green's function $G^<_{n,k\eta}(t,t)$. We start from the contour-ordered Green's function

$$G^C_{n,k\eta}(\tau,\tau') = -i\left\langle T_C\left\{d_n(\tau)c^\dagger_{k\eta}(\tau')\right\}\right\rangle, \tag{3.66}$$

with C being the contour shown in Fig. 3.1, and afterwards use the rules for analytic continuation from Sec. 3.4 to obtain the lesser function.
In Sec. 3.3 it was shown that the nonequilibrium Green's functions have the same form as their equilibrium counterparts, so instead we consider the time-ordered equilibrium Green's function $G^t_{n,k\eta}(t,t') = -i\left\langle T_t\left\{d_n(t)c^\dagger_{k\eta}(t')\right\}\right\rangle$, where T_t is the time-ordering operator.
Now we take the derivative with respect to t' and use the Heisenberg equation for time-evolution of operators to find

$$-i\partial_{t'}G^t_{n,k\eta}(t,t') = \varepsilon_{k\eta}G^t_{n,k\eta}(t,t') + \sum_m V^*_{k\eta,m}G^t_{nm}(t,t'), \tag{3.67}$$

where the new Green's functions $G^t_{nm}(t,t') = -i\left\langle T_t\left\{d_n(t)d_m(t')\right\}\right\rangle$ for the dot have been introduced.
In case of no coupling between the leads and the dot we define the uncoupled time-ordered Green's function $g^t_{k\eta}(t_1,t') = -i\left\langle T_t\left\{c_{k\eta}(t_1)c^\dagger_{k\eta}(t')\right\}\right\rangle$ for the lead η. Because it is the Green's function for the lead in absence of tunnelling, the time-evolution of the lead operators and the average value are with respect to the first term in Eq. (3.62). Again the Heisenberg equation of motion is applied and we obtain

$$(i\partial_{t'} - \varepsilon_{k\eta})g^t_{k\eta}(t',t_1) = \delta(t_1 - t'). \tag{3.68}$$

After multiplication with the lead Green's function $g^t_{k\eta}(t',t_1)$ on both sides and carrying out a partial integration, Eq. (3.67) becomes[xx]

$$G^t_{n,k\eta}(t,t') = \sum_m \int dt_1 V^*_{k\eta,m}G^t_{nm}(t,t_1)g^t_{k\eta}(t_1,t'). \tag{3.69}$$

To obtain the nonequilibrium expression for $G^C_{n,k\eta}(\tau,\tau')$ from Eq. (3.69) we have to replace the integral along the real axis with a contour integral as showed in Sec. 3.3. We neglect the initial correlations among the electrons and replace the appearance of the contour C_V with the contour C. Afterwards it is changed into the Keldysh contour C_K using the same line of arguments as in Sec. 3.4.
Now the nonequilibrium version of Eq. (3.69) is

$$G^{C_K}_{n,k\eta}(\tau,\tau') = \sum_m \int_{C_K} d\tau_1 V^*_{k\eta,m}G^{C_K}_{nm}(\tau,\tau_1)g^{C_K}_{k\eta}(\tau_1,\tau'). \tag{3.70}$$

[xx]The details can be found in Sec. A.1.3.

and using the analytic continuation rule from Eq. (3.60) we obtain

$$G^<_{n,k\eta}(t,t') = \sum_m \int dt_1 V^*_{k\eta,m} \left[G^R_{nm}(t,t_1) g^<_{k\eta}(t_1,t') + G^<_{nm}(t,t_1) g^a_{k\eta}(t_1,t') \right]. \tag{3.71}$$

In steady state no reference is given to an initial time, so the Green's functions depend only on the difference between the time-arguments. Using the convolution theorems for Fourier transforms[xxi] leads to

$$G^<_{n,k\eta}(t,t') = \sum_m \int \frac{d\omega}{2\pi} V^*_{k\eta,m} \left[G^R_{nm}(\omega) g^<_{k\eta}(\omega) + G^<_{nm}(\omega) g^a_{k\eta}(\omega) \right] e^{i\omega(t-t')}, \tag{3.72}$$

and inserting $G^<_{n,kL}(t,t)$ in Eq. (3.64) gives

$$J_L = \frac{2e}{\hbar} \sum_{nmk} \int \frac{d\omega}{2\pi} \mathrm{Re} \left\{ V^*_{kL,m} V_{kL,n} \left[G^R_{nm}(\omega) g^<_{kL}(\omega) + G^<_{nm}(\omega) g^a_{kL}(\omega) \right] \right\}. \tag{3.73}$$

We want to replace the sum over $k\eta$ with an integral, $\sum_{k\eta} \to \int d\varepsilon_{k\eta} \mathcal{D}_\eta(\varepsilon_{k\eta})$, where $\mathcal{D}_\eta(\varepsilon_{k\eta})$ is the density of states in the lead η. If we introduce the coupling parameter

$$\Gamma^\eta_{mn}(\varepsilon) = \mathcal{D}_\eta(\varepsilon) V^*_{k\eta,m} V_{k\eta,n}, \tag{3.74}$$

and insert the expressions for the lead Green's functions, we can write J_L as

$$J_L = \frac{ie}{\hbar} \int \frac{d\omega}{2\pi} \mathrm{Tr} \left\{ \mathbf{\Gamma}^L(\omega) \left(G^<(\omega) + f_L(\omega) \left[\mathbf{G}^R(\omega) - \mathbf{G}^A(\omega) \right] \right) \right\}, \tag{3.75}$$

which is shown in Sec. A.1.5. It has been used that the lead Green's functions are for the isolated leads, and because they are treated as noninteracting the Green's functions are simple to find. The current entering the right lead, J_R, is of course given as in Eq. (3.75), but with L replaced with R.

We are only interested in the steady state behaviour of the current and do not consider time-dependent phenomena like an oscillatory applied bias or time-modified gate signals.[xxii] Due to current conservation in steady state holds $J = J_L = -J_R$, and writing the current as $J = \frac{J_L - J_R}{2}$ we get from Eq. (3.75)

$$\begin{aligned} J = \frac{ie}{2\hbar} \int \frac{d\omega}{2\pi} \mathrm{Tr} \Big\{ & \left[\mathbf{\Gamma}^L(\omega) - \mathbf{\Gamma}^R(\omega) \right] \mathbf{G}^<(\omega) \\ & + \left[f_L(\omega) \mathbf{\Gamma}^L(\omega) - f_R(\omega) \mathbf{\Gamma}^R(\omega) \right] \left[\mathbf{G}^R(\omega) - \mathbf{G}^A(\omega) \right] \Big\}. \end{aligned} \tag{3.76}$$

As we will discover later on, it is more difficult to obtain an equation for the lesser Green's function than for the retarded, so we want to eliminate the $G^<$-term from the current

[xxi] See Sec. A.1.4

[xxii] A description of how to deal with time-dependent phenomena in the nonequilibrium Green's function formalism can be found in [7].

expression. In case of proportionate couplings between the left and the right lead $\mathbf{\Gamma}^L(\varepsilon) = \lambda\mathbf{\Gamma}^R(\varepsilon)$, it is possible. Otherwise not, unfortunately.
We start by writing the current as $J = xJ_L + J_L - xJ_L = xJ_L - (1-x)J_R$, where x is an arbitrary parameter. From Eq. (3.75) we find that

$$\begin{aligned} J = \frac{ie}{\hbar}\int\frac{d\omega}{2\pi}\mathrm{Tr}\Big\{&(\lambda x - 1 + x)\mathbf{\Gamma}^R(\omega)\mathbf{G}^<(\omega) \\ &+ \left[\lambda x f_L(\omega) - (1-x)f_R(\omega)\right]\mathbf{\Gamma}^R(\omega)\left[\mathbf{G}^R(\omega) - \mathbf{G}^A(\omega)\right]\Big\}. \end{aligned} \tag{3.77}$$

We chose $x = \frac{1}{1+\lambda}$, so $\lambda x - 1 + x = 0$ and the $\mathbf{G}^<$-term vanishes. The final expression for the steady state current in case of proportionate couplings is

$$J = \frac{ie}{\hbar}\frac{\lambda}{1+\lambda}\int\frac{d\omega}{2\pi}\mathrm{Tr}\left\{\mathbf{\Gamma}^R(\omega)\left[\mathbf{G}^R(\omega) - \mathbf{G}^A(\omega)\right]\left[f_L(\omega) - f_R(\omega)\right]\right\}. \tag{3.78}$$

Eq. (3.78) is a genuine nonequilibrium expression, because no assumptions concerning the applied bias are made. Furthermore, it is valid for all values of the coupling parameter $\mathbf{\Gamma}^\eta$ and therefore even for strong coupling between the leads and the dot.
Despite the simple appearance it contains some obstacles. The coupling parameter $\mathbf{\Gamma}^\eta(\omega)$ depends on energy and is in general very hard to find. In many practical calculations it is assumed to be equal to a constant over the energy range of interest, as discussed in Chap. 4. Moreover, the dot Green's functions are full Green's functions and have to be calculated in presence of the tunnelling term in the Hamiltonian. They are in general not exactly solvable and one has to apply an approximation scheme. We will return to these issues in Chap. 6.

The derivation of the current formula ends the part concerning the theoretical background for the nonequilibrium Green's function formalism. The most important things to notice are the structural equivalence between equilibrium and nonequilibrium Green's functions and the current formula. The rules for analytic continuation will also show up to be extremely useful.
In the following two chapters we apply the Green's function formalism to the FAB model in case of noninteracting electrons on the dot. The approximation scheme valid in presence of interactions on the dot is introduced in Chap. 6, and in Chap. 7 the calculations for the FAB model is presented.

Chapter 4

The FAB model without interactions (parallel)

As a first application of the Green's function method, it will be shown how to solve the FAB model in case of no electron-electron interactions on the dot, i.e. $U = 0$, and parallel magnetizations of the leads. In this case the model can be solved exactly which is often the case for non-interacting models. Due to the simplicity of the derivation it allows for introducing and getting used to some of the concepts and the notation applied in the chapters to follow, but where the calculations are more complicated.

If the interactions on the dot are neglected the Hamiltonian introduced in Eq. (2.9) reduces to

$$H = \sum_{k\eta\sigma} \varepsilon_{k\eta\sigma} c^\dagger_{k\eta\sigma} c_{k\eta\sigma} + \sum_{k\eta\sigma\mu} \left(V_{k\eta\sigma,\mu} c^\dagger_{k\eta\sigma} c_{d\mu} + h.c. \right) + \sum_{\mu} \varepsilon_\mu c^\dagger_{d\mu} c_{d\mu} \tag{4.1}$$

with $V_{k\eta\sigma,\mu} = t_{k\eta\sigma} R_{\sigma\mu}$. Recall that there are two different spin bases.

We are interested in calculating the dot Green's functions

$$G^R_{\mu\mu'}(t) = -i\theta(t) \left\langle \left\{ c_{d\mu}(t), c^\dagger_{d\mu'} \right\} \right\rangle , \tag{4.2}$$

with $\mu = \uparrow, \downarrow$ being the spin in the dot basis and to do so we apply the equation of motion technique. The operator $c_{d\mu}(t)$ in Eq. (4.2) is written in the Heisenberg picture of quantum mechanics, so the time evolution of an operator A is given by the Heisenberg equation

$$\dot{A}(t) = i \left[H, A(t) \right] , \tag{4.3}$$

when the operator has no explicit time dependence. The time derivative of $G^R_{\mu\mu'}(t)$ is therefore

$$i\partial_t G^R_{\mu\mu'}(t) = \delta(t)\delta_{\mu\mu'} - i\theta(t) \left\langle \left\{ \left[c_{d\mu}, H \right](t), c^\dagger_{d\mu'} \right\} \right\rangle . \tag{4.4}$$

The commutator between $c_{d\mu}$ and H is

$$[c_\mu, H] = \varepsilon_\mu c_\mu + \sum_{k\eta\sigma} V^*_{k\eta\sigma,\mu} c_{k\eta\sigma} \tag{4.5}$$

so when inserted in Eq. (4.4) we get

$$\left(i\partial_t - \varepsilon_\mu\right) G^R_{\mu\mu'}(t) = \delta(t)\delta_{\mu\mu'} + \sum_{k\eta\sigma} V^*_{k\eta\sigma,\mu} G^R_{k\eta\sigma,\mu'}(t), \tag{4.6}$$

where the new Green's function

$$G^R_{k\eta\sigma,\mu'}(t) = -i\theta(t) \left\langle \left\{ c_{k\eta\sigma}(t), c^\dagger_{d\mu'} \right\} \right\rangle \tag{4.7}$$

has been introduced. As for $G^R_{\mu\mu'}(t)$ the equation of motion can be found

$$(i\partial_t - \varepsilon_{k\eta\sigma}) G^R_{k\eta\sigma,\mu'}(t) = \sum_{\mu_1} V_{k\eta\sigma,\mu_1} G^R_{\mu_1\mu'}(t), \tag{4.8}$$

and after a Fourier transformation and rearranging the terms we obtain[i]

$$G^R_{k\eta\sigma,\mu'}(\omega) = \sum_{\mu_1} \frac{V_{k\eta\sigma,\mu_1}}{\omega - \varepsilon_{k\eta\sigma} + i0^+} G^R_{\mu_1\mu'}(\omega). \tag{4.9}$$

After a Fourier transformation of Eq. (4.6) the expression for $G^R_{k\eta\sigma,\mu'}(\omega)$ can be inserted and we get

$$(\omega - \varepsilon_\mu + i0^+) G^R_{\mu\mu'}(\omega) = \delta_{\mu\mu'} + \sum_{k\eta\sigma,\mu_1} \frac{V^*_{k\eta\sigma,\mu} V_{k\eta\sigma,\mu_1}}{\omega - \varepsilon_{k\eta\sigma} + i0^+} G^R_{\mu_1\mu'}(\omega). \tag{4.10}$$

Introducing the so-called retarded self-energy matrix $\mathbf{\Sigma}^R$ with the $\mu\mu_1$ entry

$$\Sigma^R_{\mu\mu_1} = \sum_{k\eta\sigma} \frac{V^*_{k\eta\sigma,\mu} V_{k\eta\sigma,\mu_1}}{\omega - \varepsilon_{k\eta\sigma} + i0^+}, \tag{4.11}$$

we can write Eq. (4.10) on matrix form as

$$\mathbf{G}^{R,-1}_0(\omega)\mathbf{G}^R(\omega) = \mathbf{1} + \mathbf{\Sigma}^R\mathbf{G}^R, \tag{4.12}$$

where $\mathbf{G}^{R,-1}_0(\omega)$ is the inverse Green's function for the isolated dot ($H_T = 0$) which is[1]

$$G^{R,-1}_{0,\mu\mu'}(\omega) = (\omega - \varepsilon_\mu + i0^+)\delta_{\mu\mu'}. \tag{4.13}$$

[i]The term $i0^+$ is a factor to ensure convergence.

In Eq. (4.12) we notice the Dyson equation structure known from time-dependent perturbation theory, which gives the iterative form

$$\mathbf{G}^R = \mathbf{G}_0^R + \mathbf{G}_0^R\mathbf{\Sigma}^R\mathbf{G}^R = \mathbf{G}_0^R + \mathbf{G}_0^R\mathbf{\Sigma}^R\mathbf{G}_0^R + \mathbf{G}_0^R\mathbf{\Sigma}^R\mathbf{G}_0^R\mathbf{\Sigma}^R\mathbf{G}_0^R + \dots \tag{4.14}$$

of the Green's function. Due to this form scattering processes are included to all orders through the self-energy. In case of no coupling between the dot and the leads the self-energy vanishes and we find that the Green's function is of course equal to the one for an isolated dot.

To proceed we need to calculate the expression for the self-energy, where we after splitting up the coupling matrix elements obtain

$$\Sigma^R_{\mu\mu'} = \sum_{\eta\sigma} R^*_{\sigma\mu} R_{\sigma\mu'} \sum_k \frac{|t_{k\eta\sigma}|^2}{\omega - \varepsilon_{k\eta\sigma} + i0^+}. \tag{4.15}$$

Applying the trick $\sum_k F(\varepsilon_k) = \int d\varepsilon \sum_k F(\varepsilon)\delta(\varepsilon - \varepsilon_k)$ and introducing the coupling parameter $\Gamma^\eta_\sigma(\varepsilon) = 2\pi \sum_k |t_{k\eta\sigma}|^2 \delta(\varepsilon - \varepsilon_{k\eta\sigma})$ we can write the self-energy as

$$\begin{aligned} \Sigma^R_{\mu\mu'} &= \sum_{\eta\sigma} R^*_{\sigma\mu} R_{\sigma\mu'} \int d\varepsilon \sum_k \frac{|t_{k\eta\sigma}|^2}{\omega - \varepsilon + i0^+} \delta(\varepsilon - \varepsilon_{k\eta\sigma}) \\ &= \sum_{\eta\sigma} R^*_{\sigma\mu} R_{\sigma\mu'} \int \frac{d\varepsilon}{2\pi} \frac{\Gamma^\eta_\sigma(\varepsilon)}{\omega - \varepsilon + i0^+}. \end{aligned} \tag{4.16}$$

The coupling parameter $\Gamma^\eta_\sigma(\varepsilon)$ can after a change from sum to integral be written as

$$\begin{aligned} \Gamma^\eta_\sigma(\varepsilon) &= 2\pi \int d\varepsilon_k \; \rho_{\eta\sigma}(\varepsilon_k) |t_{\eta\sigma}(\varepsilon_k)|^2 \delta(\varepsilon - \varepsilon_k) \\ &= 2\pi \rho_{\eta\sigma}(\varepsilon) |t_{\eta\sigma}(\varepsilon)|^2, \end{aligned} \tag{4.17}$$

where $\rho_{\eta\sigma}(\varepsilon)$ is the density of states for electron in the lead η with spin σ.
In order to progress from Eq. (4.16) it is necessary to assume that $\Gamma^\eta_\sigma(\varepsilon)$ is independent of energy, which from Eq. (4.17) implies that the density of states and the tunnelling matrix elements are constant.
The approximation is known as the Wide Band Limit and it will be used several times in the following chapters. To determine the size and energy dependence of Γ^η_σ requires more involved calculations and is in particular difficult in nonequilibrium. One way to proceed is to determine the electron structure for the leads and the molecule in equilibrium by a Density Functional Theory (DFT) calculation, and then assume that the results also can be applied to nonequilibrium in some cases, e.g. for low bias voltage or weak coupling.

In the Wide Band Limit and using $\frac{1}{\omega + i0^+} = \mathcal{P}\int \frac{1}{\omega} - i\pi\delta(\omega)$ (where $\mathcal{P}$ means principal integral) the self-energy in Eq. (4.16) becomes

$$\Sigma^R_{\mu\mu'} = -\frac{i}{2} \sum_{\eta\sigma} R^*_{\sigma\mu} R_{\sigma\mu'} \Gamma^\eta_\sigma, \tag{4.18}$$

or in matrix form

$$\mathbf{\Sigma}^R = -\frac{i}{2}\sum_\eta \begin{pmatrix} \Gamma^\eta_{\uparrow'}\cos^2\frac{\theta}{2} + \Gamma^\eta_{\downarrow'}\sin^2\frac{\theta}{2} & (\Gamma^\eta_{\uparrow'} - \Gamma^\eta_{\downarrow'})\cos\frac{\theta}{2}\sin\frac{\theta}{2} \\ (\Gamma^\eta_{\uparrow'} - \Gamma^\eta_{\downarrow'})\cos\frac{\theta}{2}\sin\frac{\theta}{2} & \Gamma^\eta_{\uparrow'}\sin^2\frac{\theta}{2} + \Gamma^\eta_{\downarrow'}\cos^2\frac{\theta}{2} \end{pmatrix} \equiv -\frac{i}{2}\tilde{\mathbf{\Gamma}}. \tag{4.19}$$

We notice that the coupling matrix $\tilde{\mathbf{\Gamma}} = \tilde{\mathbf{\Gamma}}^L + \tilde{\mathbf{\Gamma}}^R$ is nothing but the the coupling matrix $\Gamma_{\sigma\sigma'} = \delta_{\sigma\sigma'}\Gamma_\sigma$ expressed in the dot spin basis.

The expression Eq. (4.19) can be inserted in Eq. (4.12) an the Green's function can be determined, but instead we will exploit the assumption that the leads are fully polarized, meaning that there is no spin- $\downarrow'$ electrons in the leads and consequently $\Gamma^L_{\downarrow'} = \Gamma^R_{\downarrow'} = 0$. The self-energy simplifies and we finally have an expression for the Green's function

$$\mathbf{G}^R(\omega) = \left(\mathbf{G}_0^{R,-1} - \mathbf{\Sigma}^R\right)^{-1} \tag{4.20}$$

with

$$\mathbf{\Sigma}^R = -\frac{i}{2}\left(\Gamma^L_{\uparrow'} + \Gamma^R_{\uparrow'}\right)\begin{pmatrix} \cos^2\frac{\theta}{2} & \cos\frac{\theta}{2}\sin\frac{\theta}{2} \\ \cos\frac{\theta}{2}\sin\frac{\theta}{2} & \sin^2\frac{\theta}{2} \end{pmatrix}. \tag{4.21}$$

4.1 Calculation of the current in linear response

After having derived the expression for Green's function we are able to apply the general current formula from Sec. 3.5

$$J = \frac{ie}{\hbar}\frac{\lambda}{1+\lambda}\int\frac{d\omega}{2\pi}\mathrm{Tr}\left[\tilde{\mathbf{\Gamma}}^R(\omega)\left(\mathbf{G}^R(\omega) - \mathbf{G}^A(\omega)\right)\right]\left[f_L(\omega) - f_R(\omega)\right] \tag{4.22}$$

which is valid in case of proportionate couplings $\tilde{\mathbf{\Gamma}}^L = \lambda\tilde{\mathbf{\Gamma}}^R$. Notice that the Green's functions and $\tilde{\mathbf{\Gamma}}^R$ are given in the same basis.[ii]
In the Wide Band Limit $\tilde{\mathbf{\Gamma}}^R$ is assumed energy independent and the integral can be carried out numerically. However, instead we derive the linear response result which in some limits can be found analytically.

In linear response it is assumed that the bias voltage eV is small, so only the lowest order term in the expansion of the Fermi functions needs to be kept. In Sec. 2.1 we have defined the chemical potentials to be situated at $\mu_L = \frac{eV}{2}$ and $\mu_R = -\frac{eV}{2}$ so we obtain

$$f_L(\omega) - f_R(\omega) = f\left(\omega - \frac{eV}{2}\right) - f\left(\omega + \frac{eV}{2}\right) \approx -eV\frac{\partial f(\omega)}{\partial\omega}. \tag{4.23}$$

At low temperatures the derivative of the Fermi function tends to $\delta(\omega)$, which is inserted in Eq. (4.22) to give[iii]

$$J = \frac{-ie^2V}{2\pi\hbar}\frac{\lambda}{1+\lambda}\mathrm{Tr}\left[\tilde{\mathbf{\Gamma}}^R\left(\mathbf{G}^R(0) - \mathbf{G}^A(0)\right)\right]. \tag{4.24}$$

[ii] In the next chapter we will derive a current formula which is valid for arbitrary couplings in case of noninteracting electrons on the dot, see Eq. (5.11).

[iii] The assumption of low temperatures is reasonable if the Green's function can be considered as constant in an interval of the size k_bT around $\mu = 0$.

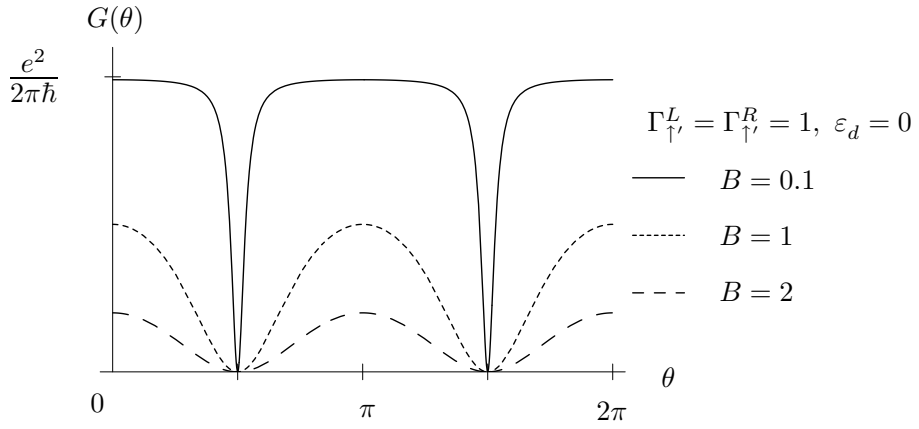

Figure 4.1: The conductance found from Eq. (4.25) is plotted for different values of the magnetic field strength B.

If we furthermore assume that the dot energy level in case of no magnetic field, ε_d, is fixed at the equilibrium chemical potential of the leads $\mu = 0$, the energy levels of the dot with the applied magnetic field are $\varepsilon_\downarrow = -\varepsilon_\uparrow = B$.

With these approximations an analytic expression for the Green's function $\mathbf{G}^R(0)$ can be obtained after some algebra (see Sec. A.2). When we recall that $\mathbf{G}^A = (\mathbf{G}^R)^\dagger$ the trace can be carried out and we finally arrive at

$$J = e^2 V \frac{\Gamma^L_{\uparrow'}\Gamma^R_{\uparrow'}}{2\pi\hbar} \frac{4\cos^2\theta}{4B^2 + \Gamma^2_{\uparrow'}\cos^2\theta}, \qquad \Gamma_{\uparrow'} = \Gamma^L_{\uparrow'} + \Gamma^R_{\uparrow'}. \tag{4.25}$$

which is the linear response result for the current in case of noninteracting electrons on the dot, $\varepsilon_d = 0$, low temperature, fully polarized leads and proportionate couplings.[iv]
In Fig. 4.3 the conductance $G = \frac{dJ}{dV}$ is plotted versus the angle θ for various values of the magnetic field strength B. Note that the maximum value of the conductance

$$G_{\max} = \frac{e^2\Gamma^L_{\uparrow'}\Gamma^R_{\uparrow'}}{2\pi\hbar} \frac{4}{4B^2 + \Gamma^2_{\uparrow'}} \tag{4.26}$$

decreases for increasing B because the dot levels are moved away from the chemical potentials of the leads. Moreover, the angular dependence tends to $\cos^2\theta$ for $B \gg \Gamma_{\uparrow'}$, and the conductance is almost independent of θ for $B \ll \Gamma_{\uparrow'}$ except for a small interval around the angles $\pi/2$ and $3\pi/2$. Both limits are easily understood by considering Eq. (4.25).

The interesting feature in the angular dependence is the anti-resonances at $\pi/2$ (and $3\pi/2$). We interpret them as a resonance phenomenon which can be explained by considering the various conduction channels through the central region.

[iv] The result for $\varepsilon_d \neq 0$ is found in Sec. A.2.

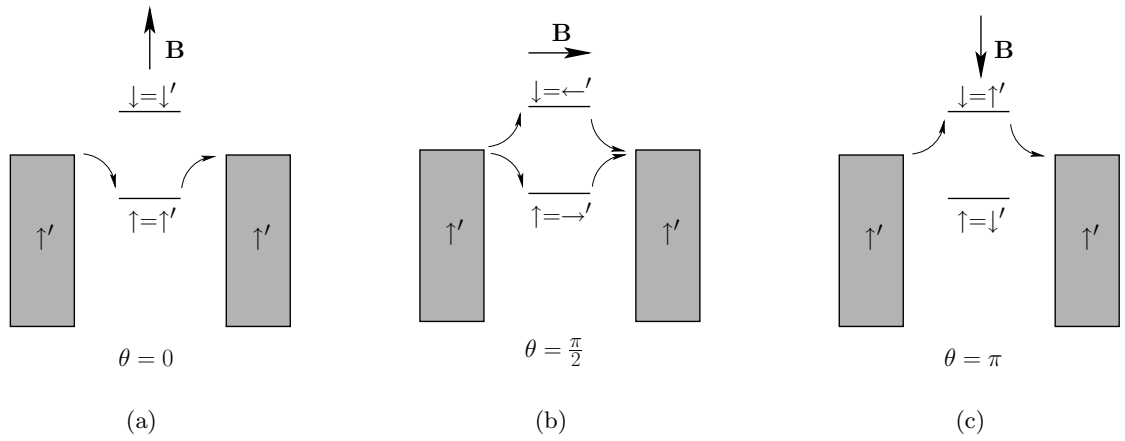

Figure 4.2: A schematic drawing of the tunnelling processes for three different angles. The spin of the dot electrons are written in both the (unprimed) dot basis and the (primed) lead basis. For $\theta = \pi/2$ the superposition of lead spin states $|\rightarrow'\rangle = \frac{1}{\sqrt{2}}(|\uparrow'\rangle + |\downarrow'\rangle)$ and $|\leftarrow'\rangle = \frac{1}{\sqrt{2}}(-|\uparrow'\rangle + |\downarrow'\rangle)$ have been introduced.

We start with $\theta = 0$. In this case the spin basis for the dot is identical to the lead spin basis. The electrons can tunnel through the central region only via the $\uparrow$=$\uparrow'$-level, because the conduction channel through the $\downarrow$=$\downarrow'$-level is blocked (see Fig. 4.2(a)). For $\theta = \pi$ is the $\uparrow$=$\downarrow'$-level blocked and the current flows through the $\downarrow$=$\uparrow'$-level, see Fig. 4.2(c).
At $\theta = \frac{\pi}{2}$ is $|\uparrow\rangle = \frac{1}{\sqrt{2}}(|\uparrow'\rangle + |\downarrow'\rangle)$ and $|\downarrow\rangle = \frac{1}{\sqrt{2}}(-|\uparrow'\rangle + |\downarrow'\rangle)$ so the electrons can tunnel through the dot via both levels as shown in Fig. 4.2(b). The superposition of the tunnelling amplitude from the two paths give rise to the destructive interference resulting in the anti-resonances at $\frac{\pi}{2}$ and $\frac{3\pi}{2}$.
The resonance phenomenon will be further discussed in Chap. 9 where we consider the co-tunnelling results for different values of the interaction on the dot, U.
The conductance is also calculated when the bare dot energy ε_d is away from resonance using Eqs. (4.20) and (4.24), see Fig. 4.3. For $\varepsilon_d \neq 0$ almost the same angular dependence as for $\varepsilon_d = 0$ is observed but the conductance at the points $\theta = 0$ and $\theta = \pi$ is changed, because the energy of the open channel is moved relative to the chemical potentials of the leads. Furthermore, the anti-resonance points are slightly shifted.
In [5] it is shown that the anti-resonances also exist in case of not fully polarized leads, but the resonance effect gets smeared out, i.e. the conductance is finite at the anti-resonance points. A finite temperature has the same effect.

For the case of noninteracting electrons on the dot a current formula can be derived for arbitrary coupling to the leads, i.e. the current can be calculated with antiparallel magnetizations of the leads [16]. The results are presented in the next chapter.

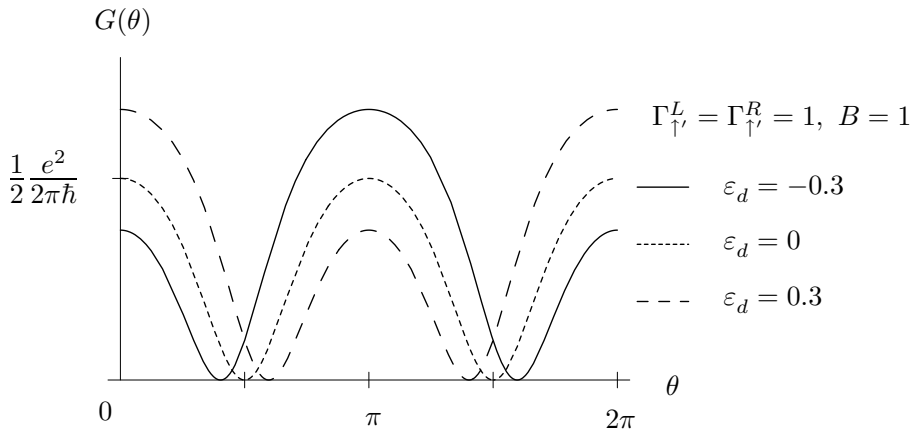

Figure 4.3: Using Eqs. (4.20) and (4.24) the conductance is plotted for various values of the bare dot energy ε_d.

Chapter 5

The FAB model without interactions (antiparallel)

In the previous chapter we considered the FAB model in case of parallel magnetizations of the leads and no interactions on the dot. The current was calculated with a current formula which is valid only in case of proportionate couplings. However, in case of noninteracting electrons on the dot ($U = 0$) the current formula in Eq. (3.76) can be simplified even for arbitrary magnetizations of the leads, as we will show in this chapter. Afterwards, the current is calculated for the noninteracting FAB model with antiparallel magnetizations of the leads.

5.1 Current formula

We start by deriving a current formula which is valid when the electrons on the dot are noninteracting.[i] The derivation is only sketched, but it is very similar to the derivation of the current formula in Sec. 3.5, and the starting point is Eq. (3.76). We want to show that for noninteracting electrons an expression for $\mathbf{G}^<$ can be obtained in terms of the advanced and retarded Green's functions.

In Chap. 4 a Dyson equation for the retarded nonequilibrium Green's function G^R was obtained (see Eq. (4.14)). In equilibrium the same Dyson equation is found for a general time-ordered dot Green's function using the equation of motion technique,

$$\mathbf{G}^t = \mathbf{G}_0^t + \mathbf{G}_0^t \mathbf{\Sigma}^t \mathbf{G}^t, \tag{5.1}$$

where the integration over the internal time variables have been suppressed. $\mathbf{G}_0^t$ is the time-ordered Green' function in absence of tunnelling and the self-energy is

$$\Sigma_{nm}^t(t,t') = \sum_{k\eta} V_{k\eta,n}^* V_{k\eta,m} g_{k\eta}^t(t,t'), \tag{5.2}$$

[i] The current formula was first derived in [16]

with $g^t_{k\eta}(t,t')$ being the time-ordered Green's function for the isolated lead η. The key point in the derivation in case of noninteracting electrons on the dot is the explicit expression for the self-energy in Eq. (5.2). Unfortunately a similar one cannot be found for interacting electrons.

Like when deriving the current formula in Sec. 3.5 we exploit that the contour-ordered nonequilibrium Green's function have the same form as $\mathbf{G}^t$ and therefore satisfies the same Dyson equation

$$\mathbf{G}^C = \mathbf{G}_0^C + \mathbf{G}_0^C \mathbf{\Sigma}^C \mathbf{G}^C. \tag{5.3}$$

The curve C is showed in Fig. 3.1[ii], and with the same arguments as in Sec. 3.5 it is transformed into the Keldysh contour C_K, see Fig. 3.4. Applying the rules for analytic continuation from Sec. 3.4 on the previous equation gives

$$\mathbf{G}^< = \mathbf{G}_0^< + \mathbf{G}_0^R \mathbf{\Sigma}^R \mathbf{G}^< + \mathbf{G}_0^R \mathbf{\Sigma}^< \mathbf{G}^A + \mathbf{G}_0^< \mathbf{\Sigma}^A \mathbf{G}^A, \tag{5.4}$$

which after iteration can be brought on the form[iii]

$$\mathbf{G}^< = (\mathbf{1} + \mathbf{G}^R \mathbf{\Sigma}^R)\mathbf{G}_0^<(\mathbf{1} + \mathbf{\Sigma}^A \mathbf{G}^A) + \mathbf{G}^R \mathbf{\Sigma}^< \mathbf{G}^A. \tag{5.5}$$

From Eq. (5.3) an expression for the retarded Green's function can also be found, and after rearranging the terms we get $\mathbf{1} + \mathbf{\Sigma}^R \mathbf{G}^R = \mathbf{G}^R (\mathbf{G}_0^R)^{-1}$. For noninteracting electrons on the isolated dot holds $[(G_0^R)^{-1}]_{nm} = \delta_{nm}(i\partial_t - \varepsilon_n)$, leading to $(\mathbf{G}_0^R)^{-1}\mathbf{G}_0^< = 0$, which is easily verified. So for $U = 0$ the first term in Eq. (5.5) vanishes and therefore

$$\mathbf{G}^< = \mathbf{G}^R \mathbf{\Sigma}^< \mathbf{G}^A. \tag{5.6}$$

The expression for the greater Green's function is found by interchanging ¡ with ¿.

Recall that in Eq. (5.6) is the integration over the internal time variables suppressed. In steady state do the Green's functions only depend on the difference between the time-arguments, so after performing a Fourier transformation and applying the convolution theorem for Fourier transforms (see Sec. A.1.4) we find in Fourier space

$$\mathbf{G}^<(\omega) = \mathbf{G}^R(\omega)\mathbf{\Sigma}^<(\omega)\mathbf{G}^A(\omega). \tag{5.7}$$

The lesser self-energy in Fourier space is easily found using Eqs. (5.2) and (A.28), and after introducing the coupling parameter $\Gamma^\eta_{mn}(\omega)$ from Eq. (3.74) we get

$$\mathbf{G}^<(\omega) = i f_L(\omega)\mathbf{G}^R(\omega)\mathbf{\Gamma}^L(\omega)\mathbf{G}^A(\omega) + i f_R(\omega)\mathbf{G}^R(\omega)\mathbf{\Gamma}^R(\omega)\mathbf{G}^A(\omega). \tag{5.8}$$

The lesser Green's function is now expressed in terms of the retarded and advanced Green's functions, but the expression can be further simplified.
The greater Green's function is found in the same way as the lesser function,

$$\mathbf{G}^>(\omega) = -i[1 - f_L(\omega)]\mathbf{G}^R(\omega)\mathbf{\Gamma}^L(\omega)\mathbf{G}^A(\omega) - i[1 - f_R(\omega)]\mathbf{G}^R(\omega)\mathbf{\Gamma}^R(\omega)\mathbf{G}^A(\omega), \tag{5.9}$$

[ii] With the same arguments as when deriving the current formula in Sec. 3.5 we neglect the initial correlations between the electrons.

[iii] Eq. (5.5) is called the Keldysh quantum kinetic equation.

and using the property $\mathbf{G}^{>} - \mathbf{G}^{<} = \mathbf{G}^{R} - \mathbf{G}^{A}$ we obtain from Eqs. (5.8) and (5.9)

$$\mathbf{G}^{R}(\omega) - \mathbf{G}^{A}(\omega) = -i\mathbf{G}^{R}(\omega)\left[\mathbf{\Gamma}^{L}(\omega) + \mathbf{\Gamma}^{L}(\omega)\right]\mathbf{G}^{A}(\omega). \tag{5.10}$$

The expressions in Eqs. (5.8) and (5.10) is inserted in Eq. (3.76) and we finally arrive at

$$J = \frac{e}{\hbar}\int \frac{d\omega}{2\pi}\mathrm{Tr}\left[\mathbf{G}^{A}(\omega)\mathbf{\Gamma}^{R}(\omega)\mathbf{G}^{R}(\omega)\mathbf{\Gamma}^{L}(\omega)\right]\left\{f_{L}(\omega) - f_{R}(\omega)\right\} \tag{5.11}$$

which is the current formula in case of noninteracting electrons on the dot and arbitrary magnetizations of the leads.

5.2 Calculation of the current in linear response

In Chap. 4 an expression for the retarded Green's function for the FAB model was obtained. In case of arbitrary magnetization of the leads we found

$$\mathbf{G}^{R}(\omega) = \left(\mathbf{G}_{0}^{R,-1} - \mathbf{\Sigma}^{R}\right)^{-1}, \tag{5.12}$$

with the self-energy

$$\mathbf{\Sigma}^{R} = -\frac{i}{2}\sum_{\eta}\begin{pmatrix} \Gamma^{\eta}_{\uparrow'}\cos^{2}\frac{\theta}{2} + \Gamma^{\eta}_{\downarrow'}\sin^{2}\frac{\theta}{2} & (\Gamma^{\eta}_{\uparrow'} - \Gamma^{\eta}_{\downarrow'})\cos\frac{\theta}{2}\sin\frac{\theta}{2} \\ (\Gamma^{\eta}_{\uparrow'} - \Gamma^{\eta}_{\downarrow'})\cos\frac{\theta}{2}\sin\frac{\theta}{2} & \Gamma^{\eta}_{\uparrow'}\sin^{2}\frac{\theta}{2} + \Gamma^{\eta}_{\downarrow'}\cos^{2}\frac{\theta}{2} \end{pmatrix}. \tag{5.13}$$

Now both leads are assumed fully polarized, but having the magnetizations in opposite directions. We define that the left lead contains only spin-$\uparrow'$ electrons and the right only spin-$\downarrow'$ electrons, so the coupling matrices are in the lead spin basis

$$\mathbf{\Gamma}^{L} = \begin{pmatrix} \Gamma^{L}_{\uparrow'} & 0 \\ 0 & 0 \end{pmatrix}, \qquad \mathbf{\Gamma}^{R} = \begin{pmatrix} 0 & 0 \\ 0 & \Gamma^{R}_{\downarrow'} \end{pmatrix}. \tag{5.14}$$

Transforming them to the dot spin basis using $\mathbf{R}(\theta)$ from Eq. (2.7) gives

$$\tilde{\mathbf{\Gamma}}^{L} = \Gamma^{L}_{\uparrow'}\begin{pmatrix} \cos^{2}\frac{\theta}{2} & \cos\frac{\theta}{2}\sin\frac{\theta}{2} \\ \cos\frac{\theta}{2}\sin\frac{\theta}{2} & \sin^{2}\frac{\theta}{2} \end{pmatrix}, \qquad \tilde{\mathbf{\Gamma}}^{R} = \Gamma^{R}_{\downarrow'}\begin{pmatrix} \sin^{2}\frac{\theta}{2} & -\cos\frac{\theta}{2}\sin\frac{\theta}{2} \\ -\cos\frac{\theta}{2}\sin\frac{\theta}{2} & \cos^{2}\frac{\theta}{2} \end{pmatrix}, \tag{5.15}$$

and the self-energy can now be expressed as

$$\mathbf{\Sigma}^{R} = -\frac{i}{2}\left(\tilde{\mathbf{\Gamma}}^{L} + \tilde{\mathbf{\Gamma}}^{R}\right). \tag{5.16}$$

Again we are only interested in the linear response result and replace $f_{L}(\omega) - f_{R}(\omega)$ in Eq. (5.11) with $-eV\frac{\partial f(\omega)}{\partial\omega}$, and finally we use $\mathbf{G}^{A}(\omega) = \left[\mathbf{G}^{R}(\omega)\right]^{\dagger}$ to find the advanced Green's function.

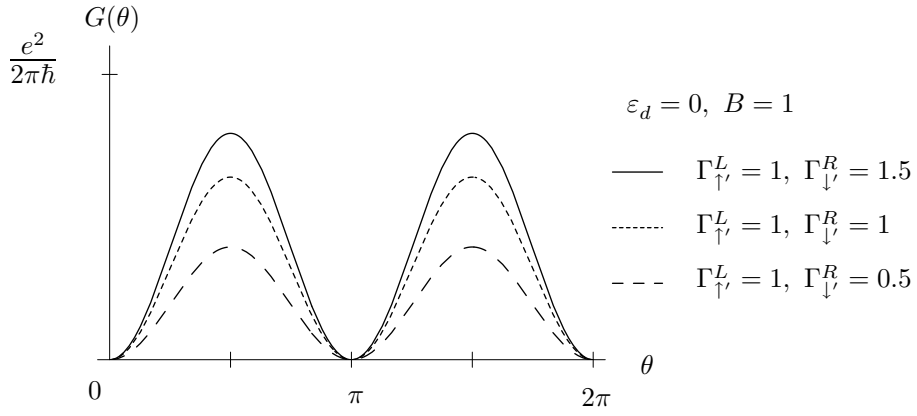

Figure 5.1: The Green's function result for the conductance. ($U = 0$). The results are plotted for $\varepsilon_d = 0$ and with different values for the coupling to the leads.

From the above equations the current can be calculated in the Wide Band Limit[iv] using Eq. (5.11). In linear response and at zero temperature we obtain

$$J(\theta) = e^2 V \frac{\Gamma^L_{\uparrow'}\Gamma^R_{\downarrow'}}{2\pi\hbar} \frac{16B^2 \sin^2\theta}{\Upsilon(\theta)}, \tag{5.17}$$

where Υ is

$$\begin{aligned}\Upsilon(\theta) = 16B^2 + B^2(8\Gamma^L_{\uparrow'}\Gamma^R_{\downarrow'} - 32\varepsilon_d^2) + [4\varepsilon_d^2 + (\Gamma^L_{\uparrow'})^2][4\varepsilon_d^2 + (\Gamma^R_{\downarrow'})^2] \\ + 4B\cos\theta(\Gamma^L_{\uparrow'} - \Gamma^R_{\downarrow'})[2\varepsilon_d(\Gamma^L_{\uparrow'} + \Gamma^R_{\downarrow'}) + B(\Gamma^L_{\uparrow'} - \Gamma^R_{\downarrow'})\cos\theta].\end{aligned} \tag{5.18}$$

For $\varepsilon_d = 0$ the expression simplifies to

$$J(\theta) = e^2 V \frac{\Gamma^L_{\uparrow'}\Gamma^R_{\downarrow'}}{2\pi\hbar} \frac{16B^2 \sin^2\theta}{(4B^2 + \Gamma^L_{\uparrow'}\Gamma^R_{\downarrow'})^2 + 4B^2(\Gamma^L_{\uparrow'} - \Gamma^R_{\downarrow'})^2\cos^2\theta}. \tag{5.19}$$

The current expression for antiparallel magnetizations of the leads is far more complicated than for parallel magnetizations.
If we assume $\varepsilon_d = 0$ and $\Gamma^L_{\uparrow'} = \Gamma^R_{\downarrow'}$ we get from Eq. (5.19) that $J(\theta) \propto \sin^2\theta$. This can be understood by considering Fig. 4.2, but with spin-$\downarrow'$ electrons in the right lead. For $\theta = 0$ (π) both conductance channels are closed because the leads have opposite magnetizations. For $\theta = \frac{\pi}{2}$ is the dot spin state a superposition of spin-$\uparrow'$ and spin-$\downarrow'$ which allows tunnelling.
The same behaviour is seen for $\varepsilon_d \neq 0$ and $\Gamma^L_{\uparrow'} \neq \Gamma^R_{\downarrow'}$.

A peculiar feature is the existence of an optimal value for the magnetic field strength B which is different from zero. Consider $\varepsilon_d = 0$. For a given value of B is the maximum

[iv] See Chap. 4.

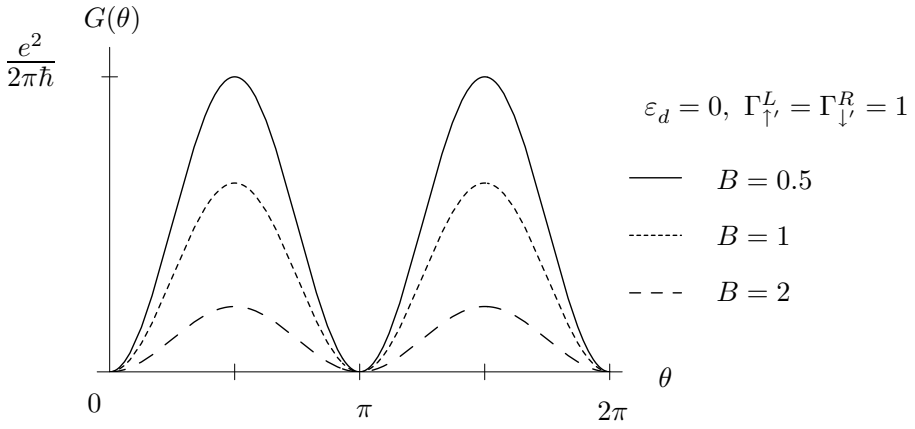

Figure 5.2: The conductance calculated using Green's functions ($U = 0$). The results are plotted for $\varepsilon_d = 0$, $\Gamma^L_{\uparrow'} = \Gamma^R_{\downarrow'} = 1$ and different values for the magnetic field strength B.

current ($\theta = \frac{\pi}{2}$)

$$J_{\max}(B) = e^2 V \frac{\Gamma^L_{\uparrow'}\Gamma^R_{\downarrow'}}{2\pi\hbar} \frac{16B^2}{(4B^2 + \Gamma^L_{\uparrow'}\Gamma^R_{\downarrow'})^2}. \tag{5.20}$$

Finding the maximum with respect to B gives the optimal value

$$B_{\text{opt}} = \sqrt{\frac{\Gamma^L_{\uparrow'}\Gamma^R_{\downarrow'}}{4}}. \tag{5.21}$$

No such value was found in case of parallel magnetization of the leads, where the current decreased monotonically when increasing B (see Eq. (4.26)). Moreover, for antiparallel magnetizations the current vanishes for $B = 0$.
The feature can be explained as a competition between two different effects. The conductance vanishes for $B = 0$ due to spin blockade because the spin states on the dot are identical to the lead spin states, which excludes tunnelling. For large values of B the dot energy levels are far from the chemical potentials of the leads which suppress tunnelling, and the conductances decreases as $\frac{1}{B^2}$ (see Eq. (5.20)).
Therefore is the optimal value a compromise between the two effects. It is not seen for the parallel geometry where tunnelling is allowed even for $B = 0$ because of the equal magnetizations of the leads.

We return to the antiparallel geometry in Sec. 9.3, where we using a scattering formalism can find the conductance in presence of interactions on the dot, but only if one state is always occupied and the other always empty, i.e. B much larger than the coupling strength.

Chapter 6

Unified description of tunnelling through QDs

In Chap. 4 it was shown how the retarded Green's function for the dot and therefore the current can be found for the FAB model, but only when the Coulomb repulsion on the dot is neglected. In case of Coulomb repulsion the equation of motion generates an infinite number of new Green's functions, which is a well known problem when working with the Anderson Hamiltonian[i].
For the Anderson model one way to deal with this is to apply a mean-field approximation as in [1], where the Coulomb repulsion term in the Hamiltonian is replaced with

$$H_U^{\mathrm{MF}} = U \left\langle n_{d\uparrow} \right\rangle n_{d\downarrow} + U \left\langle n_{d\downarrow} \right\rangle n_{d\uparrow} - U \left\langle n_{d\downarrow} \right\rangle \left\langle n_{d\uparrow} \right\rangle . \tag{6.1}$$

The series of equations of motion close with this approximation and a result can be obtain. However, this approach is not successful when dealing with a tunnelling setup like the FAB model. In the Coulomb blockade regime where U is large, the probability for an electron entering the dot depends on whether the dot is already occupied or not, and not on the mean occupation of the dot [1].

Alternatively one can apply the original Anderson Hamiltonian and generate new Green's functions, and then use some physical insight in the problem to close the equations. This allows for a description which goes beyond the mean-field approximation.
In [5] it is shown how the series of equations for the FAB model could be closed for a finite U using an approximation scheme as in the paper by Meir, Wingreen and Lee [8]. When solving the equations the limit $U \to \infty$ had to be taken because it allowed for considerable simplifications.[ii].

In this chapter we present a general formalism for writing up the equation of motion for the retarded Green's function of a generic system consisting of a quantum dot contacted to

[i] The Anderson Hamiltonian is introduced in Sec. 2.1.
[ii] There is still some discussion about the results obtained.

two leads. The method will be referred to as the unified description. With this approach an expression for the retarded dot Green's function for the FAB model can be found, even for a nonzero U. The derivation of the method is from [6], but here more details are added.

6.1 Derivation of the retarded Green's function

The basic assumption in the the procedure is knowledge about the eigenstates and eigenenergies of the central region. A similar approach is used in other branches of physics. An example is high-T_C superconductors in the Hubbard model where new fermion- and boson-like operators are introduced. These so-called "slave"-operators or "slave"-particles forms a new algebra and are directly linked to the eigenstates of the atoms.[iii]

For our tunnelling model the aim is to find the equation of motion for the retarded Green's function of the dot by generating a series of coupled equations. At a certain level in the calculations two particle Green's functions occur, which generates new higher-order Green's functions. To close the equations an approximation scheme similar to Meir, Wingreen and Lee [8] is invoked. It relies on weak dot-lead coupling which implies that the leads can be considered as unaffected by the coupling to the dot and therefore treated as non-interacting electron gasses. Furthermore, it is assumed that correlations between the leads and the dot vanish. With these approximations rather compact expressions for the Green's functions are obtained.

If the eigenstates and eigenenergies of the molecule are known we can write the Hamiltonian of the molecule as

$$H_{\text{dot}} = \sum_{\alpha} \varepsilon_{\alpha} |\alpha\rangle\langle\alpha| \tag{6.2}$$

where $|\alpha\rangle$ is a many-particle state of the molecule. If the state $|\alpha\rangle$ contains, lets say, N_α electrons it can be written on the form

$$|\alpha\rangle = \sum_{n_1,\ldots,n_{n_\alpha}} C_{n_1,\ldots,n_{n_\alpha}} c^\dagger_{dn_1} \ldots c^\dagger_{dn_{N_\alpha}} |0\rangle \tag{6.3}$$

where $c^\dagger_{dn_1}$ is the operator for creating an electron in the single-particle state n_1 on the dot.
The part of the Hamiltonian which connects the leads and the molecule has the form

$$H_T = \sum_{kn\eta} \left(t^*_{k\eta n} c^\dagger_{k\eta} c_{dn} + t_{k\eta n} c^\dagger_{dn} c_{k\eta} \right), \tag{6.4}$$

where $\eta = L, R$ corresponds to the left and right lead, respectively. $k\eta$ is supposed to be a collection of quantum numbers for an electron in the lead η.
The retarded Green's function for the dot is a matrix, where the nn'-entry is

$$G^R_{nn'}(t) = -i\theta(t) \left\langle \left\{ c_{dn}(t), c^\dagger_{dn'} \right\} \right\rangle. \tag{6.5}$$

[iii] See for instance [17] and references therein.

Now we take advantage of the knowledge about the eigenstates of the molecule, and insert a complete set of dot eigenstates $\sum_\alpha |\alpha\rangle\langle\alpha| = 1$ into H_T giving

$$H_T = \sum_{kn\eta,\alpha,\beta} \left(t^*_{k\eta n} c^\dagger_{k\eta} |\alpha\rangle\langle\beta| F_{\alpha\beta,n} + t_{k\eta n} c_{k\eta} |\alpha\rangle\langle\beta| F^*_{\alpha\beta,n} \right), \qquad F_{\alpha\beta,n} = \langle\alpha|c_{dn}|\beta\rangle. \tag{6.6}$$

Also for the retarded Green's function a complete set of dot states are inserted, and we find

$$G^R_{nn'}(t) = \sum_{\alpha\beta,\alpha'\beta'} F_{\alpha\beta,n} F^*_{\alpha'\beta',n'} G^R_{\alpha\beta,\alpha'\beta'}(t), \tag{6.7}$$

where the new auxiliary Green's functions are defined as

$$G^R_{\alpha\beta,\alpha'\beta'}(t) = -i\theta(t) \left\langle \left\{ \left(|\alpha\rangle\langle\beta| \right)(t), |\beta'\rangle\langle\alpha'| \right\} \right\rangle. \tag{6.8}$$

If we take a closer look at $|\alpha\rangle\langle\beta|$ it is seen that it is an annihilation operator. This is clear because it stems from $|\alpha\rangle\langle\alpha|d_n|\beta\rangle\langle\beta| = F_{\alpha\beta,n}|\alpha\rangle\langle\beta|$. $F_{\alpha\beta,n}$ is nonzero only if the many-particle state $|\beta\rangle$ can be written on the form $|\beta\rangle = d^\dagger_n|\alpha\rangle$, meaning that $|\beta\rangle$ is identical to $|\alpha\rangle$ except that it contains an extra n-electron. So the operator $|\alpha\rangle\langle\beta|$ removes one electron from the dot.
When dealing with operators like $|\gamma\rangle\langle\nu|$ it is important to be aware of what type of operator it is.

6.2 Equation of motion for $G^R_{\alpha\beta,\alpha'\beta'}$

As when we calculated the retarded Green's function for the FAB model in the limit $U = 0$, we will apply the equation of motion technique. Recall that the time-development of operators in the Heisenberg picture are given as

$$\dot{A}(t) = i\,[H, A(t)] \tag{6.9}$$

when the operator A has no explicit time-dependence.
We want to find the equation of motion for the auxiliary Green's functions defined in Eq. (6.8) and then insert the result in Eq. (6.7), where the Hamilton governing the time evolution is

$$\begin{aligned} H &= \sum_{k\eta} \xi_{k\eta} c^\dagger_{k\eta} c_{k\eta} + \sum_{kn\eta,\alpha,\beta} \left(t^*_{k\eta n} c^\dagger_{k\eta} |\alpha\rangle\langle\beta| F_{\alpha\beta,n} + h.c. \right) + \sum_\alpha E_\alpha |\alpha\rangle\langle\alpha| \\ &= H_C + H_T + H_{\text{dot}}. \end{aligned} \tag{6.10}$$

After calculating the commutator $[H, |\alpha\rangle\langle\beta|]$ the time derivative of the Green's function in Eq. (6.8) is

$$\left(i\partial_t + E_{\alpha\beta} \right) G^R_{\alpha\beta,\alpha'\beta'}(t) = \delta(t) \left\langle \left\{ |\alpha\rangle\langle\beta|, |\beta'\rangle\langle\alpha'| \right\} \right\rangle - L^R_{\alpha\beta,\alpha'\beta'}(t), \tag{6.11}$$

where $E_{\alpha\beta} \equiv \varepsilon_\alpha - \varepsilon_\beta$ and

$$L^R_{\alpha\beta,\alpha'\beta'}(t) = -i\theta(t) \left\langle \left\{ \left[H_T, |\alpha\rangle\langle\beta| \right], |\beta'\rangle\langle\alpha'| \right\} \right\rangle. \tag{6.12}$$

Writing out the commutator gives

$$\begin{aligned}\left[H_T, |\alpha\rangle\langle\beta|\right] = &\sum_{k\eta n\gamma} t^*_{k\eta n} c^\dagger_{k\eta} \left(F_{\gamma\alpha,n}|\gamma\rangle\langle\beta| + F_{\beta\gamma,n}|\alpha\rangle\langle\gamma|\right) \\ &- \sum_{k\eta n\nu} t_{k\eta n} c_{k\eta} \left(F^*_{\alpha\nu,n}|\nu\rangle\langle\beta| + F^*_{\nu\beta,n}|\alpha\rangle\langle\nu|\right),\end{aligned} \tag{6.13}$$

and from the F constants it is seen that $|\gamma\rangle\langle\beta|$ and $|\alpha\rangle\langle\gamma|$ corresponds to creation and annihilation of two dot electrons, respectively. Therefore they both commute with $c^\dagger_{k\eta}$ and $c_{k\eta}$, which has been used in Eq. (6.13). Likewise $|\nu\rangle\langle\beta|$ and $|\alpha\rangle\langle\nu|$ conserve the number of dot electrons and therefore also commute with the lead operators.

Introducing the new Green's functions

$$D^R_{k\eta,\gamma\beta\alpha'\beta'}(t) = -i\theta(t)\left\langle\left\{\left(c^\dagger_{k\eta}|\gamma\rangle\langle\beta|\right)(t), |\beta'\rangle\langle\alpha'|\right\}\right\rangle \tag{6.14}$$

$$E^R_{k\eta,\nu\beta\alpha'\beta'}(t) = -i\theta(t)\left\langle\left\{\left(c_{k\eta}|\nu\rangle\langle\beta|\right)(t), |\beta'\rangle\langle\alpha'|\right\}\right\rangle, \tag{6.15}$$

the function $L^R_{\alpha\beta,\alpha'\beta'}(t)$ becomes

$$\begin{aligned}L^R_{\alpha\beta,\alpha'\beta'}(t) = &\sum_{k\eta n\gamma} t^*_{k\eta n}\left(F_{\gamma\alpha,n} D^R_{k\eta,\gamma\beta\alpha'\beta'}(t) + F_{\beta\gamma,n} D^R_{k\eta,\alpha\gamma\alpha'\beta'}(t)\right) \\ &- \sum_{k\eta n\nu} t^*_{k\eta n}\left(F^*_{\gamma\nu,n} E^R_{k\eta,\nu\beta\alpha'\beta'}(t) + F^*_{\nu\beta,n} E^R_{k\eta,\alpha\nu\alpha'\beta'}(t)\right),\end{aligned} \tag{6.16}$$

and inserting this into the equation of motion for $G^R_{\alpha\beta\alpha'\beta'}(t)$ gives

$$\begin{aligned}(i\partial_t + E_{\alpha\beta}) G^R_{\alpha\beta\alpha'\beta'}(t) = &\delta(t)\left(\langle|\alpha\rangle\langle\alpha'|\rangle\,\delta_{\beta\beta'} + \langle|\beta'\rangle\langle\beta|\rangle\,\delta_{\alpha\alpha'}\right) \\ &- \sum_{k\eta n\gamma} t^*_{k\eta n}\left(F_{\gamma\alpha,n} D^R_{k\eta,\gamma\beta\alpha'\beta'}(t) + F_{\beta\gamma,n} D^R_{k\eta,\alpha\gamma\alpha'\beta'}(t)\right) \\ &+ \sum_{k\eta n\nu} t^*_{k\eta n}\left(F^*_{\gamma\nu,n} E^R_{k\eta,\nu\beta\alpha'\beta'}(t) + F^*_{\nu\beta,n} E^R_{k\eta,\alpha\nu\alpha'\beta'}(t)\right).\end{aligned} \tag{6.17}$$

So far it is exact. Now we go one step further and find the equations of motion for the new Green's functions D^R and E^R.

6.2.1 Equation of motion for D^R and E^R

For D^R we obtain

$$\begin{aligned}(i\partial_t + E_{\gamma\beta} + \xi_{k\eta}) D^R_{k\eta,\gamma\beta\alpha'\beta'}(t) = &\delta(t)\left(\left\langle c^\dagger_{k\eta}|\gamma\rangle\langle\alpha'|\right\rangle\delta_{\beta\beta'} + \left\langle|\beta'\rangle\langle\beta|c^\dagger_{k\eta}\right\rangle\right) \\ &- L^R_{D,k\eta\gamma\beta\alpha'\beta'}(t),\end{aligned} \tag{6.18}$$

where

$$L^R_{D,k\eta\gamma\beta\alpha'\beta'}(t) = -i\theta(t)\left\langle\left\{\left[H_T, c^\dagger_{k\eta}|\gamma\rangle\langle\beta|\right], |\beta'\rangle\langle\alpha'|\right\}\right\rangle \tag{6.19}$$

and the commutator gives

$$\begin{aligned}\left[H_T, c^\dagger_{k\eta}|\gamma\rangle\langle\beta|\right] = \sum_{nk'\eta'\alpha''\beta''} \Big(& t^*_{k\eta n} F_{\alpha''\beta'',n}\left[c^\dagger_{k'\eta'}|\alpha''\rangle\langle\beta''|, c^\dagger_{k\eta}|\gamma\rangle\langle\beta|\right] \\ &+ t_{k'\eta' n} F_{\alpha''\beta'',n}\left[|\beta''\rangle\langle\alpha''|c_{k'\eta'}, c^\dagger_{k\eta}|\gamma\rangle\langle\beta|\right]\Big).\end{aligned} \tag{6.20}$$

The commutators in Eq. (6.20) can be written as

$$\left[c^\dagger_{k'\eta'}|\alpha''\rangle\langle\beta''|, c^\dagger_{k\eta}|\gamma\rangle\langle\beta|\right] = -c^\dagger_{k'\eta'}c^\dagger_{k\eta}|\alpha''\rangle\langle\beta|\delta_{\beta''\gamma} + c^\dagger_{k\eta}c^\dagger_{k'\eta'}|\gamma\rangle\langle\beta''|\delta_{\alpha''\beta} \tag{6.21}$$

$$\left[|\beta''\rangle\langle\alpha''|c_{k'\eta'}, c^\dagger_{k\eta}|\gamma\rangle\langle\beta|\right] = |\beta''\rangle\langle\beta|c_{k'\eta'}c^\dagger_{k\eta}\delta_{\alpha''\gamma} + c^\dagger_{k\eta}c_{k'\eta'}|\gamma\rangle\langle\alpha''|\delta_{\beta\beta''} \tag{6.22}$$

The signs in Eq. (6.21) can be determined by noticing that the dot operators correspond to the annihilation of three dot electrons when inserted in the sum in Eq. (6.20). In the same way, the operators in Eq. (6.22) are the annihilation of a single dot electron when inserted in Eq. (6.20).

At this stage the important approximations are invoked in order to truncate the series of equations. First we assume that the lead operators are almost equal to their mean values at all times, which allows us to write

$$c^\dagger_{k'\eta'}c^\dagger_{k\eta} = \left(c^\dagger_{k'\eta'}c^\dagger_{k\eta} - \left\langle c^\dagger_{k'\eta'}c^\dagger_{k\eta}\right\rangle\right) + \left\langle c^\dagger_{k'\eta'}c^\dagger_{k\eta}\right\rangle \approx \left\langle c^\dagger_{k'\eta'}c^\dagger_{k\eta}\right\rangle, \tag{6.23}$$

$$c^\dagger_{k\eta}c_{k'\eta'} = \left(c^\dagger_{k\eta}c_{k'\eta'} - \left\langle c^\dagger_{k\eta}c_{k'\eta'}\right\rangle\right) + \left\langle c^\dagger_{k\eta}c_{k'\eta'}\right\rangle \approx \left\langle c^\dagger_{k\eta}c_{k'\eta'}\right\rangle. \tag{6.24}$$

If the contacts are considered as non-interacting electron gasses we obtain $\left\langle c^\dagger_{k'\eta'}c^\dagger_{k\eta}\right\rangle = 0$ and $\left\langle c^\dagger_{k\eta}c_{k'\eta'}\right\rangle = \delta_{k\eta,k'\eta'}f_\eta(\xi_k)$, with $f_\eta(\xi_k)$ being the Fermi function for the lead η.
Furthermore, we assume that terms like $\left\langle c^\dagger_{k\eta}|\gamma\rangle\langle\alpha'|\right\rangle$ in Eq. (6.18) vanish. These terms describe correlations between the dot and the leads and are therefore assumed small in case of weak coupling.

The approach is exact in two limits. In case of non-interacting electrons on the dot (for the FAB model $U = 0$) this point in the derivation of the equation of motion for $G^R_{nn'}(t)$ is never reached, so the method is exact. Likewise if the coupling between the leads and the dot vanishes. Then the term H_T in the Hamiltonian can be neglected, and the Green's function of the dot can be determined without any approximations. In this limit it is also exact.
In general one has to be careful when applying this approximation scheme to the Anderson model. We will save this discussion to Sec. 7.5 where the method is applied to the FAB model.

After the approximations made $L^R_{D,k\eta\gamma\beta\alpha'\beta'}(t)$ becomes,

$$\begin{aligned} L^R_{D,k\eta\gamma\beta\alpha'\beta'}(t) \approx &\sum_{\gamma' n'} t_{k\eta n'} F^*_{\gamma\gamma',n'}[1-f_\eta(\xi_k)]G^R_{\gamma'\beta\alpha'\beta'}(t) \\ &+ \sum_{\gamma' n'} t_{k\eta n'} F^*_{\gamma'\beta',n'} f_\eta(\xi_k) G^R_{\gamma\gamma'\alpha'\beta'}(t), \end{aligned} \tag{6.25}$$

and when inserted in Eq. (6.18) we finally arrive at the following equation in Fourier space

$$\begin{aligned} D^R_{k\eta,\gamma\beta\alpha'\beta'}(\omega) = \frac{-1}{\omega+\xi_{k\eta}+E_{\gamma\beta}+i0^+} \sum_{\gamma' n'} \Big(&t_{k\eta n'} F^*_{\gamma'\beta,n'} f_\eta(\xi_{k\eta}) G^R_{\gamma\gamma'\alpha'\beta'}(\omega) \\ &+ t_{k\eta n'} F^*_{\gamma\gamma',n'}[1-f_\eta(\xi_{k\eta})]G^R_{\gamma'\beta\alpha'\beta'}(\omega)\Big). \end{aligned} \tag{6.26}$$

Doing exactly the same kind of calculations and invoking the same approximations the following expression for $E^R_{k\eta,\nu\beta\alpha'\beta'}(\omega)$ is found[iv]

$$\begin{aligned} E^R_{k\eta,\nu\beta\alpha'\beta'}(\omega) = \frac{-1}{\omega-\xi_{k\eta}+E_{\nu\beta}+i0^+} \sum_{\nu' n'} \Big(&t^*_{k\eta n'} F_{\beta\nu',n'}[1-f_\eta(\xi_{k\eta})]G^R_{\nu\nu'\alpha'\beta'}(\omega) \\ &+ t^*_{k\eta n'} F^*_{\nu'\nu,n'} f_\eta(\xi_{k\eta}) G^R_{\nu'\beta\alpha'\beta'}(\omega)\Big). \end{aligned} \tag{6.27}$$

[iv] See Sec. A.3.

6.3 Unified expression for $G^R_{\alpha\beta,\alpha'\beta'}$

Now we can collect the pieces and insert the expressions for D^R and E^R in Eq. (6.17) and in Fourier space the result reads

$$\begin{aligned}
(\omega + E_{\alpha\beta} + i0^+)G^R_{\alpha\beta,\alpha'\beta'}(\omega) = &\left\langle |\alpha\rangle\langle\alpha'| \right\rangle \delta_{\beta\beta'} + \left\langle |\beta'\rangle\langle\beta| \right\rangle \delta_{\alpha\alpha'} \\
&+ \sum_{\gamma\gamma' nn'} F_{\gamma\alpha,n} F^*_{\gamma\gamma',n'} K^h_{nn'}(\omega + E_{\gamma\beta}) G^R_{\gamma'\beta,\alpha'\beta'}(\omega) \\
&+ \sum_{\beta\gamma nn'} F_{\gamma\alpha,n} F^*_{\gamma'\beta,n'} K^e_{nn'}(\omega + E_{\gamma\beta}) G^R_{\gamma\gamma',\alpha'\beta'}(\omega) \\
&+ \sum_{\gamma\gamma' nn'} F_{\beta\gamma,n} F^*_{\alpha\gamma',n'} K^h_{nn'}(\omega + E_{\alpha\gamma}) G^R_{\gamma'\gamma,\alpha'\beta'}(\omega) \\
&+ \sum_{\gamma\gamma' nn'} F_{\beta\gamma,n} F^*_{\gamma'\gamma,n'} K^e_{nn'}(\omega + E_{\alpha\gamma}) G^R_{\alpha\gamma',\alpha'\beta'}(\omega) \\
&+ \sum_{\nu\nu' nn'} F^*_{\alpha\nu,n} F_{\nu'\nu,n'} \Lambda^e_{nn'}(\omega + E_{\nu\beta}) G^R_{\nu'\beta,\alpha'\beta'}(\omega) \\
&+ \sum_{\nu\nu' nn'} F^*_{\alpha\nu,n} F_{\beta\nu',n'} \Lambda^h_{nn'}(\omega + E_{\nu\beta}) G^R_{\nu\nu',\alpha'\beta'}(\omega) \\
&+ \sum_{\nu\nu' nn'} F^*_{\nu\beta,n} F_{\nu'\alpha,n'} \Lambda^e_{nn'}(\omega + E_{\alpha\nu}) G^R_{\nu'\nu,\alpha'\beta'}(\omega) \\
&+ \sum_{\nu\nu' nn'} F^*_{\nu\beta,n} F_{\nu\nu',n'} \Lambda^h_{nn'}(\omega + E_{\alpha\nu}) G^R_{\alpha\nu',\alpha'\beta'}(\omega),
\end{aligned} \tag{6.28}$$

where we have introduced the functions

$$K^{e,h}_{nn'}(\omega) = \sum_{k\eta} \begin{pmatrix} f_\eta(\xi_{k\eta}) \\ 1 - f_\eta(\xi_{k\eta}) \end{pmatrix} \frac{t^*_{k\eta n} t_{k\eta n'}}{\omega + \xi_{k\eta} + i0^+}, \tag{6.29}$$

$$\Lambda^{e,h}_{nn'}(\omega) = \sum_{k\eta} \begin{pmatrix} f_\eta(\xi_{k\eta}) \\ 1 - f_\eta(\xi_{k\eta}) \end{pmatrix} \frac{t^*_{k\eta n} t_{k\eta n'}}{\omega - \xi_{k\eta} + i0^+}. \tag{6.30}$$

The task is to solve the equations for the auxiliary Green's functions and insert the results in Eq. (6.7). Eventually, a general expression for the retarded Green's function has been derived for a system consisting of a quantum dot coupled to two leads. It shall be emphasized that the method is only supposed to work in the limit of weak coupling.

K. Flensberg showed in [6] that the method gives the same result for the model with a singe spinful level with interactions, as the one obtained in [8]. Furthermore, it is proved that the method is exact for non-interacting electrons.
The method was also applied in [9] where a model for a single level coupled to a vibrational mode was considered.

6.4 Discussion of the unified description

Even though the expression in Eq. (6.28) looks rather compact it hides some serious complications, because it depends on expectation values like $\langle|\alpha\rangle\langle\alpha'|\rangle$. These expectation values have to be calculated self-consistently, and we note that they are related to lesser Green's function. Consider for instance

$$\big\langle(|\alpha\rangle\langle\alpha'|)(t)\big\rangle = -iG^{<}_{0\alpha',0\alpha}(t,t). \tag{6.31}$$

In steady state $\langle(|\alpha\rangle\langle\alpha'|)(t)\rangle$ is assumed constant, and we obtain

$$\big\langle|\alpha\rangle\langle\alpha'|\big\rangle = -i\int\frac{d\omega}{2\pi}G^{<}_{0\alpha',0\alpha}(\omega) \tag{6.32}$$

but we do not know how to determine the lesser Green's functions. A tempting approach would be to use the same equation of motion approach as for the retarded Green's functions. This gives an equation system identical to Eq. (6.28) except that the constant on the right-hand side is zero,[v] so we have a homogeneous equation system for all ω. However, among the infinitely many solutions we do not know which to chose.

To progress we have to assume a pesudo-equilibrium situation. An example is a setup where the dot is strongly coupled to one of the leads, so they are in equilibrium. That is in fact often the case in an experiment. In this situation the equilibrium fluctuation-dissipation theorem can be applied, e.g. (see Eq. (3.26))

$$\big\langle|\alpha\rangle\langle\alpha'|\big\rangle = i\int\frac{d\omega}{2\pi}\left[G^{R}_{0\alpha',0\alpha}(\omega) - \big(G^{R}_{0\alpha,0\alpha'}(\omega)\big)^{*}\right]f_{\eta}(\omega), \tag{6.33}$$

where $f_\eta(\omega)$ is the Fermi function for the lead with the strong coupling to the molecule. Eqs. (6.28) and (6.33) then define a self-consistent equation system for the retarded Green's functions $G^R_{0\alpha,0\alpha'}(\omega)$.
Another pseudo-equilibrium situation occurs when we are only interested in the linear response result, i.e. we consider only a small bias voltage which can be treated to lowest order. Therefore the fluctuation-dissipation theorem can be used to determine the occupancies, but remember that calculating the current also requires proportionate couplings. When applying Green's functions to solve the FAB model for a finite U only the linear response result will be considered, and therefore solely the parallel geometry.

For some models the lesser function can be determined through a diagrammatic expansion giving a true nonequilibrium expression, but determining the lesser function is in general a problem when dealing with nonequilibrium Green's functions. That was also the reason for assuming proportionate couplings when we derived the current formula in Sec. 3.5, because it eliminated the lesser function.

In Chap. 7 an attempt to apply the unified description on the FAB model is presented. At that point a further discussion of the validity of the approach is also given (see Sec. 7.5).

[v] Recall that the constant on the right-hand side in Eq. (6.28) stems from the δ-function in the definition of the retarded Green's function.

Chapter 7

Green's function approach to the FAB model

After the derivation of the unified description of tunnelling we can proceed and apply the method to the FAB model.
At first we translate the FAB Hamiltonian into the notation used in the unified description, and from Eq. (6.28) we can write up an equation system for the auxiliary Green's functions. The next task is to determine self-consistently the occupancies entering the expressions for the auxiliary Green's functions and use them to find the original Green's functions. Finally the current is calculated in linear response and for low temperatures.

Already at this state it should be mentioned that we have only partially succeeded. However, the unclear/uncorrect results give rise to a discussion of the validity of the method and the approximations used. That will be found in the last section.

7.1 The FAB model in the unified description

We want to find the retarded Green's function for the dot

$$G^R_{\mu\mu'}(t) = -i\theta(t)\left\langle\{c_{d\mu}(t), c^\dagger_{d\mu'}\}\right\rangle, \tag{7.1}$$

where μ and μ' is either $\uparrow$ or $\downarrow$, using the method derived in the previous section.
When applying the unified description the first thing to do is to identify the eigenstates of the dot. For the FAB model this has already been sorted out in Sec. 2.3, and the eigenstates are $|0\rangle$, $|\uparrow\rangle$, $|\downarrow\rangle$ and $|2\rangle = c^\dagger_{d\downarrow}c^\dagger_{d\uparrow}|0\rangle$, where the spin is in the dot spin basis.
With these eigenstates it is easy to see that only the following $F_{\alpha\beta,\mu} = \langle\alpha|c_{d\mu}|\beta\rangle$ coefficients are non-vanishing [i]

$$F_{0\uparrow,\uparrow} = F_{0\downarrow,\downarrow} = F_{\uparrow 2,\downarrow} = -F_{\downarrow 2,\uparrow} = 1. \tag{7.2}$$

[i] The minus sign is due to order of the operators in the definition of the double occupied state.

The tunnelling part of the Hamiltonian is with the degrees of freedom for the FAB model

$$H_T = \sum_{k\eta\sigma,\mu,\alpha\beta} V_{k\eta\sigma,\mu} c^\dagger_{k\eta\sigma} |\alpha\rangle\langle\beta| F_{\alpha\beta,\mu} + V^*_{k\eta\sigma,\mu} |\beta\rangle\langle\alpha| F^*_{\alpha\beta,\mu} c_{k\eta\sigma}, \tag{7.3}$$

which will be used in the definition of the K and Λ functions.

From the $F_{\alpha\beta,\mu}$-coefficients and the definition of the Green's function in terms of the auxiliary Green's functions[ii], the Green's functions $G^R_{\mu\mu'}(t)$ can be expressed as

$$\begin{aligned}
G^R_{\uparrow\uparrow} &= G^R_{0\uparrow,0\uparrow} - G^R_{\downarrow 2,0\uparrow} - G^R_{0\uparrow,\downarrow 2} + G^R_{\downarrow 2,\downarrow 2},\\
G^R_{\downarrow\downarrow} &= G^R_{0\downarrow,0\downarrow} + G^R_{\uparrow 2,0\downarrow} + G^R_{0\downarrow,\uparrow 2} + G^R_{\uparrow 2,\uparrow 2},\\
G^R_{\uparrow\downarrow} &= G^R_{0\uparrow,0\downarrow} + G^R_{0\uparrow,\uparrow 2} - G^R_{\downarrow 2,0\downarrow} - G^R_{\downarrow 2,\uparrow 2},\\
G^R_{\downarrow\uparrow} &= G^R_{0\downarrow,0\uparrow} - G^R_{0\downarrow,\downarrow 2} + G^R_{\uparrow 2,0\uparrow} - G^R_{\uparrow 2,\downarrow 2}.
\end{aligned} \tag{7.4}$$

Here the time-dependence of the Green's functions has been suppressed.
The task is to calculate the 16 Green's functions on the right-hand sides and then insert the result into Eq. (7.4) in order to obtain $\mathbf{G}^R(\omega)$.

From Eq. (6.28) and Eq. (7.2) we obtain the following expressions for the auxiliary Green's functions in Eq. (7.4)

$$\begin{aligned}
&\Big[\omega + E_{\downarrow 2} - K^h_{\downarrow\downarrow}(\omega + E_{02}) - \Lambda^e_{\uparrow\uparrow}(\omega) - \Lambda^h_{\uparrow\uparrow}(\omega) - \Lambda^h_{\downarrow\downarrow}(\omega + E_{\downarrow\uparrow})\Big] G^R_{\downarrow 2,\alpha'\beta'}\\
&\quad = \left[\delta_{\downarrow\alpha'} \langle|\beta'\rangle\langle 2|\rangle + \delta_{2\beta'} \langle|\downarrow\rangle\langle\alpha'|\rangle\right]\\
&\qquad + \left[K^e_{\downarrow\downarrow}(\omega + E_{02}) + \Lambda^e_{\downarrow\downarrow}(\omega + E_{\downarrow\uparrow})\right] G^R_{0\uparrow,\alpha'\beta'}\\
&\qquad + \Big[K^h_{\downarrow\uparrow}(\omega + E_{02}) - \Lambda^e_{\uparrow\downarrow}(\omega)\Big] G^R_{\uparrow 2,\alpha'\beta'}\\
&\qquad - \left[K^e_{\downarrow\uparrow}(\omega + E_{02}) + \Lambda^e_{\uparrow\downarrow}(\omega)\right] G^R_{0\downarrow,\alpha'\beta'},
\end{aligned} \tag{7.5}$$

and

$$\begin{aligned}
&\Big[\omega + E_{0\uparrow} - K^e_{\downarrow\downarrow}(\omega + E_{02}) - \Lambda^e_{\uparrow\uparrow}(\omega) - \Lambda^h_{\uparrow\uparrow}(\omega) - \Lambda^e_{\downarrow\downarrow}(\omega + E_{\downarrow\uparrow})\Big] G^R_{0\uparrow,\alpha'\beta'}\\
&\quad = \left[\delta_{0\alpha'} \langle|\beta'\rangle\langle\uparrow|\rangle + \delta_{\uparrow\beta'} \langle|0\rangle\langle\alpha'|\rangle\right]\\
&\qquad + \Big[K^h_{\downarrow\downarrow}(\omega + E_{02}) + \Lambda^h_{\downarrow\downarrow}(\omega + E_{\downarrow\uparrow})\Big] G^R_{\downarrow 2,\alpha'\beta'}\\
&\qquad + \Big[\Lambda^h_{\uparrow\downarrow}(\omega) - K^e_{\downarrow\uparrow}(\omega + E_{02})\Big] G^R_{0\downarrow,\alpha'\beta'}\\
&\qquad + \Big[K^h_{\downarrow\uparrow}(\omega + E_{02}) + \Lambda^h_{\uparrow\downarrow}(\omega)\Big] G^R_{\uparrow 2\alpha'\beta'},
\end{aligned} \tag{7.6}$$

[ii] See Eq. (6.7) and Eq. (6.8)

and

$$\begin{aligned}
&\Big[\omega + E_{0\downarrow} - K^e_{\uparrow\uparrow}(\omega + E_{02}) - \Lambda^e_{\downarrow\downarrow}(\omega) - \Lambda^h_{\downarrow\downarrow}(\omega) - \Lambda^e_{\uparrow\uparrow}(\omega + E_{\uparrow\downarrow})\Big]\, G^R_{0\downarrow,\alpha'\beta'} \\
&\quad = \left[\delta_{0\alpha'}\langle|\beta'\rangle\langle\downarrow|\rangle + \delta_{\downarrow\beta'}\langle|0\rangle\langle\alpha'|\rangle\right] \\
&\qquad - \Big[K^h_{\uparrow\uparrow}(\omega + E_{02}) + \Lambda^h_{\uparrow\uparrow}(\omega + E_{\uparrow\downarrow})\Big]\, G^R_{\uparrow 2,\alpha'\beta'} \\
&\qquad - \Big[K^h_{\uparrow\downarrow}(\omega + E_{02}) + \Lambda^h_{\downarrow\uparrow}(\omega)\Big]\, G^R_{\downarrow 2,\alpha'\beta'} \\
&\qquad + \Big[\Lambda^h_{\downarrow\uparrow}(\omega) - K^e_{\uparrow\downarrow}(\omega + E_{02})\Big]\, G^R_{0\uparrow,\alpha'\beta'},
\end{aligned} \tag{7.7}$$

and finally

$$\begin{aligned}
&\Big[\omega + E_{\uparrow 2} - K^h_{\uparrow\uparrow}(\omega + E_{02}) - \Lambda^e_{\downarrow\downarrow}(\omega) - \Lambda^h_{\downarrow\downarrow}(\omega) - \Lambda^h_{\uparrow\uparrow}(\omega + E_{\uparrow\downarrow})\Big]\, G^R_{\uparrow 2,\alpha'\beta'} \\
&\quad = \left[\delta_{\uparrow\alpha'}\langle|\beta'\rangle\langle 2|\rangle + \delta_{2\beta'}\langle|\uparrow\rangle\langle\alpha'|\rangle\right] \\
&\qquad - \left[K^e_{\uparrow\uparrow}(\omega + E_{02}) + \Lambda^e_{\uparrow\uparrow}(\omega + E_{\uparrow\downarrow})\right]\, G^R_{0\downarrow,\alpha'\beta'} \\
&\qquad + \Big[K^h_{\uparrow\downarrow}(\omega + E_{02}) - \Lambda^e_{\downarrow\uparrow}(\omega)\Big]\, G^R_{\downarrow 2,\alpha'\beta'} \\
&\qquad + \left[K^e_{\uparrow\downarrow}(\omega + E_{02}) + \Lambda^e_{\downarrow\uparrow}(\omega)\right]\, G^R_{0\uparrow,\alpha'\beta'},
\end{aligned} \tag{7.8}$$

The constants $K^{e,h}$ and $\Lambda^{e,h}$ are defined as in Eqs. (6.29) and (6.30) with

$$K^{e,h}_{\mu\mu'}(\omega) = \sum_{k\eta\sigma} \begin{pmatrix} f_\eta(\varepsilon_{k\eta\sigma}) \\ 1 - f_\eta(\varepsilon_{k\eta\sigma}) \end{pmatrix} \frac{V^*_{k\eta\sigma,\mu} V_{k\eta\sigma,\mu'}}{\omega + \varepsilon_{k\eta\sigma} + i0^+}, \tag{7.9}$$

and

$$\Lambda^{e,h}_{\mu\mu'}(\omega) = \sum_{k\eta\sigma} \begin{pmatrix} f_\eta(\varepsilon_{k\eta\sigma}) \\ 1 - f_\eta(\varepsilon_{k\eta\sigma}) \end{pmatrix} \frac{V^*_{k\eta\sigma,\mu} V_{k\eta\sigma,\mu'}}{\omega - \varepsilon_{k\eta\sigma} + i0^+}. \tag{7.10}$$

The Eqs. (7.5)-(7.8) look terrifying, but we note that according to Eqs. (6.7) and (7.2) there are only four possibilities for $\alpha'\beta'$. Moreover, the Green's functions depend only on other Green's functions which have the same indices for $\alpha'\beta'$, e.g. $G^R_{0\uparrow,0\uparrow}$ depends only on $G^R_{0\downarrow,0\uparrow}$, $G^R_{\uparrow 2,0\uparrow}$ and $G^R_{\downarrow 2,0\uparrow}$.
With this in mind, we put Eqs. (7.5)-(7.8) on matrix form

$$\left(\mathbf{M}^R\right)^{-1} \begin{pmatrix} G^R_{0\uparrow,\alpha'\beta'} \\ G^R_{0\downarrow,\alpha'\beta'} \\ G^R_{\downarrow 2,\alpha'\beta'} \\ G^R_{\uparrow 2,\alpha'\beta'} \end{pmatrix} = \begin{pmatrix} \delta_{0\alpha'}\langle|\beta'\rangle\langle\uparrow|\rangle + \delta_{\uparrow\beta'}\langle|0\rangle\langle\alpha'|\rangle \\ \delta_{0\alpha'}\langle|\beta'\rangle\langle\downarrow|\rangle + \delta_{\downarrow\beta'}\langle|0\rangle\langle\alpha'|\rangle \\ \delta_{\downarrow\alpha'}\langle|\beta'\rangle\langle 2|\rangle + \delta_{2\beta'}\langle|\downarrow\rangle\langle\alpha'|\rangle \\ \delta_{\uparrow\alpha'}\langle|\beta'\rangle\langle 2|\rangle + \delta_{2\beta'}\langle|\uparrow\rangle\langle\alpha'|\rangle \end{pmatrix}. \tag{7.11}$$

It is the same matrix for all $\alpha'\beta'$ because the matrix elements (depending on $K^{e,h}$, $\Lambda^{e,h}$ etc.) are independent of $\alpha'\beta'$.
Furthermore, the matrix $\mathbf{M}^R$ can be split up into two parts as

$$\mathbf{M}^R = (\mathbf{M}^R_0)^{-1} - \mathbf{M}^R_\Sigma, \tag{7.12}$$

where $\mathbf{M}_0^R$ is the auxiliary Green's function for the isolated quantum dot and $\mathbf{M}_\Sigma^R$ has the form of a self-energy.[iii]
The equations defined through Eq. (7.11) can in principle be solved for any values of the parameters.

From Eq. (7.4) and Eq. (7.11) it follows that

$$\begin{aligned} G^R_{\uparrow\uparrow} = &(P_0 + P_\uparrow)\left(M^R_{11} - M^R_{31}\right) + (P_2 + P_\downarrow)\left(M^R_{33} - M^R_{13}\right) \\ &+ P_{\uparrow\downarrow}\left(M^R_{12} - M^R_{32} - M^R_{14} + M^R_{34}\right), \end{aligned} \tag{7.13}$$

where $P_{\alpha\beta} = \langle|\alpha\rangle\langle\beta|\rangle$ and $P_{\alpha\alpha} = P_\alpha$.

The occupancies, $P_{\alpha,\beta}$, are not independent, and because the eigenstates for the dot Hamiltonian form a complete dot set we find $P_0 + P_\uparrow + P_\downarrow + P_2 = 1$. Moreover holds $P_\downarrow + P_2 = \left\langle c^\dagger_\downarrow c_\downarrow \right\rangle = \langle n_\downarrow\rangle$, which gives $P_0 + P_\uparrow = 1 - P_\downarrow - P_2 = 1 - \langle n_\downarrow\rangle$. Finally, $P_{\uparrow\downarrow} = \left\langle c^\dagger_\uparrow c_\downarrow \right\rangle \equiv \langle n_{\uparrow\downarrow}\rangle$, which is seen by inserting a complete dot set in $\left\langle c^\dagger_\uparrow c_\downarrow \right\rangle$.

So Eq. (7.13) becomes

$$\begin{aligned} G^R_{\uparrow\uparrow} = &\left(M^R_{11} - M^R_{31}\right) + \langle n_\downarrow\rangle\left(M^R_{33} - M^R_{13} - M^R_{11} + M^R_{31}\right) \\ &+ \langle n_{\uparrow\downarrow}\rangle\left(M^R_{12} - M^R_{32} - M^R_{14} + M^R_{34}\right). \end{aligned} \tag{7.14}$$

For $G^R_{\downarrow\downarrow}$ we find in the same way

$$\begin{aligned} G^R_{\downarrow\downarrow} &= (P_0 + P_\downarrow)\left(M^R_{22} + M^R_{42}\right) + (P_2 + P_\uparrow)\left(M^R_{24} + M^R_{44}\right) \\ &\quad + P_{\downarrow\uparrow}\left(M^R_{21} + M^R_{41} + M^R_{23} + M^R_{43}\right) \\ &= \left(M^R_{22} + M^R_{42}\right) + \langle n_\uparrow\rangle\left(M^R_{24} + M^R_{44} - M^R_{42} - M^R_{22}\right) \\ &\quad + \langle n_{\downarrow\uparrow}\rangle\left(M^R_{21} + M^R_{41} + M^R_{23} + M^R_{43}\right), \end{aligned} \tag{7.15}$$

and for the off-diagonal Green's functions we obtain

$$\begin{aligned} G^R_{\uparrow\downarrow} &= (P_0 + P_\downarrow)\left(M^R_{12} - M^R_{32}\right) + (P_2 + P_\uparrow)\left(M^R_{14} - M^R_{34}\right) \\ &\quad + P_{\downarrow\uparrow}\left(M^R_{11} + M^R_{13} - M^R_{31} - M^R_{33}\right) \\ &= \left(M^R_{12} - M^R_{32}\right) + \langle n_\uparrow\rangle\left(M^R_{14} + M^R_{32} - M^R_{34} - M^R_{12}\right) \\ &\quad + \langle n_{\downarrow\uparrow}\rangle\left(M^R_{13} - M^R_{31} - M^R_{33} + M^R_{11}\right), \end{aligned} \tag{7.16}$$

and

$$\begin{aligned} G^R_{\downarrow\uparrow} &= (P_0 + P_\uparrow)\left(M^R_{21} + M^R_{41}\right) - (P_2 + P_\downarrow)\left(M^R_{23} + M^R_{43}\right) \\ &\quad + P_{\uparrow\downarrow}\left(M^R_{22} - M^R_{24} + M^R_{42} - M^R_{44}\right) \\ &= \left(M^R_{21} + M^R_{41}\right) - \langle n_\downarrow\rangle\left(M^R_{21} + M^R_{23} + M^R_{41} + M^R_{43}\right) \\ &\quad + \langle n_{\uparrow\downarrow}\rangle\left(M^R_{22} - M^R_{24} + M^R_{42} - M^R_{44}\right). \end{aligned} \tag{7.17}$$

[iii] The explicit form of the matrix $(\mathbf{M}_0^R)^{-1}$ can be found in Sec. A.4.3.

The occupations appearing on the left-hand sides have to be calculated self-consistently as discussed in Sec. 6.4.
We are interested in comparing the results found using the unified description with the exact analytic result derived for $U = 0$ in linear response (see Sec. 4.1). So in the following we will only be interested in the linear response result and therefore have to assume proportionate couplings in order to calculate the current.[iv] Applying the fluctuation-dissipation theorem gives

$$\langle n_\uparrow \rangle = -2\mathrm{Im} \int \frac{d\omega}{2\pi} G^R_{\uparrow\uparrow}(\omega) f(\omega) \tag{7.18}$$

$$\langle n_\downarrow \rangle = -2\mathrm{Im} \int \frac{d\omega}{2\pi} G^R_{\downarrow\downarrow}(\omega) f(\omega) \tag{7.19}$$

$$\langle n_{\uparrow\downarrow} \rangle = i \int \frac{d\omega}{2\pi} \left[G^R_{\downarrow\uparrow}(\omega) - [G^R_{\uparrow\downarrow}(\omega)]^* \right] f(\omega) \tag{7.20}$$

$$\langle n_{\downarrow\uparrow} \rangle = i \int \frac{d\omega}{2\pi} \left[G^R_{\uparrow\downarrow}(\omega) - [G^R_{\downarrow\uparrow}(\omega)]^* \right] f(\omega), \tag{7.21}$$

as derived in Sec. A.4.4, where $f(\omega)$ is the Fermi distribution function in equilibrium.
Combing Eq. (7.14)-(7.17) and Eq. (7.18)-(7.21) it is possible to calculate the occupancies, which will be done in the following section.

7.2 Numerical solution of the FAB model

At this point we have to use numerical methods in order to solve the equations for the Green's functions and the occupancies self-consistently.
We proceed in three steps. In Eq. (7.14)-(7.17) we see that the Green's functions $G^R_{\mu\mu'}$ depend on the elements of the $\mathbf{M}^R$ matrix defined in Eq. (7.11). The occupancies are related to the Green's functions and therefore to the elements of $\mathbf{M}^R$, see Eq. (7.18)-(7.21). So the first step is to calculate the integral over $\mathbf{M}^R$ times the Fermi function, and the second is to obtain the occupancies from Eqs. (7.18)-(7.21) by solving the resulting matrix equation.[v] Finally, the occupancies are inserted in Eq. (7.14)-(7.17) and the Green's functions have been determined for all ω.

7.2.1 Expressions for K and Λ

In order to find the integral over $\mathbf{M}^R$ times the Fermi function we need expressions for the $K^{e,h}$ and $\Lambda^{e,h}$ functions from Eqs. (7.9) and (7.10). As an example is shown how to calculate $\Lambda^e_{\mu\mu'}(\omega)$.
As in Chap. 4 we use the trick $\sum_k F(\varepsilon_k) = \int d\varepsilon \sum_k \delta(\varepsilon - \varepsilon_k) F(\varepsilon)$ and introduce the

[iv] See Sec. 6.4.

[v] When writing down the equations for the occupancies it is advantageous to use that $\langle n_\uparrow \rangle, \langle n_\downarrow \rangle$ are reals and $\langle n_{\uparrow\downarrow} \rangle = \langle n_{\downarrow\uparrow} \rangle^*$.

coupling parameter

$$\Gamma^{\eta}_{\sigma}(\varepsilon) = 2\pi \sum_{k\sigma} |t_{k\eta\sigma}|^2 \delta(\varepsilon - \varepsilon_{k\eta\sigma}). \tag{7.22}$$

Recalling that $V_{k\eta\sigma,\mu} = R_{\sigma\mu} t_{k\eta\sigma}$, where $\mathbf{R}$ is the change-of-basis matrix from Eq. (2.7), we obtain with this definition that $\Lambda^{e}_{\mu\mu'}(\omega)$ can be written as

$$\begin{aligned} \Lambda^{e}_{\mu\mu'}(\omega) &= \sum_{k\eta\sigma} f_{\eta}(\varepsilon_{k\eta\sigma}) \frac{V^{*}_{k\eta\sigma,\mu} V_{k\eta\sigma,\mu'}}{\omega - \varepsilon_{k\eta\sigma} + i0^{+}} \\ &= \sum_{\eta\sigma} R^{*}_{\sigma\mu} R_{\sigma\mu'} \int \frac{d\varepsilon}{2\pi} \frac{f_{\eta}(\varepsilon)}{\omega - \varepsilon + i0^{+}} \Gamma^{\eta}_{\sigma}(\varepsilon). \end{aligned} \tag{7.23}$$

With the same line of arguments as in Chap. 4 we assume that $\Gamma^{\eta}_{\sigma}(\varepsilon)$ is independent of energy (the Wide Band Limit) and therefore can be pulled outside the integral. This approximation gives the following expression for Λ^{e}

$$\Lambda^{e}_{\mu\mu'}(\omega) = \sum_{\eta} \tilde{\Gamma}^{\eta}_{\mu\mu'} \int \frac{d\varepsilon}{2\pi} \frac{f_{\eta}(\varepsilon)}{\omega - \varepsilon + i0^{+}}, \tag{7.24}$$

where $\tilde{\Gamma}^{\eta}_{\mu\mu'}$ is the coupling matrix defined in the dot spin basis (see Eq. (4.19)). How to calculate the integral is shown in Sec. A.4.1.
In the exact same way we obtain

$$\Lambda^{h}_{\mu\mu'}(\omega) = \sum_{\eta} \tilde{\Gamma}^{\eta}_{\mu\mu'} \int \frac{d\varepsilon}{2\pi} \frac{1 - f_{\eta}(\varepsilon)}{\omega - \varepsilon + i0^{+}}, \tag{7.25}$$

$$K^{e,h}_{\mu\mu'}(\omega) = \sum_{\eta} \tilde{\Gamma}^{\eta}_{\mu\mu'} \int \frac{d\varepsilon}{2\pi} \begin{pmatrix} f_{\eta}(\varepsilon) \\ 1 - f_{\eta}(\varepsilon) \end{pmatrix} \frac{1}{\omega - \varepsilon - i0^{+}}. \tag{7.26}$$

7.2.2 Condition for $\mathbf{M}^{R}$

In the Wide Band Limit and after rewriting the expressions for $K^{e,h}$ and $\Lambda^{e,h}$ in the preceding section, it is, at least in principle, possible to solve the linear equation systems in Eq. (7.11) for all θ, where θ is the angle between the magnetization of the leads and the applied magnetic field.
As already mentioned, calculating the occupations in Eqs. (7.18)-(7.21) involves integration over all entries in the matrix $\mathbf{M}^{R} = [(\mathbf{M}^{R}_{0})^{-1} - \mathbf{M}^{R}_{\Sigma}]^{-1}$ from Eq. (7.11) times the Fermi function. But before doing so we will show a condition which $\mathbf{M}^{R}$ has to fulfil, and it might explain why the calculations fail for $U \neq 0$.
In the following section a method to obtain the occupations is presented.

Recall that the equation system in Eq. (7.11) has the form[vi]

$$(\mathbf{M}^{R}_{0})^{-1} \overline{G}^{R}_{\alpha'\beta'} = \overline{v}_{\alpha'\beta'} + \mathbf{M}^{R}_{\Sigma} \overline{G}^{R}_{\alpha'\beta'}, \tag{7.27}$$

[vi] Notice that $\overline{G}$ is the vector defined on the right-hand side of Eq. (7.11), not to be confused with $\mathbf{G}^{R}$ having the elements $G^{R}_{\mu\mu'}$ with $\mu, \mu' = \uparrow, \downarrow$.

where $\overline{v}_{\alpha'\beta'}$ is a vector containing the occupancies, $\mathbf{M}_0^R$ the retarded Green's function for the isolated quantum dot, $\mathbf{M}_\Sigma^R$ the retarded self-energy and

$$\overline{G}^R_{\alpha'\beta'} = (G^R_{0\uparrow,\alpha'\beta'}, G^R_{0\downarrow,\alpha'\beta'}, G^R_{\downarrow 2,\alpha'\beta'}, G^R_{\uparrow 2,\alpha'\beta'}) \tag{7.28}$$

is a vector containing the full auxiliary retarded Green's functions.
Integration over $\overline{G}^R_{\alpha'\beta'}$ for all energies gives

$$\begin{aligned}\int \frac{d\omega}{2\pi}\overline{G}^R_{\alpha'\beta'}(\omega) &= \int \frac{d\omega}{2\pi}\left[\mathbf{M}_0^R(\omega)\overline{v}_{\alpha'\beta'} + \mathbf{M}_0^R(\omega)\mathbf{M}_\Sigma^R(\omega)\overline{G}^R_{\alpha'\beta'}(\omega)\right] \\ &= -\frac{i}{2}\overline{v}_{\alpha'\beta'},\end{aligned} \tag{7.29}$$

where the remaining term comes from[vii]

$$\begin{aligned}\left[\mathbf{M}_0^R(\omega)\right]_{nm} &= \delta_{nm}\frac{1}{\omega + E^{nm} + i0^+} \\ &= \mathcal{P}\int \frac{d\omega}{\omega + E^{nm}} - i\pi\delta(\omega + E^{nm})\delta_{nm} \\ &= -i\pi\delta(\omega + E^{nm})\delta_{nm}.\end{aligned} \tag{7.30}$$

The second term cancels. $\overline{G}^R_{\alpha'\beta'}(\omega)$, $\mathbf{M}_\Sigma^R(\omega)$ and $\mathbf{M}_0^R(\omega)$ are retarded functions, so after analytic continuation $\omega + i0^+ \to z$ they will have poles on same side of the real axis. Moreover, $\mathbf{M}_0(z)\mathbf{M}_\Sigma(z)\overline{G}_{\alpha'\beta'}(z) < \frac{K}{|z|^2}$ for $|z| \to \infty$, with K being a constant. Using the Residue Theorem by making a closed contour along the real axis closed in the pole free half plane does the job.

From Eq. (7.11) we get $\overline{G}^R_{\alpha'\beta'}(\omega) = \mathbf{M}^R(\omega)\overline{v}_{\alpha'\beta'}$, so

$$\int \frac{d\omega}{2\pi}\overline{G}^R_{\alpha'\beta'}(\omega) = \int \frac{d\omega}{2\pi}\mathbf{M}^R(\omega)\overline{v}_{\alpha'\beta'} = -\frac{i}{2}\overline{v}_{\alpha'\beta'} \tag{7.31}$$

from which it follows

$$\int \frac{d\omega}{2\pi}\ \mathbf{M}^R(\omega) = -\frac{i}{2}\mathbf{1}. \tag{7.32}$$

When performing the integral over $\mathbf{M}^R$ the condition was not fulfilled for all values of the parameters[viii] and angles. We assumed that this was due to numerical integration problems because the entries in the $\mathbf{M}^R(\omega)$ matrix are very peaked and therefore difficult to integrate. However, it might be because of problems caused by the approximations used in the derivation of the unified description. The will be discussed in the last section of this chapter.

[vii] For the explicit form of $\mathbf{M}_0^R(\omega)$ see Sec. A.4.3.

[viii] The parameters are the strength of the magnetic field B, U, $\Gamma^\eta_{\uparrow'}$, $\Gamma^\eta_{\downarrow'}$ and temperature.

7.2.3 Calculation of the occupations

Because we assumed that the condition in Eq. (7.32) was not satisfied due to numerical problems, we now show how the integral over $\mathbf{M}^R(\omega)f(\omega)$ can be carried out using the Residue Theorem from complex analysis. This is a very elegant way of doing numerical integrations because it involves summing over discrete values in the complex plane instead of integration over a complicated function.

So the task in this section is to calculate the integral

$$\int \frac{d\omega}{2\pi}\, \mathbf{M}^R(\omega)f(\omega), \tag{7.33}$$

and we start be writing $\mathbf{M}^R(\omega)$ as

$$\mathbf{M}^R(\omega) = \Big(\big[(\mathbf{M}_0^R)^{-1}(\omega) - \mathbf{M}_\Sigma^R(\omega)\big]^{-1} - \mathbf{M}_0^R(\omega)\Big) + \mathbf{M}_0^R(\omega) \equiv \mathbf{Q}^R(\omega) + \mathbf{M}_0^R(\omega). \tag{7.34}$$

The integral over $\mathbf{M}_0^R(\omega)f(\omega)$ can be calculated when we recall that $\frac{1}{\omega+i0^+} = \mathcal{P}\int \frac{1}{\omega} - i\pi\delta(\omega)$. The imaginary part of the integral gives[ix]

$$\mathrm{Im}\int \frac{d\omega}{2\pi}\left[\mathbf{M}_0^R(\omega)\right]_{nm} f(\omega) = -\frac{1}{2}f(-E^n)\delta_{nm}, \tag{7.35}$$

and this diagonal matrix will be denoted $\mathrm{Im}_{\mathbf{M}_0^R}$.
The principal integral is more cumbersome and no simple expression is found, but it can be calculated using the same method as when calculating the integrals contained in the $K^{e,h}$ and $\Lambda^{e,h}$ functions, and the derivation is found in Sec. A.4.1. The resulting diagonal matrix will be denoted $\mathrm{Re}_{\mathbf{M}_0^R}$.

For $\mathbf{Q}^R(\omega)$ we perform the analytic continuation $\omega + i0^+ \to z$. $\mathbf{Q}(z)$ has poles only in the half plane below the real axis because $\mathbf{M}_0^R(\omega)$ and $\mathbf{M}_\Sigma^R(\omega)$ are a retarded Green's function and a retarded self-energy, respectively. $f(z)$ has poles for

$$z = i\frac{(2n+1)\pi}{\beta} = ik_n, \qquad \beta = \frac{1}{k_B T}. \tag{7.36}$$

According to the Residue Theorem integration along the curve $\tilde{\mathcal{D}}$ shown in Fig. 7.1 will give[x]

$$-\int_{\mathcal{C}} \frac{dz}{2\pi i}\mathbf{Q}(z)f(z) = -\left(\int_L + \int_{L'}\right)\frac{dz}{2\pi i}\mathbf{Q}(z)f(z) = \frac{1}{\beta}\sum_{ik_n}\mathbf{Q}(ik_n), \tag{7.37}$$

because $\mathrm{Res}\left[\mathbf{Q}(z)f(z); ik_n\right] = -\frac{1}{\beta}\mathbf{Q}(ik_n)$.
For $|z| \to \infty$ holds $\left[\mathbf{M}_0^{-1}(z) - \mathbf{M}_\Sigma(z)\right]^{-1} \to \mathbf{M}_0(z)$, because the $K^{e,h}$ and $\Lambda^{e,h}$ functions

[ix] The exact expression for $\mathbf{M}_0^R$ is found in Sec. A.4.3.
[x] See e.g. [1].

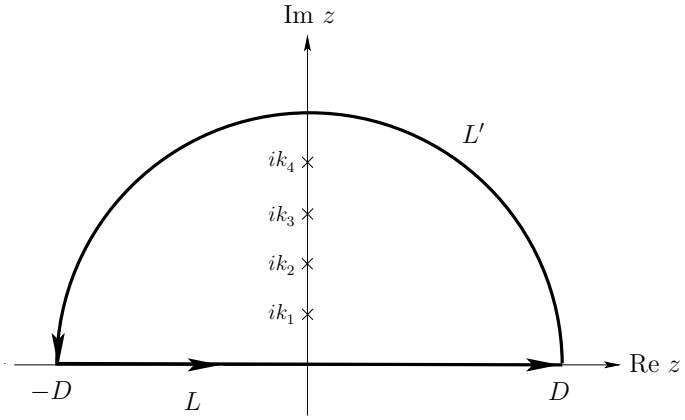

Figure 7.1: The integration contour $\tilde{\mathcal{D}}$=L+L' (L running from -D to D along the real axis).

tend to zero. So the integral along L' vanishes for $D \to \infty$.
Collecting the pieces gives

$$\int \frac{d\omega}{2\pi}\, \mathbf{M}^R(\omega) f(\omega) = \frac{-i}{\beta} \sum_{ik_n} \mathbf{Q}(ik_n) + \mathrm{Im}_{\mathbf{M}_0^R} + \mathrm{Re}_{\mathbf{M}_0^R}. \tag{7.38}$$

To evaluate $\mathbf{Q}(ik_n)$ requires $K^{e,h}_{\mu\mu'}(ik_n + E)$ and $\Lambda^{e,h}_{\mu\mu'}(ik_n + E)$, where E is a (real valued) energy, which is the arguments for $K^{e,h}$ and $\Lambda^{e,h}$ in Eqs. (7.5)-(7.8).

The value D on the integration contour $\tilde{\mathcal{D}}$ corresponds to half the energy band for the lead electrons. So far we have considered the limit $D \to \infty$, i.e. the leads contain electrons with all energies. Instead, we now assign a finite value to D, so the energy of the lead electron are bound by the cut-off, $-D < \varepsilon_{k\eta\sigma} < D$. Moreover, it is assumed symmetric around the equilibrium chemical potential $\mu = 0$, and only temperatures $T \approx 0$ are considered.
From Eq. (7.23) we get

$$\begin{aligned}
\Lambda^e_{\mu\mu'}(ik_n + E) &= \sum_\eta \frac{\tilde{\Gamma}^\eta_{\mu\mu'}}{2\pi} \left[\int_{-D}^{D} d\varepsilon \frac{f_\eta(\varepsilon)}{ik_n + E - \varepsilon} \right] \\
&\approx \sum_\eta \frac{\tilde{\Gamma}^\eta_{\mu\mu'}}{2\pi} \left[\int_{-D}^{0} d\varepsilon \frac{-ik_n + E - \varepsilon}{(E-\varepsilon)^2 + k_n^2} \right] \\
&= \sum_\eta \frac{\tilde{\Gamma}^\eta_{\mu\mu'}}{2\pi} \left[\frac{1}{2} \ln \left[\frac{(E+D)^2 + k_n^2}{E^2 + k_n^2} \right] - i \left(\tan^{-1} \left[\frac{E+D}{k_n} \right] - \tan^{-1} \left[\frac{E}{k_n} \right] \right) \right].
\end{aligned} \tag{7.39}$$

With the same approximation $\Lambda^h_{\mu\mu'}(ik_n + E)$ becomes

$$\Lambda^h_{\mu\mu'}(ik_n + E) = \sum_\eta \frac{\tilde{\Gamma}^\eta_{\mu\mu'}}{2\pi}\left[\frac{1}{2}\ln\left[\frac{E^2+k_n^2}{(E-D)^2+k_n^2}\right] - i\left(\tan^{-1}\left[\frac{E}{k_n}\right] - \tan^{-1}\left[\frac{E-D}{k_n}\right]\right)\right], \tag{7.40}$$

and furthermore holds

$$K^e_{\mu\mu'}(ik_n + E) = \Lambda^h_{\mu\mu'}(ik_n + E), \tag{7.41}$$

$$K^h_{\mu\mu'}(ik_n + E) = \Lambda^e_{\mu\mu'}(ik_n + E). \tag{7.42}$$

From Eq. (7.38) and Eqs. (7.39)-(7.42) the integral over $\mathbf{M}^R(\omega)f(\omega)$ can be obtained, and then the occupancies can be found using Eqs. (7.18)-(7.21). Finally, the Green's functions are determined from Eqs. (7.14)-(7.17).

7.3 Calculation of the current

With the occupancies calculated in the previous section, it is possible to find the Green's function

$$\mathbf{G}^R(\omega) = \begin{pmatrix} G^R_{\uparrow\uparrow}(\omega) & G^R_{\uparrow\downarrow}(\omega) \\ G^R_{\uparrow\downarrow}(\omega) & G^R_{\downarrow\downarrow}(\omega) \end{pmatrix}, \tag{7.43}$$

If $\tilde{\mathbf{\Gamma}}(\omega)$ is independent of energy and it is used that $\mathbf{G}^A(\omega) = \left(\mathbf{G}^R(\omega)\right)^\dagger$ the current formula from Eq. (3.78) can be written as[xi]

$$J = \frac{ie}{\hbar}\frac{\lambda}{1+\lambda}\mathrm{Tr}\left[\tilde{\mathbf{\Gamma}}\int\frac{d\omega}{2\pi}\left(\mathbf{G}^R(\omega) - \left(\mathbf{G}^R(\omega)\right)^\dagger\right)\left(f_L(\omega) - f_R(\omega)\right)\right]. \tag{7.44}$$

The chemical potentials for the leads are defined as

$$\mu_L = \mu + \frac{eV}{2}, \qquad \mu_R = \mu - \frac{eV}{2}, \tag{7.45}$$

where μ is the chemical potential in equilibrium and eV is the applied bias. We could only calculate the Green's function in linear response, so the current calculation is also restricted to linear response, and expanding to first order in eV gives $f_L(\omega) - f_R(\omega) \approx -eV\frac{\partial f(\omega)}{\partial\omega}$. The current formula becomes

$$J = -\frac{ie^2V}{\hbar}\frac{\lambda}{1+\lambda}\mathrm{Tr}\left[\tilde{\mathbf{\Gamma}}\int\frac{d\omega}{2\pi}\left(\mathbf{G}^R(\omega) - \left(\mathbf{G}^R(\omega)\right)^\dagger\right)\frac{\partial f(\omega)}{\partial\omega}\right], \tag{7.46}$$

and after introducing the constant

$$\mathbf{K} = \int\frac{d\omega}{2\pi}\mathbf{G}^R(\omega)\frac{\partial f(\omega)}{\partial\omega} \tag{7.47}$$

[xi] $f_i(\omega) = f(\omega - \mu_i)$, where μ_i is the chemical potential of the i-lead, and $\tilde{\mathbf{\Gamma}}$ is the coupling matrix in the dot spin basis.

we arrive at

$$J = -\frac{ie^2V}{\hbar}\frac{\lambda}{1+\lambda}\mathrm{Tr}\left[\tilde{\mathbf{\Gamma}}(\mathbf{K}-\mathbf{K}^\dagger)\right]. \tag{7.48}$$

Before calculating $\mathbf{K}$, we note that it requires an integral over $\mathbf{M}^R\frac{\partial f(\omega)}{\partial\omega}$ due to Eqs. (7.14)-(7.17). If this integral is calculated on the real axis, the same problems as when calculating the occupancies are encountered. Once again we perform the analytic continuation $\omega + i\eta \to z$ and calculate $\mathbf{K}$ from a contour integral in the complex plane.

The function $\mathbf{G}(z) - \mathbf{G}_0(z)$ does not have poles in the upper half plane, while $\frac{\partial f(z)}{\partial z}$ has poles of order two at $z = ik_n = i\frac{(2n+1)\pi}{\beta}$. As in Sec. A.4.4 the Residue Theorem is applied to obtain

$$\begin{aligned}\mathbf{K} &= \int\frac{d\omega}{2\pi}\left[\mathbf{G}^R(\omega)-\mathbf{G}_0^R(\omega)\right]\frac{\partial f(\omega)}{\partial\omega} + \int\frac{d\omega}{2\pi}\mathbf{G}_0^R(\omega)\frac{\partial f(\omega)}{\partial\omega}\\ &= \int_{\mathcal{C}}\frac{dz}{2\pi}\left[\mathbf{G}(z)-\mathbf{G}_0(z)\right]\frac{\partial f(z)}{\partial z} + \int\frac{d\omega}{2\pi}\mathbf{G}_0^R(\omega)\frac{\partial f(\omega)}{\partial\omega}\\ &= i\sum_n \mathrm{Res}\left[\left(\mathbf{G}(z)-\mathbf{G}_0(z)\right)\frac{\partial f(z)}{\partial z}; ik_n\right] + \int\frac{d\omega}{2\pi}\mathbf{G}_0^R(\omega)\frac{\partial f(\omega)}{\partial\omega}\end{aligned} \tag{7.49}$$

with the same contour as in Fig. 7.1.
The residues are[xii]

$$\mathrm{Res}\left[\left(\mathbf{G}(z)-\mathbf{G}_0(z)\right)\frac{\partial f(z)}{\partial z}; ik_n\right] = \frac{1}{\beta}\left[\mathbf{G}'(ik_n)-\mathbf{G}_0'(ik_n)\right], \tag{7.50}$$

and the derivative of the function $\mathbf{G}(z)$ at ik_n is found numerically as

$$\mathbf{G}'(ik_n) \approx \frac{\mathbf{G}(ik_{n+1})-\mathbf{G}(ik_{n-1})}{4\pi i/\beta}, \tag{7.51}$$

which is valid for large β as we have in our calculation.
The last term in Eq. (7.49) gives

$$\int\frac{d\omega}{2\pi}\mathbf{G}_0^R(\omega)\frac{\partial f(\omega)}{\partial\omega} = \mathcal{P}_{\mathbf{G}_0^R} - \frac{i}{2}\begin{pmatrix}\frac{\partial f}{\partial\omega}(\varepsilon_\uparrow) & 0\\ 0 & \frac{\partial f}{\partial\omega}(\varepsilon_\downarrow)\end{pmatrix}, \tag{7.52}$$

where $\mathcal{P}_{\mathbf{G}_0^R}$ is the principal part of the integral.[xiii]
Now $\mathbf{K}$ can be written as

$$\mathbf{K} = i\sum_{ik_n}\frac{1}{\beta}\left[\mathbf{G}'(ik_n)-\mathbf{G}_0'(ik_n)\right] + \mathcal{P}_{\mathbf{G}_0^R} - \frac{i}{2}\begin{pmatrix}\frac{\partial f}{\partial\omega}(\varepsilon_\uparrow) & 0\\ 0 & \frac{\partial f}{\partial\omega}(\varepsilon_\downarrow)\end{pmatrix} \tag{7.53}$$

[xii] The derivation is in Sec. A.4.2.

[xiii] The principal integral over $\mathbf{G}_0^R$ gives a diagonal matrix with real-valued entries. From Eq. (7.48) it is seen that this part drops out.

and from this expression

$$J = -\frac{ie^2V}{\hbar}\frac{\lambda}{1+\lambda}\mathrm{Tr}\left[\tilde{\mathbf{\Gamma}}(\mathbf{K}-\mathbf{K}^\dagger)\right]. \tag{7.54}$$

can be found.
The results are presented in the next section.

7.4 Results

Everything is ready for solving the equations for the Green's functions and calculating the current. The equations have been implemented in both *Mathematica* and *Matlab*, and the results are identical.
In this section two different cases are considered. First we show that the unified description gives the exact solution in absence of Coulomb repulsion between the electrons on the dot. Then we consider $U \neq 0$ and find some dubious results depending on the value of the coupling strength $\Gamma_{\uparrow'}$.

We are restricted to low temperatures, i.e. that temperature is much smaller than the other energies in the problem, due to the approximations used in Sec. 7.2.3 to obtain the analytic expressions for $K^{e,h}(ik_n)$ and $\Lambda^{e,h}(ik_n)$. The energy unit is chosen to be 200 k_BT. When the residue sums are evaluated to find the occupancies and the current, the number of points in the sums are fixed such that the maximum n, $n_{\max}$, is the largest integer satisfying

$$\frac{(2n+1)\pi}{\beta} < D, \tag{7.55}$$

with D being the band width and $\beta = 1/k_bT$.
The leads are assumed fully polarized, i.e. $\Gamma^{\eta}_{\downarrow'} = 0$, and for simplicity they are also assumed identical, $\Gamma^{L}_{\uparrow'} = \Gamma^{R}_{\uparrow'}$, so $\lambda = 1$.
All the results shown are for the bare dot energy fixed at resonance, $\varepsilon_d = \mu = 0$.[xiv]

Only a very brief interpretation of the results are given in this section. In Chap. 9, where perturbation theory in the tunnelling Hamiltonian is considered, a more thorough examination of the results are given.

7.4.1 No Coulomb repulsion on the dot

As already mentioned in Sec. 6.4, the unified description is exact in the noninteracting limit, $U = 0$, so the results could be calculated directly from the equations in Chap. 4. However, it offers a valuable check of the implementation.

[xiv] The implementation can also calculate the current in case of not fully polarized leads and the bare dot energy away from resonance.

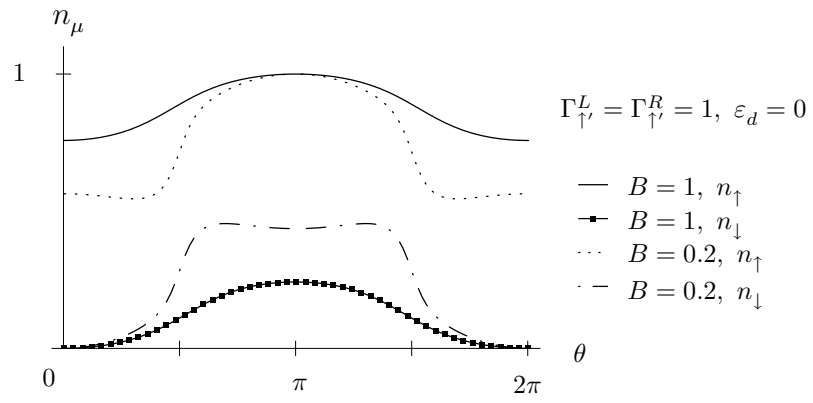

Figure 7.2: The occupations of the dot levels for noninteracting electrons on the dot. The band width is $D = 20$.

The unified description is only supposed to be valid in the weak coupling limit, but for noninteracting electrons this restriction is not needed, so we assign $\Gamma^L_{\uparrow'} = \Gamma^R_{\uparrow'} = 1$ and set $B = 0.2$ and $B = 1$.
Due to tunnelling, a broadening of the dot energy levels occurs and the width of the energy levels are equal to the imaginary part of the self-energy. For the FAB model the self-energy depend on the angle θ, but for noninteracting electrons it is at most equal to $\Gamma_{\uparrow'} = \Gamma^L_{\uparrow'} + \Gamma^R_{\uparrow'}$, see Eq. (4.21). The value for the band width is unimportant as long as the dot energy levels are well inside the band, i.e. $\left|\varepsilon_\mu\right| + \Gamma_{\uparrow'} \ll D$, and it is therefore fixed at $D = 20$.

Fig. 7.2 shows the occupations of the dot levels, $n_\uparrow$ and $n_\downarrow$. If $B = 0.2$ both energy levels are close to resonance and for $\theta = 0$ the lower energy level, $\varepsilon_\uparrow$, is half-filled because electrons tunnel through it (see Fig. 4.2). The other level is blocked due to spin blockade, and because the energy is above the chemical potentials of the leads it is empty.
For $\theta = \frac{\pi}{2}$ the spin-$\uparrow$ level is blocked, but because the energy is below the chemical potentials it is always occupied. Current flow through the spin-$\downarrow$ state giving a half-filled level. When B is increased the energy levels are moved further away from resonance and the lower energy level gets more filled, while the spin-$\downarrow$ level is emptied.

In Fig. 7.3 the results obtained with the unified description are compared with the exact results derived in Chap. 4. For $B = 1$ perfect agreement is seen whereas for $B = 0.2$ the results also match, except in a very tiny region around the resonance points.

It can be concluded that the unified approach and the implementation gives the exact result in the limit $U = 0$.

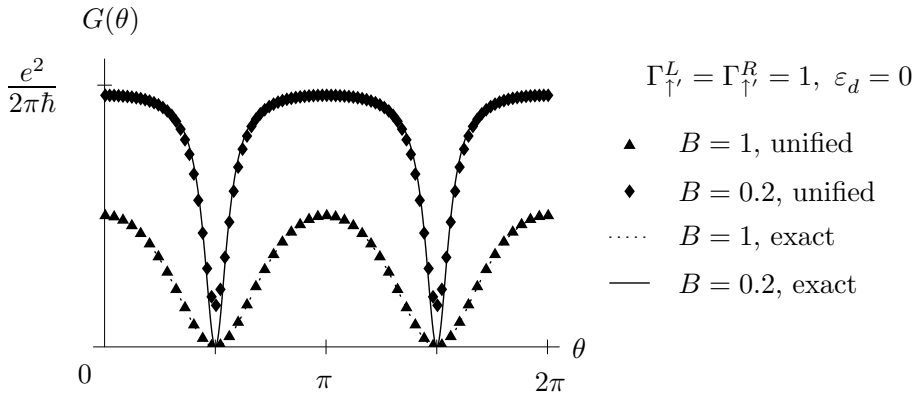

Figure 7.3: The conductance for noninteracting electrons on the dot calculated with the unified description of tunnelling and the exact expression, Eq. (4.25). The band width is $D = 20$.

7.4.2 Interacting electrons on the dot

For interacting electrons on the dot the unified description should only be applied in the weak tunnelling limit. In this section results are shown for different values of the coupling parameter and the Coulomb repulsion. In the rest of this section $B = 1$.

For interacting electrons on the dot the level widths are unknown. However, in the weak tunnelling limit they are assumed to be almost equal to their values in case of non-interacting electrons on the dot. Values of U up to 15 is considered, giving $\varepsilon_2 = 15$, so the band width is set to $D = 50$.

We start with $\Gamma^L_{\uparrow'} = \Gamma^R_{\uparrow'} = 0.01$. The energy levels are far from the chemical potentials of the lead and the occupancies (not shown) are $n_\uparrow \approx 1$ and $n_\downarrow \approx 0$ for all θ.
The results for $U = 0.1,\ 0.5$ and 0.7 are shown in Fig. 7.4.
At the resonance points $\theta = \frac{\pi}{2}$ and $\theta = \frac{3\pi}{2}$ the conductance is enhanced, because the destructive interference existing for $U = 0$ is destroyed (see Sec. 4.1). Moreover, the conductance diminishes at $\theta = \pi$ because the current has to flow through the doubled occupied state, which has an increased energy.[xv]
For $U = 0.1$ and $U = 0.5$ the conductance appear to be slightly negative. This is of course clearly unphysical, but might be due to numerical problems. It becomes even worse for $U = 1,\ 1.2$ and 2 where the results are obviously wrong, as shown in Fig. 7.5. The spin-$\downarrow$ level and the doubled occupied state are degenerate for $U = 1$ which could cause numerical difficulties.
The conductance becomes positive if U is further increased (see Fig. 7.6) and the conductance is finite for all angles. For large values of U the current cannot flow through the spin-$\downarrow$ level due to the high energy of the doubled occupied state. A simple spin blockade

[xv] The physical mechanism behind the new features for increasing U is explained in detail in Chap. 9.

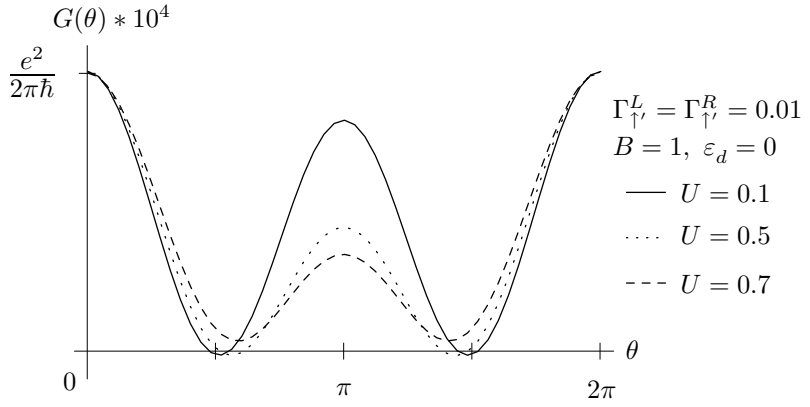

Figure 7.4: Conductance for small values of the magnetic field strength B. The band width is $D = 50$.

behaviour is observed, where the conductance decreases monotonically from $\theta = 0$ to π as the spin-$\uparrow$ level is gradually closed.
The large U limit resembles the results found in Chap. 9, where the co-tunnelling results are presented. However, they show that the conductance vanishes at $\theta = \pi$.

The results seems reasonable for $U < \left|\varepsilon_\mu\right|$, but are clearly wrong for $U \approx B$. In the large U limits they are very doubtful.

Increasing $\Gamma_{\uparrow'}$ by a factor of 10 gives almost the same results, as shown in Sec. A.4.5. The only difference is the appearance of a considerable negative conductance even for small values of U.
Eventually, results are plotted for $\Gamma^L_{\uparrow'} = \Gamma^L_{\uparrow'} = 0.5$, see Fig. 7.7. The unified description is not supposed to hold for that strong couplings and the results show negative conductance even for small values of U, and also for $U = 10$. Moreover, the occupation of the spin-$\downarrow$ level is negative for $\theta \approx 0$ and for the spin-$\uparrow$ level the occupation is greater than one for $\theta \approx \pi$. This is obviously not a valid result.

7.5 Discussion of the results

The doubtful results in the last section give rise to questioning the unified description and the implementation of the model.

The approximation scheme applied to derive the unified description was also used by LaCroix [18] for dealing with the Anderson Hamiltonian. She pointed out that cross-terms like $\left\langle c^\dagger_{k\eta}|\gamma\rangle\langle\alpha'|\right\rangle$ in the equations of motion diverge for temperatures below a certain temperature T_K. So neglecting them, as we did in our derivation, is not correct for $T < T_K$. The temperature T_K is the so-called Kondo temperature and the Kondo effect in quan-

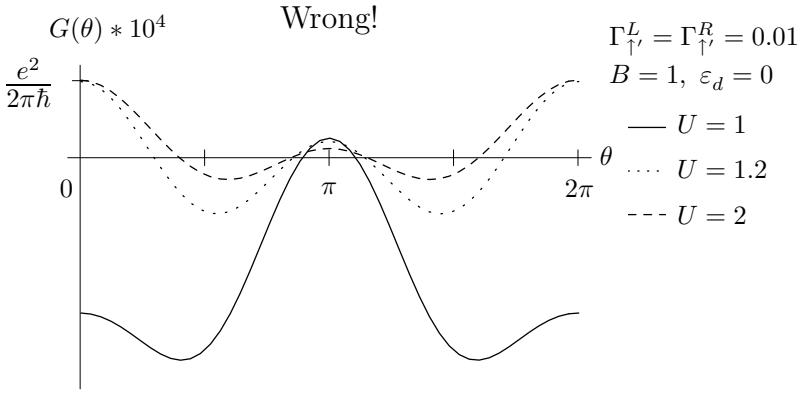

Figure 7.5: The conductance for various values of $U \approx B$. The results are clearly unphysical because of the negative values for the conductance. The band width is $D = 50$.

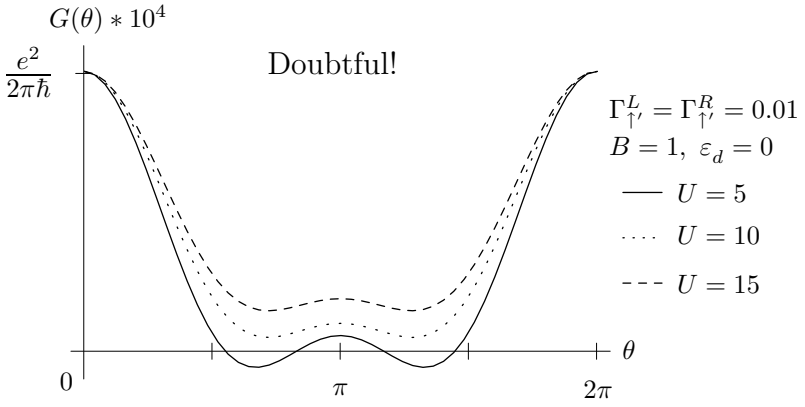

Figure 7.6: Increasing U gives positive conductance for $U > 5$. The band width is $D = 50$.

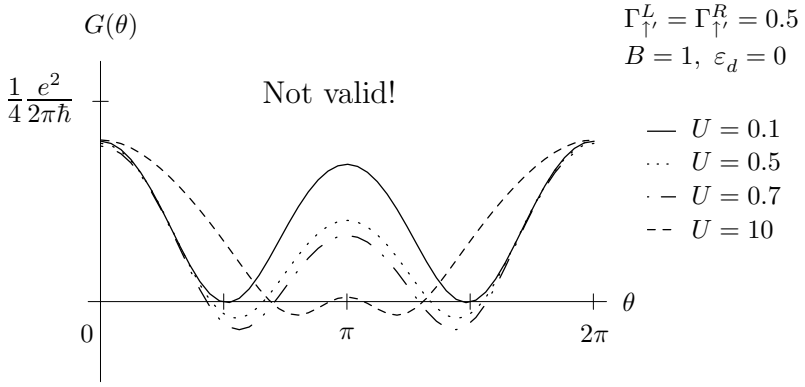

Figure 7.7: Plot of the conductance outside the range of weak tunnelling. The band width is $D = 50$.

tum dots is a well known phenomenon. It appears due to the interactions between the lead electrons and a localized spin on the dot, and it is described via the so-called Kondo Hamiltonian.[xvi] Studying the Kondo effect is a field of it own and an introduction to it is not given here. It is just noticed that the effect gives rise to an enhanced conductance below T_K, and in the same temperature limit a sharp peak in the density of states appear at the chemical potentials of the leads because of logaritmic singularities. If the energy level of the localized spin state is well below the chemical potentials of the leads, the Anderson Hamiltonian can be mapped onto the Kondo Hamiltonian [19], so the Kondo effect is present in the Anderson Hamiltonian.
In the Kondo problem the leads are not assumed fully polarized because the effect is due to the presence of two different spins and there has been a debate concerning the influence of ferromagnetic leads on the Kondo effect. Recent work has shown that the ferromagnetic leads suppress the effect, but also the possibility of restoring it by applying an external magnetic field. However, not for fully polarized leads.[xvii]
Our model contains both fully polarized leads and an applied magnetic field, but maybe the possibility of having logaritmic divergences exists. The rotation of the magnetic field introducing different spin bases complicates the problem and makes it even more difficult to find the regime, where the approximation scheme can be safely applied.

In the implementation it was assumed that the temperature is low, which gave a simple analytic expression for the $K^{e,h}$ and $\Lambda^{e,h}$ on the imaginary axis. If temperature is increased they have to be calculated numerically which requires more computer time and no effect is observed in the low temperature limit.
When calculating the residue sums, the arc L' in the complex plane is neglected in the contour integral along $\tilde{\mathcal{D}}$ (see Fig. 7.1). When D is sufficiently large this approach is valid because the integrand tends to zero faster than $\frac{1}{|z|^2}$. An attempt to calculate the integral along L' has been done, but it is difficult for numerical reasons. Remember that the spacing between the poles on the real axis are proportional to $1/\beta$, so the contour runs close to the poles at low temperatures.

Solving the FAB model using the unified description have not given a clear answer to the question of how the conductance changes for increasing U. It seems like the conductance is enhanced at the resonance angles and suppressed at $\theta = \pi$, as already explained. The effect of increasing U is further discussed in Chap. 9.

[xvi] It is same effect which gives the enhanced zero-temperature resistivity in metals with magnetic impurities.
[xvii] See [20] and [21].

Chapter 8

Rate equation approach to a single level with spin

In this chapter, we will introduce another way of dealing with quantum transport, known as the quantum rate equation approach. It amounts to finding an expression for the time-derivative of the elements of the density matrix. In steady state these equations can be solved and an expression for the current can be obtained.
The reason for the name quantum rate equations is that they involve the non-diagonal elements of the density matrix which is not the case for a classical rate equation. The non-diagonal elements deal with the superposition of different quantum states and therefore account for the coherence effects we are interested in. An example of the superposition of states could be two coupled quantum dots, where the tunnelling between the dots will create a bonding and an anti-bonding state. When an electron tunnels into the system, it will "see" these states rather than the states for the isolated dots. This gives rise to interference effects which can be observed in the current.

There are several ways of deriving the rate equations. In [12] the equations are derived from the classical rate equations for some specific systems and the method is used in [11] to deal with two coupled quantum dots. A more rigorous approach is presented by Gurvitz and Prager [10] where the quantum rate equations are derived from a microscopic Hamiltonian for a general mesoscopic system. However, both methods are only valid in case of a large bias voltage, and for the FAB model we are interested in the interference effect, which takes place when the energy levels are close to the chemical potentials of the leads. Therefore none of the two methods can be applied.
Instead an attempt to derive the rate equations for the FAB model is presented based on an article by Bing Dong *et al.* [4]. They derive the rate equations for an Anderson model using nonequilibrium Green's functions, and with some modifications the result can be applied to the FAB model. In the article they claim that the equations are valid for arbitrary bias voltages and temperatures. We will show that it is *not* the case and that the equations only hold in the large bias limit, and consequently it is not an extension of the previously published results ([10],[12]). Moreover, we found several inconsistencies in

the derivation which we have corrected or just pointed out.
That the approach could not be applied to the FAB model in linear response was first realized after the calculations had been carried out. Nevertheless, this chapter is kept in the thesis because the rate equation approach is widely used when treating quantum transport.

First we give a very brief introduction to the idea of rate equations, and afterwards the ideas behind the derivation of the rate equations are presented. The mathematical derivation is rather technical and lengthy but some of it is sketched in Sec. 8.3, and the rest can be derived in exactly the same way. Finally, it is shown why the equations are only valid for high temperatures or in the large bias limit.

8.1 Density matrix and rate equations

We start by considering the simple situation were we have a system in a state described by the normalized wave function ψ. The density operator $\hat{\rho}$ is defined through the relation[i]

$$\langle A\rangle = \langle\psi|\hat{A}|\psi\rangle \equiv \mathrm{Tr}\left[\hat{\rho}\hat{A}\right] \tag{8.1}$$

where $\hat{A}$ is any operator for some physical observable A and $\langle\cdot\rangle$ means expectation value. If $\{|n\rangle\}$ is a complete set spanning the Hilbert space, we find

$$\begin{aligned}\langle A\rangle &= \sum_{nm}\langle\psi|n\rangle\langle n|\hat{A}|m\rangle\langle m|\psi\rangle \\ &= \sum_{nm}\rho_{mn}A_{nm}\end{aligned} \tag{8.2}$$

where we have made the identification $\hat{\rho} = |\psi\rangle\langle\psi|$. It is simple to show that $\hat{\rho}$ fulfills $\mathrm{Tr}[\hat{\rho}] = 1$.

Now we instead consider a system in a so-called mixed state, meaning that the probability of finding the system in the state ψ_i is given by a weight factor w_i. The weight factors are classical probabilities, $w_i \in [0,1]$, and they obey the sum rule $\sum_i w_i = 1$.
An example of a mixed ensemble could be a system in thermal equilibrium. If the states $|\nu\rangle$ are eigenstates of the Hamiltonian with eigenenergies E_ν, them the probability of finding the system in the state $|\nu\rangle$ is $e^{-\beta E_\nu}/Z$, with Z being the partition function $Z = \sum_\nu e^{-\beta E_\nu}$ and $\beta = k_bT$. Another example could be spin-$\frac{1}{2}$ particles where a certain fraction have the spin along the x-axis, another fraction have along the y-axis and the remaining have along the z-axis.[ii]
For the mixed ensemble the expectation value (often called the ensemble average) of an operator A is given as

$$\langle A\rangle = \sum_i w_i A^i = \sum_i w_i\langle\psi_i|\hat{A}|\psi_i\rangle = \sum_{inm} w_i\rho^i_{mn}A_{nm} = \mathrm{Tr}\left[\left(\sum_i w_i\hat{\rho}^i\right)\hat{A}\right]. \tag{8.3}$$

[i] This section is written on basis of [25], [24] and [1]. Solely in this section operators are marked with a hat.

[ii] See [25].

This leads to the following definition of the density operator for the mixed ensemble

$$\hat{\rho} = \sum_i w_i \hat{\rho}^i = \sum_i w_i |\psi_i\rangle\langle\psi_i|. \tag{8.4}$$

The elements of the density matrix are

$$\rho_{mn} = \sum_i w_i \langle m|\psi_i\rangle\langle\psi_i|n\rangle = \sum_i w_i \langle\psi_i|n\rangle\langle m|\psi_i\rangle = \langle |n\rangle\langle m| \rangle \,. \tag{8.5}$$

So finally we have obtained that the elements of the density operator for the mixed ensemble are the expectation values of the operators $|n\rangle\langle m|$. This will be used in the following sections.
Note that the trace is independent of basis, and therefore can the traces in Eqs. (8.1)-(8.3) be carried out in the most convenient basis.

We end this this section by pointing out that knowing the density matrix gives information about any physical observable. This is often used in the branch of physics known as quantum statistical mechanics, were the problems are so complex that the wave functions are not known and one has to use statistical arguments instead.
In the next section we will show how the current can be found when the elements of the density matrix are determined.

8.2 The idea behind the derivation of the rate equations

In this section it is presented how the rate equations are derived in [4], but also where we have made necessary corrections. However, they consider the Hamiltonian

$$\begin{aligned} H^{BD} = &\sum_{\eta,k,\sigma} \varepsilon_{\eta k\sigma} c^\dagger_{\eta k\sigma} c_{\eta k\sigma} + \sum_{\eta,\sigma} \left(V_{\eta\sigma} c^\dagger_{\eta k\sigma} c_{d\sigma} + h.c. \right) \\ &+ \varepsilon_d \sum_\sigma c^\dagger_{d\sigma} c_{d\sigma} + \sum_\sigma R_\sigma c^\dagger_{d\bar{\sigma}} c_{d\sigma} + U n_{d\uparrow} n_{d\downarrow} \end{aligned} \tag{8.6}$$

whereas we derive the rate equations for a system described by the model Hamiltonian introduced in section Sec. 2.1

$$\begin{aligned} H = &\sum_{\eta,k,\sigma} \varepsilon_{\eta k\sigma} c^\dagger_{\eta k\sigma} c_{\eta k\sigma} + \sum_{\eta,\sigma} \left(V_{\eta k\sigma} c^\dagger_{\eta k\sigma} c_{d\sigma} + h.c. \right) \\ &+ \sum_\sigma (\varepsilon_\sigma - \sigma B \cos\theta) c^\dagger_{d\sigma} c_{d\sigma} - \sum_\sigma B \sin\theta c^\dagger_{d\bar{\sigma}} c_{d\sigma} + U n_{d\uparrow'} n_{d\downarrow'}, \end{aligned} \tag{8.7}$$

In the beginning write the spin of the dot electrons in the lead spin basis.

The starting point is to realize that the dot annihilation operator can be written in terms of the the four states $|0\rangle$, $|\uparrow'\rangle$, $|\downarrow'\rangle$, $|2\rangle = c^\dagger_{d\downarrow'} c^\dagger_{d\uparrow'} |0\rangle$ corresponding to the empty state, a single electron with spin up, a single electron with spin down and the double

occupied state. By comparison when acting on the different dot states, it is seen that $c_{d\sigma}$ can be written as[iii]

$$c_{d\sigma} = |0\rangle\langle\sigma| + \sigma|\bar{\sigma}\rangle\langle 2|. \tag{8.8}$$

The four states spans the dot Hilbert space, so the operators satisfy

$$|0\rangle\langle 0| + \sum_{\sigma} |\sigma\rangle\langle\sigma| + |2\rangle\langle 2| = 1, \tag{8.9}$$

and from the Dirac kets it is easy to check that the commutator relations for the operators $c_{d\sigma}$ are fulfilled. In terms of the new operators the Hamiltonian reads

$$\begin{aligned} H = &\sum_{\eta,k,\sigma} \varepsilon_{\eta k\sigma} c^{\dagger}_{\eta k\sigma} c_{\eta k\sigma} + \sum_{\eta,\sigma} \left(V_{\eta\sigma} c^{\dagger}_{\eta k\sigma} (|0\rangle\langle\sigma| + \sigma|\bar{\sigma}\rangle\langle 2|) + h.c. \right) \\ &+ \sum_{\sigma} (\varepsilon_{\sigma} - \sigma B\cos\theta)|\sigma\rangle\langle\sigma| - \sum_{\sigma} B\sin\theta|\bar{\sigma}\rangle\langle\sigma| + U|2\rangle\langle 2| \end{aligned} \tag{8.10}$$

Recall from Eq. (8.5) that the elements of the density matrix ρ_{mn} in the lead spin basis are the expectation values of the operators $|n\rangle\langle m|$ (with $n, m = 0, \uparrow', \downarrow', 2$) so we can write[iv]

$$\rho_{00} = \langle |0\rangle\langle 0| \rangle , \qquad \rho_{\sigma\sigma} = \langle |\sigma\rangle\langle\sigma| \rangle , \tag{8.11}$$

$$\rho_{22} = \langle |2\rangle\langle 2| \rangle , \quad \langle \rho_{\sigma\bar{\sigma}} \rangle = \langle |\bar{\sigma}\rangle\langle\sigma| \rangle . \tag{8.12}$$

The other non-diagonal elements of the density matrix are not calculated, because they do not appear in the expression for the current.
The time evolution of the density matrix elements can be expressed in terms of the expectation values for the new operators. For instance,

$$i\dot{\rho}_{00} = i\frac{\partial}{\partial t} \langle |0\rangle\langle 0| \rangle = \langle [|0\rangle\langle 0|, H] \rangle . \tag{8.13}$$

Now the setup is ready for deriving the rate equations. Using the Hamiltonian written in terms of the new operators and the commutator rules for the pseudo-operators, we easily find the commutators for the operators $|0\rangle\langle 0|$, $|\sigma\rangle\langle\sigma|$, $|2\rangle\langle 2|$ and $|\sigma\rangle\langle\bar{\sigma}|$ with H. Taking the expectation values gives the equation of motion for the elements of the density matrix, but expectation values like $\left\langle (c^{\dagger}_{\eta,k,\bar{\sigma}} |\sigma\rangle\langle 2|)(t) \right\rangle$ have to be calculated. This is where the nonequilibrium Green's functions (NGFs) come into play, because these expectation values

[iii] In the article by Bing Dong *et al.* they introduce a slave-particle formlism inspired by the work in [17]. That is not needed and furthermore it is done incorrectly, because the commutator relations between the operators defined in the article are wrong.

[iv] In the following the time dependence of the operators and the elements of the density matrix will be suppressed.

correspond to the time-diagonal parts of the NGFs

$$G^{<}_{\sigma' 2,\eta k\sigma}(t,t') \equiv i\left\langle c^{\dagger}_{\eta k\sigma}(t')(|\sigma'\rangle\langle 2|)(t)\right\rangle, \tag{8.14}$$

$$G^{<}_{0\sigma,\eta k\sigma'}(t,t') \equiv i\left\langle c^{\dagger}_{\eta k\sigma'}(t')(|0\rangle\langle\sigma|)(t)\right\rangle, \tag{8.15}$$

$$G^{<}_{\eta k\sigma',0\sigma,}(t,t') \equiv i\left\langle (|\sigma\rangle\langle 0|)(t')c^{\dagger}_{\eta k\sigma'}(t)\right\rangle, \tag{8.16}$$

$$G^{<}_{\eta k\sigma,\sigma' 2}(t,t') \equiv i\left\langle (|2\rangle\langle\sigma'|)(t')c_{\eta k\sigma}(t)\right\rangle. \tag{8.17}$$

They are named current Greens's functions because they describe tunnelling between the leads and and the dot. The theory for NGFs can be applied to get expressions for these lesser and greater Green's functions in terms of the lead and dot Green's functions, exactly as in Sec. 3.5. However, in [4] they do not derive the expressions for the time-ordered Green's function properly as we will show[v], because they neglect Green's functions which are of higher order in the coupling. It turns out that it does not change the final result due to approximations made at some later stage.
As in Chap. 4 we take the Wide Band Limit, i.e. we assume that the density of states and the transition matrix elements for tunnelling from the lead to the dot are constant for the energies of interest. We end up with an expression for e.g. $\rho_{\sigma\sigma}$ which is

$$\begin{aligned}\dot{\rho}_{\sigma\sigma} = \frac{i}{2\pi}\int d\omega \sum_{\eta=L,R}\Big\{&\Gamma^{\eta}_{\sigma} f_{\eta}(\omega) G^{>}_{0\sigma\sigma}(\omega) + \Gamma^{\eta}_{\sigma}\left[1-f_{\eta}(\omega)\right] G^{<}_{0\sigma\sigma}(\omega)\\ &- \Gamma^{\eta}_{\bar{\sigma}} f_{\eta}(\omega) G^{>}_{2\sigma\sigma}(\omega) - \Gamma^{\eta}_{\bar{\sigma}}\left[1-f_{\eta}(\omega)\right] G^{<}_{2\sigma\sigma}(\omega)\Big\} - iB\sin\theta\left[\rho_{\sigma\bar{\sigma}} - \rho_{\bar{\sigma}\sigma}\right].\end{aligned} \tag{8.18}$$

The constant $\Gamma^{\eta}_{\sigma} = 2\pi\sum_k |V_{\eta k\sigma}|^2 \delta(\varepsilon - \varepsilon_{\eta k\sigma})$ is the (energy independent) coupling parameter and $f_{\eta}(\omega)$ is the Fermi function for the η-lead. The coupling parameters Γ^{η}_{σ} are in this formalism named (scattering) rates because they are related to the rate of change in the occupancies of the dot states, see Eqs. (8.55)-(8.58). Each term in the sum is the probability per unit time for a transition where an electron in state $\eta k\sigma$ leaves the lead η and enters the dot (or the opposite process). It is identical to Fermi's Golden Rule, which is often directly used when writing up rate equations for less complicated systems.

The new Green's functions in Eq. (8.18) are dot Green's functions defined as

$$G^{<}_{0\sigma\sigma'}(t,t') \equiv i\left\langle (|\sigma'\rangle\langle 0|)(t')(|0\rangle\langle\sigma|)(t)\right\rangle, \tag{8.19}$$

$$G^{>}_{0\sigma\sigma'}(t,t') \equiv -i\left\langle (|0\rangle\langle\sigma|)(t)(|\sigma'\rangle\langle 0|)(t')\right\rangle, \tag{8.20}$$

$$G^{<}_{2\sigma\sigma'}(t,t') \equiv i\sigma\sigma'\left\langle (|2\rangle\langle\sigma'|)(t')(|\sigma\rangle\langle 2|)(t)\right\rangle, \tag{8.21}$$

$$G^{>}_{2\sigma\sigma'}(t,t') \equiv -i\sigma\sigma'\left\langle (|\sigma\rangle\langle 2|)(t)(|2\rangle\langle\sigma'|)(t')\right\rangle. \tag{8.22}$$

Again we use the assumption of weak coupling, but in a somewhat subtle way which is not well explained in [4].
First we consider the Green's function for the isolated dot, i.e. in absence of coupling.

[v] See Sec. A.5.

Bing Dong *et al.* use the approximation that the spin-flip term $R_\sigma c^\dagger_{d\sigma} c_{d\bar{\sigma}}$ in Eq. (8.6) is small, so the term is neglected when calculating the Green's functions for the isolated dot. As we will explain later this is clearly inconsistent, so instead we choose to diagonalize the dot Hamiltonian and introduce a new spin basis. The diagonalization was already done in Sec. 2.3, and in the diagonal basis the dot Green's functions are easy to calculate, e.g.

$$G^{<,0}_{0\mu\mu'}(t,t') = \left\langle (|\mu'\rangle\langle 0|)(t')(|0\rangle\langle\mu|)(t)\right\rangle_0 = ie^{-i\varepsilon_\mu(t-t')}\rho^0_{\mu\mu'}, \tag{8.23}$$

where the subscript indicates that the average is with respect to the dot Hamiltonian, and μ and μ' are spins in the diagonal basis. The Green's functions in Eqs. (8.19)-(8.22), which are written in the nondiagonal basis, can of course be expressed in the terms of the diagonal Green's function (see Eq. (8.48)).
The Green's function for the isolated dot depends only on the difference between the time arguments, so after a Fourier transformation $G^{<,0}_{0\mu\mu'}(t,t')$ becomes

$$G^{<,0}_{0\mu\mu'}(\omega) = 2\pi i\rho^0_{\mu\mu'}\delta(\omega-\varepsilon_\mu), \tag{8.24}$$

which means that the spin-μ level is peaked right at ε_μ.
No we can invoke the assumption of weak coupling and assume that the Green's function in presence of tunnelling can be written on the same form as the decoupled Green's function, i.e.

$$G^{<}_{0\mu\mu'}(t,t') = ie^{-i\varepsilon_\mu(t-t')}\rho_{\mu\mu'}(t,t), \tag{8.25}$$

where the Green's function consists of a rapidly varying phase depending on the difference between the time arguments, and an occupation which is local in time. The assumption that the occupation is local in time is the so-called Markov approximation. It has the physical meaning that the probability of a tunnelling event at a given time t depend only on the occupation at that particular time, i.e. there is no memory-structure in the system. This is reasonable when tunnelling happens rarely and the system is in the same state at each tunnelling event, i.e. when the coupling is weak. Moreover, it turns out that in order to proceed in the calculations we have to assume that the occupations are constant. In the end we are only interested in the steady state result, and there this approximation is valid.
After a Fourier transformation we find

$$G^{<}_{0\mu\mu'}(\omega) = 2\pi i\rho_{\mu\mu'}\delta(\omega-\varepsilon_\mu). \tag{8.26}$$

It is seen that the assumptions imply that that no broadning of the energy level occurs due to tunnelling, so the state is still peaked right at the energy ε_μ. The approximation is only valid when the coupling is much smaller than the temperature.
The Green's function for the dot in presence of coupling is inserted in Eq. (8.18), and after carrying out the trivial ω integral we have obtained an expression for $\dot{\rho}_{\sigma\sigma}$. Remembering that we have assumed steady state and the occupations therefore are constant, we have that $\dot{\rho}_{\sigma\sigma}$ is equal to zero.

Finally, we end up with a matrix equation on the form

$$\overline{0} = \mathbf{\Xi}\ \overline{\rho}, \tag{8.27}$$

where $\mathbf{\Xi}$ is a coefficient matrix and $\overline{\rho} = (\rho_{00}, \rho_{\uparrow\uparrow}, \rho_{\downarrow\downarrow}, \rho_{22}, \rho_{\uparrow\downarrow}, \rho_{\downarrow\uparrow})$. The resulting homogenous equation system can be solved using the normalization $\rho_{00} + \rho_{22} + \sum_\mu \rho_{\mu\mu} = 1$.

The current operator is defined in terms of the operator

$$N_\eta(t) = \sum_{k\sigma} c^\dagger_{\eta k\sigma}(t) c_{\eta k\sigma}(t), \tag{8.28}$$

which counts the number of electrons in the lead η at time t. The current I_η is the rate of change in electrons in the η-lead, i.e.

$$I_\eta(t) = -e\left\langle \frac{dN_\eta(t)}{dt} \right\rangle = -ie\left\langle \left[H, \sum_{k\sigma} c^\dagger_{\eta k\sigma} c_{\eta k\sigma} \right] \right\rangle, \tag{8.29}$$

and the derivation of $I_\eta(t)$ is done in the same way as for the occupancies. We end up with an expression for the current in terms of the elements of the density matrix.

We return to the corrections we have made when deriving the rate equations presented in the article by Bing Dong *et al.*.
First we note that the incorrect derivation of the current Green's functions have no consequences. The time-ordered Green's function they have neglected are of the type

$$G^t_{0\sigma,\sigma' 2}(t,t') = -i\left\langle T_t\left[(|0\rangle\langle\sigma|)(t)(|2\rangle\langle\sigma'|)(t') \right] \right\rangle. \tag{8.30}$$

It is easily verified that Green's functions of this type vanish if the dot is isolated. Again we assume that the Green's functions in presence of tunnelling resemble those for the isolated dot, so therefore these Green's functions are neglected even in presence of tunnelling. This approximation is only valid in case of weak coupling between the leads and the dot. Furthermore, when calculating $G^{<,>,0}$ they use in [4] the approximation that the spin-flip term $R_\sigma c^\dagger_{d\sigma} c_{d\bar{\sigma}}$ in Eq. (8.6) is small, so the term is neglected when calculating the Green's functions for the isolated dot. This assumption has the apparent advantage that the rate equations becomes very simple and intuitive. Furthermore, the limit of strong Coulomb repulsion or strong bias can be taken analytically, and the result can be compared to other ways of deriving the rate equations for a system described by the model Hamiltonian H^{BD} ([10],[12]).
Although this way of handling the Green's functions seems very appealing it is obviously not consistent, because the term proportional to R_σ is kept in the expression for the rate equations (for our model the term $-iB\sin\theta[\rho_{\sigma\bar{\sigma}} - \rho_{\bar{\sigma}\sigma}]$ in Eq. (8.18)). This term couples the diagonal matrix elements with the non-diagonal parts of the density matrix. In order to be consistent this term should also be treated as small, but that will destroy the coherence effect we are interested in.
We go beyond this approximation by diagonalizing the dot Hamiltonian. The equations

get more complicated, but they are valid for all values of the magnetic field.

In the next section the derivation will be presented.

8.3 Derivation of the rate equations

As already mentioned the derivation is rather long and cumbersome, and it will only be shown how to calculate the equation for $\dot{\rho}_{\sigma\sigma}$ in Eq. (8.27). The other equations are derived in the exact same way and only the final results will be presented here.

The time-derivative of $\hat{\rho}_{\sigma\sigma}$ is $\dot{\hat{\rho}}_{\sigma\sigma} = i\left[H, |\sigma\rangle\langle\sigma|\right]$. Using the commutator rules for the new operators we find

$$\begin{aligned} i\left[H, |\sigma\rangle\langle\sigma|\right] = i\sum_{\eta k}\Big[V_{\eta k\sigma}c^{\dagger}_{\eta k\sigma}|0\rangle\langle\sigma| - \bar{\sigma}V_{\eta k\bar{\sigma}}c^{\dagger}_{\eta k\bar{\sigma}}|\sigma\rangle\langle 2| - V^{*}_{\eta k\bar{\sigma}}|\sigma\rangle\langle 0|c_{\eta k\sigma} + \bar{\sigma}V^{*}_{\eta k\bar{\sigma}}|2\rangle\langle\bar{\sigma}|c_{\eta k\bar{\sigma}}\Big] \\ - iB\sin\theta\left(|\bar{\sigma}\rangle\langle\sigma| - |\sigma\rangle\langle\bar{\sigma}|\right) \end{aligned} \tag{8.31}$$

Taking the expectation value on both sides and using Eqs.(8.14)-(8.17) we obtain

$$\begin{aligned} \dot{\rho}_{\sigma\sigma} = \sum_{\eta k}\Big[V_{\eta k\sigma}G^{<}_{0\sigma,\eta k\sigma}(t,t) - \bar{\sigma}V_{\eta k\bar{\sigma}}G^{<}_{2\sigma,\eta k\bar{\sigma}}(t,t) - V^{*}_{\eta k\sigma}G^{<}_{\eta k\sigma,0\sigma}(t,t) + \bar{\sigma}V^{*}_{\eta k\bar{\sigma}}G^{<}_{\eta k\bar{\sigma},\sigma 2}(t,t)\Big] \\ - iB\sin\theta\left[\rho_{\sigma\bar{\sigma}} - \rho_{\bar{\sigma}\sigma}\right] \end{aligned} \tag{8.32}$$

where the NGFs from Eqs. (8.19)-(8.22) have been inserted. Like when deriving the current formula in Sec. 3.5 the lesser current Green's functions can be found from the contour-ordered Green's functions using the rules for analytic continuation. In the article the expressions for the current Green's functions in Eqs. (8.33)-(8.36) are stated as the exact expressions, but they have neglected/forgotten the Green's which couple the doubled occupied and the empty state, as shown in Sec. A.5. It is consistent with the approximation where the Green's functions are on the same form as those for the isolated dot, so it does not change their final result.
The approximated current Green's functions are

$$\hat{G}^{<}_{0\sigma,\eta k\sigma'}(t,t') = \int dt_1\Big[G^{R}_{0\sigma\sigma'}(t,t_1)V_{\eta k\sigma'}g^{<}_{\eta k\sigma'}(t_1,t') + G^{<}_{0\sigma\sigma'}(t,t_1)V_{\eta k\sigma'}g^{A}_{\eta k\sigma'}(t_1,t')\Big], \tag{8.33}$$

$$\hat{G}^{<}_{\sigma 2,\eta k\sigma'}(t,t') = \sigma'\int dt_1\Big[G^{R}_{2\sigma\bar{\sigma'}}(t,t_1)V_{\eta k\sigma'}g^{<}_{\eta k\sigma'}(t_1,t') + G^{<}_{2\sigma\bar{\sigma'}}(t,t_1)V_{\eta k\sigma'}g^{A}_{\eta k\sigma'}(t_1,t')\Big], \tag{8.34}$$

$$\hat{G}^{<}_{\eta k\sigma',0\sigma}(t,t') = \int dt_1\Big[g^{R}_{\eta k\sigma'}(t,t_1)V_{\eta k\sigma'}G^{<}_{0\sigma'\sigma}(t_1,t') + g^{<}_{\eta k\sigma'}(t,t_1)V_{\eta k\sigma'}G^{A}_{0\sigma'\sigma}(t_1,t')\Big], \tag{8.35}$$

$$\hat{G}^{<}_{\eta k\sigma',\sigma 2}(t,t') = \sigma'\int dt_1\Big[g^{R}_{\eta k\sigma'}(t,t_1)V_{\eta k\sigma'}G^{<}_{2\bar{\sigma'}\sigma}(t_1,t') + g^{<}_{\eta k\sigma'}(t,t_1)V_{\eta k\sigma'}G^{A}_{2\bar{\sigma'}\sigma}(t_1,t')\Big]. \tag{8.36}$$

$G_{0\sigma\sigma'}$ and $G_{2\sigma\sigma'}$ are the NGFs for the dot, while $g_{\eta k\sigma}$ is the Green's function for the η-lead in absence of tunnelling. If it is assumed that the dot Green's functions only depend on the difference between the time arguments, meaning that the system is in steady state with no initial effects present, the Fourier transformed Green's functions can be found. From the convolution theorem for Fourier transforms we get

$$\int dt_1 A(t-t_1)B(t_1-t) = \int du A(u)B(-u) = \int \frac{d\omega}{2\pi} A(\omega)B(\omega), \tag{8.37}$$

and inserting the approximated current Green's functions from Eqs. (8.33)-(8.36) into Eq. (8.32) and rearranging the terms gives

$$\begin{aligned}\dot{\rho}_{\sigma\sigma} = \int \Big\{ \frac{d\omega}{2\pi} \sum_{\eta k} \Big[& |V_{\eta k\sigma}|^2 \Big(G^R_{0\sigma\sigma}(\omega) - G^A_{0\sigma\sigma}(\omega) \Big) g^<_{\eta k\sigma}(\omega) \\ & + |V_{\eta k\sigma}|^2 \big(g^A_{\eta k\sigma}(\omega) - g^R_{\eta k\sigma}(\omega) \big) G^<_{0\sigma\sigma}(\omega) \\ & + |V_{\eta k\bar{\sigma}}|^2 \big(G^A_{2\sigma\sigma}(\omega) - G^R_{2\sigma\sigma}(\omega) \big) g^<_{\eta k\bar{\sigma}}(\omega) \\ & + |V_{\eta k\bar{\sigma}}|^2 \big(g^R_{\eta k\bar{\sigma}}(\omega) - g^A_{\eta k\bar{\sigma}}(\omega) \big) G^<_{2\sigma\sigma}(\omega) \Big] \Big\} \\ & - iB \sin\theta \left[\rho_{\sigma\bar{\sigma}} - \rho_{\bar{\sigma}\sigma} \right].\end{aligned} \tag{8.38}$$

Using the general property for Green's functions $G^> - G^< \equiv G^R - G^A$ the previous equation becomes

$$\begin{aligned}\dot{\rho}_{\sigma\sigma} = \int \Big\{ \frac{d\omega}{2\pi} \sum_{\eta k} \Big[& |V_{\eta k\sigma}|^2 \Big(G^>_{0\sigma\sigma}(\omega) - G^<_{0\sigma\sigma}(\omega) \Big) g^<_{\eta k\sigma}(\omega) \\ & + |V_{\eta k\sigma}|^2 \big(g^<_{\eta k\sigma}(\omega) - g^>_{\eta k\sigma}(\omega) \big) G^<_{0\sigma\sigma}(\omega) \\ & + |V_{\eta k\bar{\sigma}}|^2 \big(G^<_{2\sigma\sigma}(\omega) - G^>_{2\sigma\sigma}(\omega) \big) g^<_{\eta k\bar{\sigma}}(\omega) \\ & + |V_{\eta k\bar{\sigma}}|^2 \big(g^>_{\eta k\bar{\sigma}}(\omega) - g^<_{\eta k\bar{\sigma}}(\omega) \big) G^<_{2\sigma\sigma}(\omega) \Big] \Big\} \\ & - iB \sin\theta \left[\rho_{\sigma\bar{\sigma}} - \rho_{\bar{\sigma}\sigma} \right].\end{aligned} \tag{8.39}$$

The lead Green's functions are for the isolated leads, so the average and time evolution are solely with respect to the contact part of the Hamiltonian, $H_C = \sum_{\eta,k,\sigma} \varepsilon_{\eta k\sigma} c^\dagger_{\eta k\sigma} c_{\eta k\sigma}$. For the lesser Green's function, we get[vi]

$$\begin{aligned} g^<_{\eta k\sigma}(t) &\equiv \left\langle c^\dagger_{\eta k\sigma} c_{\eta k\sigma}(t) \right\rangle \\ &= i e^{-i\varepsilon_{\eta k\sigma} t} \left\langle c^\dagger_{\eta k\sigma} c_{\eta k\sigma} \right\rangle \\ &= i e^{-i\varepsilon_{\eta k\sigma} t} f_\eta(\varepsilon_{\eta k\sigma}), \end{aligned} \tag{8.40}$$

with $f_\eta(\varepsilon) = f(\varepsilon - \mu_\eta)$, where $f(\varepsilon)$ is the Fermi function.
Performing a Fourier transformation yields

$$g^<_{\eta k\sigma}(\omega) = 2\pi i f_\eta(\varepsilon_{\eta k\sigma}) \delta(\omega - \varepsilon_{\eta k\sigma}), \tag{8.41}$$

[vi] Without loss of generality we can set $t' = 0$.

and similarly

$$g^{>}_{\eta k\sigma}(\omega) = -2\pi i[1 - f_\eta(\varepsilon_{\eta k\sigma})]\delta(\omega - \varepsilon_{\eta k\sigma}). \tag{8.42}$$

As in Chap. 4 we introduce a coupling parameter $\Gamma^\eta_\sigma(\varepsilon) = 2\pi \sum_k |V_{\eta k\sigma}|^2 \delta(\varepsilon - \varepsilon_{\eta k\sigma})$ and in the WBL it is assumed to be independent of energy.
The new expressions for the contact NGFs and the coupling constants are inserted in Eq. (8.39) and the result is

$$\begin{aligned}\dot\rho_{\sigma\sigma} = \frac{i}{2\pi}\int d\omega \sum_\eta \Big\{&\Gamma^\eta_\sigma f_\eta(\omega) G^{>}_{0\sigma\sigma}(\omega) + \Gamma^\eta_\sigma[1 - f_\eta(\omega)]G^{<}_{0\sigma\sigma}(\omega) \\ &- \Gamma^\eta_{\bar\sigma} f_\eta(\omega) G^{>}_{2\sigma\sigma}(\omega) + \Gamma^\eta_{\bar\sigma}[1 - f_\eta(\omega)]G^{<}_{2\sigma\sigma}(\omega)\Big\} \\ &- iB\sin\theta\left[\rho_{\sigma\bar\sigma} - \rho_{\bar\sigma\sigma}\right].\end{aligned} \tag{8.43}$$

The other rate equations are derived in exactly the same manner and we obtain[vii]

$$\dot\rho_{00} = -\frac{i}{2\pi}\int d\omega \sum_{\eta\sigma}\Big\{\Gamma^\eta_\sigma[1 - f_\eta(\omega)]G^{<}_{0\sigma\sigma}(\omega) + \Gamma^\eta_\sigma f_\eta(\omega)G^{>}_{0\sigma\sigma}(\omega)\Big\} \tag{8.44}$$

$$\dot\rho_{22} = \frac{i}{2\pi}\int d\omega \sum_{\eta\sigma}\Big\{\Gamma^\eta_\sigma[1 - f_\eta(\omega)]G^{<}_{2\bar\sigma\bar\sigma}(\omega) + \Gamma^\eta_\sigma f_\eta(\omega)G^{>}_{2\bar\sigma\bar\sigma}(\omega)\Big\} \tag{8.45}$$

$$\begin{aligned}\dot\rho_{\sigma\bar\sigma} = \frac{i}{2\pi}\int d\omega \sum_\eta \Big[&\Gamma^\eta_{\bar\sigma}\Big\{f_\eta(\omega)G^R_{0\sigma\bar\sigma}(\omega) + \frac{1}{2}G^{<}_{0\sigma\bar\sigma}(\omega) - f_\eta(\omega)G^R_{2\bar\sigma\sigma}(\omega) - \frac{1}{2}G^{<}_{2\bar\sigma\sigma}(\omega)\Big\} \\ &- \Gamma^\eta_\sigma\Big\{f_\eta(\omega)G^A_{0\sigma\bar\sigma}(\omega) - \frac{1}{2}G^{<}_{0\sigma\bar\sigma}(\omega) - \frac{1}{2}G^{<}_{2\bar\sigma\sigma} + f_\eta(\omega)G^A_{2\bar\sigma\sigma}(\omega)\Big\}\Big] \\ &- iB\sin\theta[\rho_{\sigma\sigma} - \rho_{\bar\sigma\bar\sigma}]\end{aligned} \tag{8.46}$$

Recall that the Green's functions in Eqs. (8.43)-(8.46) are the dot Green's functions defined in Eqs. (8.19)-(8.22). As explained in Sec. 8.2, we assume that the dot Green's functions in Eqs. (8.43)-(8.46) are on the same form as the Green's functions for the isolated dot, so the latter have to be determined, e.g.

$$G^{<,0}_{0\sigma\sigma'}(t) \equiv i\left\langle |\sigma'\rangle\langle 0|(|0\rangle\langle\sigma|)(t)\right\rangle_0, \tag{8.47}$$

where the subscript indicates that the average and time-dependence are with respect to the dot Hamiltonian.
The decoupled Green's functions are easiest to calculate in the basis where $H_{\rm dot}$ is diago-

[vii] In [4] they have an expression for the non-diagonal elements which only depend on lesser and greater Green's functions for the dot. We have not been able to reproduce it. However, the advanced and retarded Green's functions for the isolated dot and leads are easy to find, and in the Wide Band Limit where the coupling constant is independent of energy, we can obtain the same final result as in [4].

nal[viii], so the following change of basis is performed

$$\begin{aligned} G^{<,0}_{0\sigma\sigma'}(t) &= i\sum_{\mu\mu'} R^*_{\sigma'\mu'} R_{\sigma\mu} \left\langle |\mu'\rangle\langle 0|(|0\rangle\langle\mu|)(t)\right\rangle_0 \\ &= \sum_{\mu\mu'} R^*_{\sigma'\mu'} R_{\sigma\mu} G^{<,0}_{e\mu\mu'}(t) \end{aligned} \tag{8.48}$$

where $\mathbf{R} = \mathbf{R}(\theta)$ is the change-of-basis matrix defined in Sec. 2.3.
The decoupled lesser Green's function in the diagonal basis is

$$\begin{aligned} G^{<,0}_{0\mu\mu'}(t) &= i\left\langle |\mu'\rangle\langle 0|(|0\rangle\langle\mu|)(t)\right\rangle_0 \\ &= i\left\langle |\mu'\rangle\langle 0|e^{iH_{\rm dot}t}|0\rangle\langle\mu|e^{-iH_{\rm dot}t}\right\rangle_0 \\ &= ie^{-i\varepsilon_\mu t}\left\langle |\mu'\rangle\langle\mu|\right\rangle_0 . \end{aligned} \tag{8.49}$$

and in Fourier space

$$G^{<,0}_{0\mu\mu'}(\omega) = 2\pi i\rho^0_{\mu\mu'}\delta(\omega - \varepsilon_\mu), \tag{8.50}$$

with $\rho^0_{\mu\mu'} = \langle |\mu'\rangle\langle\mu|\rangle_0$.
For the other decoupled Green's functions, which correspond to the full Green's functions in Eqs. (8.20)-(8.22) in absence of tunnelling, we obtain with the same change-of-basis the following expressions

$$G^{>,0}_{0\mu\mu'} = -2\pi i\rho^0_{00}\delta_{\mu\mu'}\delta(\omega - \varepsilon_\mu), \tag{8.51}$$

$$G^{<,0}_{2\mu\mu'} = 2\pi i\rho^0_{22}\delta_{\mu\mu'}\delta(\omega - (\varepsilon_{\bar\mu} + U)), \tag{8.52}$$

$$G^{>,0}_{2\mu\mu'} = -2\pi i\rho^0_{\mu'\mu}\delta(\omega - (\varepsilon_{\bar\mu} + U)). \tag{8.53}$$

The occupancies that enter are in the diagonal basis, but using the relation

$$\rho^0_{\mu\mu'} = \sum_{\sigma_1\sigma_2} R_{\sigma_1\mu'} R^*_{\sigma_2\mu} \left\langle |\sigma_1\rangle\langle\sigma_2|\right\rangle_0 \tag{8.54}$$

they can be transformed to the non-diagonal basis if necessary.

Using the assumption that the Green's functions in presence of coupling can be written on the same form as those in Eqs. (8.50)-(8.53), we obtain after inserting them in the rate

[viii] See Sec. 2.3.

equations (8.43)-(8.46) and performing the trivial integral that

$$\dot{\rho}_{00} = \sum_{\eta\sigma\mu\mu'} R_{\sigma\mu}R^*_{\sigma\mu'}\Gamma^\eta_\sigma \Big\{[1-f_\eta(\varepsilon_\mu)]\rho_{\mu\mu'} - f_\eta(\varepsilon_\mu)\delta_{\mu\mu'}\rho_{00}\Big\}, \tag{8.55}$$

$$\begin{aligned}\dot{\rho}_{\sigma\sigma} = \sum_{\eta\mu\mu'} \Big\{ & R_{\sigma\mu}R^*_{\sigma\mu'}\Gamma^\eta_\sigma\Big[f_\eta(\varepsilon_\mu)\delta_{\mu\mu'}\rho_{00} - [1-f_\eta(\varepsilon_\mu)]\rho_{\mu\mu'}\Big] \\ & + R_{\sigma\mu'}R^*_{\sigma\mu}\Gamma^\eta_{\bar\sigma}\Big[[1-f_\eta(\varepsilon_{\bar\mu}+U)]\delta_{\mu\mu'}\rho_{22} - f_\eta(\varepsilon_{\bar\mu}+U)\rho_{\mu'\mu}\Big]\Big\} \\ & - iB\sin\theta\sum_{\mu\mu'}\left[R_{\sigma\mu}R^*_{\bar\sigma\mu'} - R^*_{\sigma\mu'}R_{\bar\sigma\mu}\right]\rho_{\mu\mu'},\end{aligned} \tag{8.56}$$

$$\begin{aligned}\dot{\rho}_{\sigma\bar\sigma} = \frac{1}{2}\sum_{\eta\mu\mu'}(\Gamma^\eta_\sigma + \Gamma^\eta_{\bar\sigma}) \Big\{ & R_{\sigma\mu}R^*_{\bar\sigma\mu'}\Big[f_\eta(\varepsilon_\mu)\delta_{\mu\mu'}\rho_{00} - [1-f_\eta(\varepsilon_\mu)]\rho_{\mu\mu'}\Big] \\ & - R_{\sigma\mu'}R^*_{\bar\sigma\mu}\Big[f_\eta(\varepsilon_{\bar\mu}+U)\rho_{\mu'\mu} - [1-f_\eta(\varepsilon_{\bar\mu}+U)]\delta_{\mu\mu'}\rho_{22}\Big]\Big\} \\ & - iB\sin\theta\sum_{\mu\mu'}\left[R_{\sigma\mu}R^*_{\sigma\mu'} - R^*_{\bar\sigma\mu'}R_{\sigma\mu}\right]\rho_{\mu\mu'},\end{aligned} \tag{8.57}$$

$$\dot{\rho}_{22} = \sum_{\eta\sigma\mu\mu'} R_{\bar\sigma\mu}R^*_{\bar\sigma\mu'}\Gamma^\eta_\sigma \Big\{f_\eta(\varepsilon_{\bar\mu}+U)\rho_{\mu'\mu} - [1-f_\eta(\varepsilon_{\bar\mu}+U)]\delta_{\mu\mu'}\rho_{22}\Big\}. \tag{8.58}$$

In the derivation we have assumed the system to be in steady state, so the occupancies are constant and the left-hand sides in Eqs. (8.55)-(8.58) are equal to zero. We end up with a homogenous linear equation system consisting of six equations plus a normalization[ix] $\rho_{00} + \sum_{\mu=\uparrow,\downarrow}\rho_{\mu\mu} + \rho_{22} = 1$, and it can easily be solved numerically.[x] However, certain reservations have to been taken to this approach and that will be the subject of the coming section.

We end this section by stating the expression for the current. From Eq. (8.29) we obtain after the same type of calculations leading to the expression for the occupancies the following equation

$$\begin{aligned}I_\eta = e\sum_{\sigma\mu\mu'}\Gamma^\eta_\sigma\Big\{ & R_{\sigma\mu}R^*_{\sigma\mu}f_\eta(\varepsilon_\mu)\delta_{\mu\mu'}\rho_{00} + R_{\bar\sigma\mu}R^*_{\bar\sigma\mu}f_\eta(\varepsilon_{\bar\mu}+U)\rho_{\mu'\mu} \\ & - R_{\sigma\mu}R^*_{\sigma\mu}[1-f_\eta(\varepsilon_\mu)]\rho_{\mu\mu'} + R_{\bar\sigma\mu}R^*_{\bar\sigma\mu}[1-f_\eta(\varepsilon_{\bar\mu}+U)]\delta_{\mu\mu'}\rho_{22}\Big\},\end{aligned} \tag{8.59}$$

where the current is given in terms of the occupancies in the diagonal basis.

8.4 Range of validity for the rate equations

To explore the limits of validity for the derived equations we use the following general property for the density-matrix elements

$$\rho^*_{\alpha\alpha'} = \big\langle|\alpha'\rangle\langle\alpha|\big\rangle^* = \Big\langle(|\alpha'\rangle\langle\alpha|)^\dagger\Big\rangle = \big\langle|\alpha\rangle\langle\alpha'|\big\rangle = \rho_{\alpha'\alpha}, \tag{8.60}$$

[ix] It stems from $\sum_{\mu=\uparrow,\downarrow}|\mu\rangle\langle\mu| + |0\rangle\langle 0| + |2\rangle\langle 2| = 1$.

[x] Notice that it is the occupancies in the diagonal basis which are determined.

which implies that the diagonal elements are real numbers.
For the element $\dot{\rho}_{00}$ in equation Eq. (8.55) the complex conjugate is

$$\begin{aligned}\dot{\rho}^*_{00} &= \sum_{\eta\sigma\mu\mu'} R^*_{\sigma\mu} R_{\sigma\mu'} \Gamma^\eta_\sigma \left\{ [1 - f_\eta(\varepsilon_\mu)]\rho_{\mu'\mu} - f_\eta(\varepsilon_\mu)\delta_{\mu\mu'}\rho_{00} \right\} \\ &= \sum_{\eta\sigma\mu\mu'} R^*_{\sigma\mu'} R_{\sigma\mu} \Gamma^\eta_\sigma \left\{ [1 - f_\eta(\varepsilon_{\mu'})]\rho_{\mu\mu'} - f_\eta(\varepsilon_\mu)\delta_{\mu\mu'}\rho_{00} \right\},\end{aligned} \tag{8.61}$$

which is not equal to $\dot{\rho}_{00}$ because of the energy argument in $1 - f_\eta(\varepsilon_{\mu'})$. The same problem is encountered for the other rate equations, so the property in Eq. (8.60) is only fulfilled in the large bias limit where $1 - f_\eta(\varepsilon_{\mu'})$ is either 0 or 1, or for high temperatures where $f_\eta(\varepsilon_{\mu'}) \approx f_\eta(\varepsilon_\mu)$. Both limits are not relevant for the interesting regime of the FAB model because the interference effect is washed out in these limits and the current becomes independent of the angle θ.

In summary, we have presented a rate equation description which is an alternative to the Green's functions approach when dealing with quantum transport. The rate equations are derived rather elegantly from nonequilibrium Green's functions, but they are only valid in the large bias limit or for high temperatures, and not for arbitrary bias voltages and temperatures as claimed in the article by Bing Dong *et al.* Therefore they do not have a larger range of validity than those derived from e.g. the microscopic Hamiltonian, but the results agree in the strong bias limit for the systems considered in the article. Moreover, we cannot compare results found with the derived rate equations to the linear response results from Chap. 4, 5 and 7.
The restricted validity is not found in the article, because they do not deal properly with the central region Hamiltonian, i.e. diagonalize it and thereby treat the spin flip term R_σ to all orders finding two different eigenenergies for the dot. In the limit of infinite bias or high temperatures this error is unimportant, because the Fermi function then has the same value at the eigenenergies.
Besides the limits of high temperature or high bias, the rate equations are also valid when the off-diagonal elements in the density matrix vanish, i.e. we have the normal master equations for states with no coupling between them.

The conclusion is that we are still not able to find a set of rate equations which include the non-diagonal elements in the density matrix when the coupling is larger than both the applied bias voltage and the temperature.

In the next section the FAB model is solved using a scattering formalism.

Chapter 9

Scattering formalism

In the previous sections we have studied tunnelling through a single quantum dot with an applied magnetic field using a Green's function approach and a rate equation approach. As a last example of how to find the conductance it will in this chapter be shown how to calculate it in perturbation theory.
The derivation will be done for the parallel geometry and the results will be compared to the results obtained with the Green's function approach in order to illuminate the differences between the methods.
In Sec. 9.3 the results for the antiparallel geometry is presented.

The aim is to calculate the transition rate between an initial and a final state, where in the process electrons have been moved across the quantum dot giving rise to a current. We start by defining a Hamiltonian $H = H_0 + V$ where the eigenstates of H_0 are known and then treat V as a perturbation. To lowest order in V this is Fermi's Golden Rule, but we have to go to higher orders introducing the so-called transition operator $\hat{T}$, which gives a generalization of the golden rule.
For the FAB model we will take the Hamiltonian for the isolated dot and leads as H_0 and then treat the tunnelling Hamiltonian as a perturbation. To lowest order in H_T no contributing tunnelling processes occur, but second order processes give a contribution. These processes include two subsequent tunnelling events and are therefore named cotunnelling.

9.1 The transition operator $\hat{T}$

For many physical system one is interested in knowing the rate for transitions between different states.
Consider a general Hamiltonian H_0 which has the eigenstates $\{|n\rangle\}$ with the corresponding eigenenergies $\{E_n\}$. At times before t_0 the system is assumed to be in an initial state $|i\rangle$. A constant perturbation onsets at time t_0 and the system evolves under the influence of the full Hamiltonian $H = H_0 + V$. What is the probability per unit time Γ_{fi} for a transition from the initial state $|i\rangle$ to a final state $|f\rangle$?
We use a mathematical trick and make V time-dependent such that $V \to V(t) = Ve^{\varepsilon t}$.

If t_0 is set equal to $-\infty$ and we let $\varepsilon \to 0$ at the end of the calculation, it corresponds to a constant perturbation at all times. Now time-dependent perturbation theory can be applied to calculated the transition rate[i], and to lowest order in V we obtain ($\hbar = 1$)

$$\Gamma_{fi}^{(1)} = 2\pi \left|\langle f|V|i\rangle\right|^2 \delta(E_f - E_f) \tag{9.1}$$

which is nothing but Fermi's Golden Rule.[ii]

The transition rate can be calculated to all order via the so-called transition operator $\hat{T}$, which is defined as

$$\begin{aligned} T &= V + V\frac{1}{E_i - H_0 + i\varepsilon}T \\ &= V + V\frac{1}{E_i - H_0 + i\varepsilon}V + V\frac{1}{E_i - H_0 + i\varepsilon}V\frac{1}{E_i - H_0 + i\varepsilon}V + \ldots, \end{aligned} \tag{9.2}$$

where $\varepsilon \to 0$ in the end of the calculation. The transition operator replaces V in Eq. (9.1) such that the transition rate becomes

$$\Gamma_{fi} = 2\pi \left|\langle f|T|i\rangle\right|^2 \delta(E_f - E_f), \tag{9.3}$$

and we notice that we indeed obtain Fermi's Golden Rule when expanding to lowest order in V.
To derive the transition operator properly is rather comprehensive and it will not be done here, where we just notice that it can be done in different ways. A common way is via the Lippmann-Schwinger equation which is often used when treating the interaction between an incoming wave and a scattering potential.[iii] A different approach based on propagators is found in [23].

9.2 Applied to the FAB model (parallel geometry)

After introducing the transition operator and the transition rate we return to our problem at hand.
Before calculating the transition rate we impose the following constraints. In this section, the magnetizations of the leads will be assumed parallel[iv], and we consider fully polarized leads containing only spin-$\uparrow'$ electrons, i.e. the spin label for the lead electrons can be omitted. Furthermore, the spin-$\uparrow$ level of the dot is assumed to be far below the chemical potentials of the leads, implying that the level is always occupied. The spin-$\downarrow$ level is on the contrary always far above the chemical potential giving an always empty state.
In the weak coupling limit the leads are assumed unaffected by the coupling to the dot, and therefore treated as non-interacting electron gasses as in the previous sections. At

[i] See Eq. (3.17).
[ii] See e.g. [1] and [25].
[iii] See e.g. [25].
[iv] The results for the antiparallel geometry is found in Sec. 9.3.

zero temperature all single-particle states with an energy below the Fermi energy ε_F are occupied. This corresponds to a filled Fermi sea (FS) and the corresponding many-particle state is

$$|FS\rangle = \left(\prod_{\varepsilon_k < \varepsilon_F} c_k^\dagger \right) |0\rangle, \tag{9.4}$$

with $|0\rangle$ being the empty state.

Now we consider the system at a finite temperature T, where excitations in the filled Fermi sea can occur creating new states e.g. with one single electron-hole pair $|\nu\rangle = c_{k'}^\dagger c_k |FS\rangle$, where $\varepsilon_k < \varepsilon_F < \varepsilon_{k'}$.
W_ν is defined to be the probability to find the system in the state ν, and the probabilities fulfil the normalization $\sum_\nu W_\nu = 1$. The leads are assumed to be in thermal equilibrium, so the probabilities are distributed such that the average occupation n_k of the state $|k\rangle$ is given by the Fermi-Dirac function, i.e.

$$n_k = \sum_\nu W_\nu \langle \nu | c_k^\dagger c_k | \nu \rangle = \sum_{k \in \nu} W_\nu = f(\varepsilon_k), \tag{9.5}$$

where the second sum is over all many-particle states ν which have the single-particle state $|k\rangle$ occupied. $f(\varepsilon)$ is the Fermi-Dirac distribution function at temperature T.
The initial states for the system consisting of the leads and the dot are now given as the outer product of the lead and the dot states, i.e. $|\nu_L, \nu_R, \uparrow\rangle$ with the corresponding probability $W_{\nu_L \nu_R} = W_{\nu_L} W_{\nu_R}$, because the leads are assumed uncorrelated and the dot state with spin-$\uparrow$ is always occupied. The energy of this state is $\varepsilon_{\nu_L \nu_R} = \varepsilon_{\nu_L} + \varepsilon_{\nu_R} + \varepsilon_\uparrow$.

Because we are interested in the conductance, we only consider final states where electrons have been moved across the quantum dot leaving the system in the initial state, except than one electron has been taken from one lead an put into the other. No such process is possible to first order in H_T, but second order processes are. The current can then be calculated as $J = \frac{e}{\hbar}(\Gamma_{LR}^{(2)} - \Gamma_{RL}^{(2)})$, where $\Gamma_{LR}^{(2)}$ is a sum over all transition rates for processes which brings an electron from the left to the right lead.
First we calculate the transition rate $\Gamma_{LR}^{(2)}$, so as final states we take $|f_{kk'}\rangle = c_{kR}^\dagger c_{k'L} |\nu_L, \nu_R, \uparrow\rangle$, with energy $E_{f_{kk'}} = \varepsilon_{\nu_L \nu_R} + \varepsilon_{kR} - \varepsilon_{k'L}$. This gives[v]

$$\Gamma_{LR}^{(2)} = 2\pi \sum_{kk'} \sum_{\nu_L \nu_R} W_{\nu_L \nu_R} |\langle f_{kk'} | H_T \frac{1}{\varepsilon_{\nu_L \nu_R} - H_0} H_T | \nu_L, \nu_R, \uparrow \rangle|^2 \delta(\varepsilon_{kR} - \varepsilon_{k'L}). \tag{9.6}$$

In case of full polarization of the leads the lead spin index in the tunnelling Hamiltonian in Eq. (2.9) can be omitted and it becomes

$$H_T = \sum_{k\eta\mu} \left(V_{k\eta,\mu} c_{k\eta}^\dagger c_{d\mu} + h.c. \right), \tag{9.7}$$

[v] The $i\varepsilon$ has been omitted because we only consider processes where the energy difference between the initial and intermediate state is nonzero.

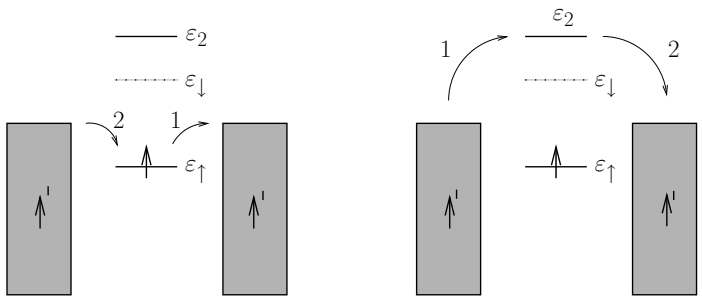

Figure 9.1: Fig. 9.1(a) shows the process A, where an electron tunnel from the always filled ↑-level to the right lead and gets refilled from the left lead. In fig. 9.1(b) the B process is shown. Here an electron tunnels from the left to the right lead via the doubled occupied state.

which contains eight terms when the sums over η and μ are written out. However only two processes will contribute to $\Gamma^{(2)}_{LR}$: (A) an electron leaving the dot entering the right lead and *afterwards* an electron entering the dot from the left lead, and (B) an electron entering and leaving the spin-↓ level, creating an intermediate doubled occupied state while going from left to right. The two processes are shown in Fig. 9.1.
With this in mind the matrix element $\langle f_{kk'}|H_T\frac{1}{\varepsilon_{\nu_L\nu_R}-H_0}H_T|\nu_L,\nu_R,\uparrow\rangle$ in Eq. (9.6) can be split into two parts corresponding to the two contributing processes

$$M_A = \sum_{k_1k_2}\langle f_{kk'}|V^*_{k_2L,\uparrow}c^\dagger_{d\uparrow}c_{k_2L}\frac{1}{\varepsilon_{\nu_L\nu_R}-H_0}V_{k_1R,\uparrow}c^\dagger_{k_1R}c_{d\uparrow}|\nu_L,\nu_R,\uparrow\rangle, \tag{9.8}$$

$$M_B = \sum_{k_1k_2}\langle f_{kk'}|V_{k_2R,\downarrow}c^\dagger_{k_2R}c_{d\downarrow}\frac{1}{\varepsilon_{\nu_L\nu_R}-H_0}V^*_{kR,\downarrow}c^\dagger_{d\downarrow}c_{k_1}|\nu_L,\nu_R,\uparrow\rangle. \tag{9.9}$$

The matrix elements M_A is

$$\begin{aligned}
M_A &= \sum_{k_1k_2}V^*_{k_2L,\uparrow}V_{k_1R,\uparrow}\langle f_{kk'}|c^\dagger_{d\uparrow}c_{k_2L}\frac{1}{\varepsilon_{\nu_L\nu_R}-(\varepsilon_{\nu_L\nu_R}-\varepsilon_\uparrow+\varepsilon_{k_1R})}c^\dagger_{k_1R}c_{d\uparrow}|\nu_L,\nu_R,\uparrow\rangle\\
&= \sum_{k_1k_2}\frac{V^*_{k_2L,\uparrow}V_{k_1R,\uparrow}}{\varepsilon_\uparrow-\varepsilon_{k_1R}}\langle f_{kk'}|c_{k_2L}c^\dagger_{k_1R}c^\dagger_{d\uparrow}c_{d\uparrow}|\nu_L,\nu_R,\uparrow\rangle\\
&= \sum_{k_1k_2}\frac{V^*_{k_2L,\uparrow}V_{k_1R,\uparrow}}{\varepsilon_\uparrow-\varepsilon_{k_1R}}\langle\nu_L,\nu_R,\uparrow|c^\dagger_{k'L}c_{kR}c_{k_2L}c^\dagger_{k_1R}|\nu_L,\nu_R,\uparrow\rangle\\
&= -\frac{V^*_{k'L,\uparrow}V_{kR,\uparrow}}{\varepsilon_\uparrow-\varepsilon_{k_1R}}\langle\nu_L,\nu_R,\uparrow|c^\dagger_{k'L}c_{k'L}\left(1-c^\dagger_{kR}c_{kR}\right)|\nu_L,\nu_R,\uparrow\rangle,
\end{aligned} \tag{9.10}$$

where we at the third equality have used that the spin-↑ state is always occupied.
M_B is calculated in the same way and the result is

$$M_B = \frac{V^*_{k'L,\downarrow} V_{kR,\downarrow}}{\varepsilon_{k'L} - \varepsilon_\downarrow - U} \langle \nu_L, \nu_R, \uparrow | c^\dagger_{k'L} c_{k'L} \left(1 - c^\dagger_{kR} c_{kR}\right) | \nu_L, \nu_R, \uparrow \rangle. \tag{9.11}$$

It is seen how the transition rate is controlled by the energy of the intermediate state through the energy denominator like in standard second order perturbation theory.
The results for the matrix elements are inserted in Eq. (9.6), and after writing out the expression for the coupling matrix elements we find

$$\begin{aligned}\Gamma^{(2)}_{LR} = 2\pi \sum_{kk'} \sum_{\nu_L \nu_R} W_{\nu_L \nu_R} &\left| \frac{t^*_{k'L\uparrow'} t_{kR\uparrow'} R_{\uparrow,\uparrow'} R_{\uparrow',\uparrow}}{\varepsilon_\uparrow - \varepsilon_{kR}} - \frac{t^*_{k'L\uparrow'} t_{kR\uparrow'} R_{\downarrow,\uparrow'} R_{\uparrow',\downarrow}}{\varepsilon_{k'L} - \varepsilon_\downarrow - U} \right|^2 \\ &\left| \langle \nu_L, \nu_R, \uparrow | c^\dagger_{k'L} c_{k'L} \left(1 - c^\dagger_{kR} c_{kR}\right) | \nu_L, \nu_R, \uparrow \rangle \right|^2 \delta(\varepsilon_{kR} - \varepsilon_{k'L}).\end{aligned} \tag{9.12}$$

The identity matrix $I = \sum_{\nu'_L \nu'_R \mu} |\nu'_L, \nu'_R, \mu\rangle\langle \nu'_L, \nu'_R, \mu|$ is inserted and the sums over the many-particle states can be carried out

$$\begin{aligned}&\sum_{\nu_L \nu_R} W_{\nu_L} W_{\nu_R} \left| \langle \nu_L, \nu_R, \uparrow | c^\dagger_{k'L} c_{k'L} | \nu_L, \nu_R, \uparrow \rangle \langle \nu_L, \nu_R, \uparrow | \left(1 - c^\dagger_{kR} c_{kR}\right) | \nu_L, \nu_R, \uparrow \rangle \right|^2 \\ &= \left(\sum_{\nu_L} W_{\nu_L} \langle \nu_L | c^\dagger_{k'L} c_{k'L} | \nu_L \rangle \right) \left(\sum_{\nu_R} W_{\nu_R} \langle \nu_R | \left(1 - c^\dagger_{kR} c_{kR}\right) | \nu_R \rangle \right) \\ &= f_L(\varepsilon_{k'L}) \left[1 - f_R(\varepsilon_{kR})\right].\end{aligned} \tag{9.13}$$

It has been used that the matrix elements are either 0 or 1, so the square can be omitted. The previous result is inserted in Eq. (9.12) and the trick $\sum_k F(\varepsilon_k) = \int d\varepsilon \sum_k F(\varepsilon) \delta(\varepsilon_k - \varepsilon)$ is invoked twice to give

$$\begin{aligned}\Gamma^{(2)}_{LR} &= 2\pi \int d\varepsilon' \int d\varepsilon \sum_{kk'} |t^*_{k'L\uparrow'}|^2 |t_{kR\uparrow'}|^2 \delta(\varepsilon_{k'L} - \varepsilon') \delta(\varepsilon_{kR} - \varepsilon) \\ &\qquad \left| \frac{R_{\uparrow,\uparrow'} R_{\uparrow',\uparrow}}{\varepsilon_\uparrow - \varepsilon} - \frac{R_{\downarrow,\uparrow'} R_{\uparrow',\downarrow}}{\varepsilon' - \varepsilon_\downarrow - U} \right|^2 f_L(\varepsilon') \left(1 - f_R(\varepsilon)\right) \delta(\varepsilon - \varepsilon') \\ &= \frac{1}{2\pi} \int d\varepsilon' \int d\varepsilon \; \Gamma^L_{\uparrow'}(\varepsilon') \Gamma^R_{\uparrow'}(\varepsilon) \\ &\qquad \left| \frac{R_{\uparrow,\uparrow'} R_{\uparrow',\uparrow}}{\varepsilon_\uparrow - \varepsilon} - \frac{R_{\downarrow,\uparrow'} R_{\uparrow',\downarrow}}{\varepsilon' - \varepsilon_\downarrow - U} \right|^2 f_L(\varepsilon') \left(1 - f_R(\varepsilon)\right) \delta(\varepsilon - \varepsilon'),\end{aligned} \tag{9.14}$$

where the elastic coupling parameters $\Gamma^\eta_{\uparrow'}(\varepsilon) = 2\pi \sum_k |t_{k\eta\uparrow'}|^2 \delta(\varepsilon_{k\eta} - \varepsilon)$ have been introduced.
As in the previous sections we take the Wide Band Limit and assume that the coupling

parameters are independent of energy and can be pulled outside the integral. Recall that this is reasonable when the density of states and the transmission matrix elements $t_{k\eta\uparrow'}$ are almost constant. When we are only interested in the current in linear response this is a good approximation because the energies of interest are situated in a small neighborhood around the chemical potentials.
So in the Wide Band Limit $\Gamma^{(2)}_{LR}$ is

$$\Gamma^{(2)}_{LR} = \frac{\Gamma^L_{\uparrow'}\Gamma^R_{\uparrow'}}{2\pi}\int d\varepsilon \left|\frac{R_{\uparrow,\uparrow'}R_{\uparrow',\uparrow}}{\varepsilon_\uparrow - \varepsilon} - \frac{R_{\downarrow,\uparrow'}R_{\uparrow',\downarrow}}{\varepsilon - \varepsilon_\downarrow - U}\right|^2 f_L(\varepsilon)\left(1 - f_R(\varepsilon)\right). \tag{9.15}$$

Because of the Fermi functions only energies in the interval of from μ_R to μ_L will contribute to the integral (at least for low temperatures). We have already supposed that the energy levels of the dot were far from this interval, so the denominators inside the integral will be dominated by these energies and can be considered as constants, giving

$$\Gamma^{(2)}_{LR} \approx \frac{\Gamma^L_{\uparrow'}\Gamma^R_{\uparrow'}}{2\pi}\left|\frac{R_{\uparrow,\uparrow'}R_{\uparrow',\uparrow}}{\varepsilon_\uparrow} + \frac{R_{\downarrow,\uparrow'}R_{\uparrow',\downarrow}}{\varepsilon_\downarrow + U}\right|^2 \int d\varepsilon f_L(\varepsilon)\left[1 - f_R(\varepsilon)\right]. \tag{9.16}$$

Using the relations [1]

$$f(\varepsilon_1)\left[1 - f(\varepsilon_2)\right] = n_B(\varepsilon_1 - \varepsilon_2)\left[f(\varepsilon_2) - f(\varepsilon_1)\right], \tag{9.17}$$

$$\int_{-\infty}^{\infty} d\varepsilon \left[f(\varepsilon) - f(\varepsilon + \omega)\right] = \omega, \tag{9.18}$$

where $n_B(\varepsilon) = \frac{1}{\exp(\varepsilon\beta)-1}$, the integral in Eq. (9.16) can be calculated and it gives[vi]

$$\int d\varepsilon f_L(\varepsilon)\left[1 - f_R(\varepsilon)\right] = -eV n_B(-eV). \tag{9.19}$$

Finally we obtain

$$\Gamma^{(2)}_{LR} = -eV\frac{\Gamma^L_{\uparrow'}\Gamma^R_{\uparrow'}}{2\pi}\left|\frac{R_{\uparrow,\uparrow'}R_{\uparrow',\uparrow}}{\varepsilon_\uparrow} + \frac{R_{\downarrow,\uparrow'}R_{\uparrow',\downarrow}}{\varepsilon_\downarrow + U}\right|^2 n_B(-eV). \tag{9.20}$$

The result for $\Gamma^{(2)}_{RL}$ is found by interchanging $L \leftrightarrow R$ in Eq. (9.16) and we find

$$\Gamma^{(2)}_{RL} = eV\frac{\Gamma^L_{\uparrow'}\Gamma^R_{\uparrow'}}{2\pi}\left|\frac{R_{\uparrow,\uparrow'}R_{\uparrow',\uparrow}}{\varepsilon_\uparrow} + \frac{R_{\downarrow,\uparrow'}R_{\uparrow',\downarrow}}{\varepsilon_\downarrow + U}\right|^2 n_B(eV), \tag{9.21}$$

which gives that the current $J = \frac{e}{\hbar}\left(\Gamma^{(2)}_{LR} - \Gamma^{(2)}_{RL}\right)$ is

$$J = e^2\frac{\Gamma^L_{\uparrow'}\Gamma^R_{\uparrow'}}{2\pi\hbar}\left|\frac{R_{\uparrow,\uparrow'}R_{\uparrow',\uparrow}}{\varepsilon_\uparrow} + \frac{R_{\downarrow,\uparrow'}R_{\uparrow',\downarrow}}{\varepsilon_\downarrow + U}\right|^2 V, \tag{9.22}$$

[vi] Remember that the chemical potentials are $\mu_L = \frac{eV}{2}$ and $\mu_R = -\frac{eV}{2}$.

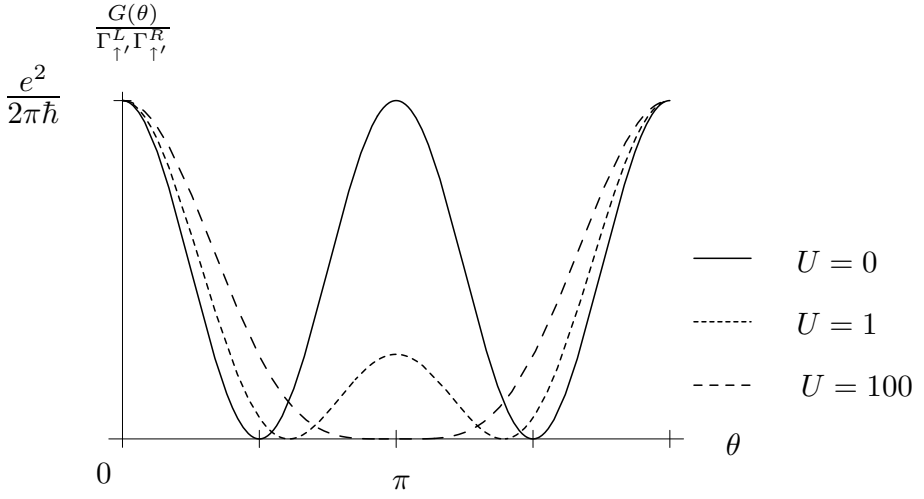

Figure 9.2: The figure shows the conductance $G(\theta)$ for $\varepsilon_d = 0$, $B = 1$ and $U = 0,\ 1$, and 100. It is seen how the anti-resonances at $\theta = \pi/2$ and $\theta = 3\pi/2$ disappear for increasing U. The result for $U = 1$ resembles the results shown in Fig. 7.4.

where it has been used that $\left[n_B(-x) + n_B(x)\right] = -1$.
It is now easy to find the conductance $G = \frac{dJ}{dV}$ as

$$G(\theta) = e^2 \frac{\Gamma^L_{\uparrow'}\Gamma^R_{\uparrow'}}{2\pi\hbar} \left| \frac{R_{\uparrow,\uparrow'}R_{\uparrow',\uparrow}}{\varepsilon_\uparrow} + \frac{R_{\downarrow,\uparrow'}R_{\uparrow',\downarrow}}{\varepsilon_\downarrow + U} \right|^2 . \tag{9.23}$$

Inserting the matrix elements from the change-of-basis matrix defined in Eq. (2.7) the result is

$$G(\theta) = e^2 \frac{\Gamma^L_{\uparrow'}\Gamma^R_{\uparrow'}}{2\pi\hbar} \left[\frac{\cos^2\frac{\theta}{2}}{\varepsilon_\uparrow} + \frac{\sin^2\frac{\theta}{2}}{\varepsilon_\downarrow + U} \right]^2 . \tag{9.24}$$

The Eq. (9.24) is the co-tunnelling result for the conductance to second order in the coupling term H_T. It should be emphasized that the expression is only valid when the energy of the spin-$\uparrow$ level is always filled and the other always empty. This is the case when the dot levels are much further away from the Fermi levels than the strength of the coupling parameter $\Gamma_{\uparrow'} = \Gamma^L_{\uparrow'} + \Gamma^R_{\uparrow'}$. This can for instance be seen from the calculation of the occupancies with the Green's functions.
No temperature dependence is present in the conductance because the temperature k_bT is assumed much smaller than the spacing between the chemical potentials of the leads and the energy levels of the dot. If the two energy scales are comparable temperature effects become important and the above analysis breaks down because the $\uparrow$-level is not always occupied.

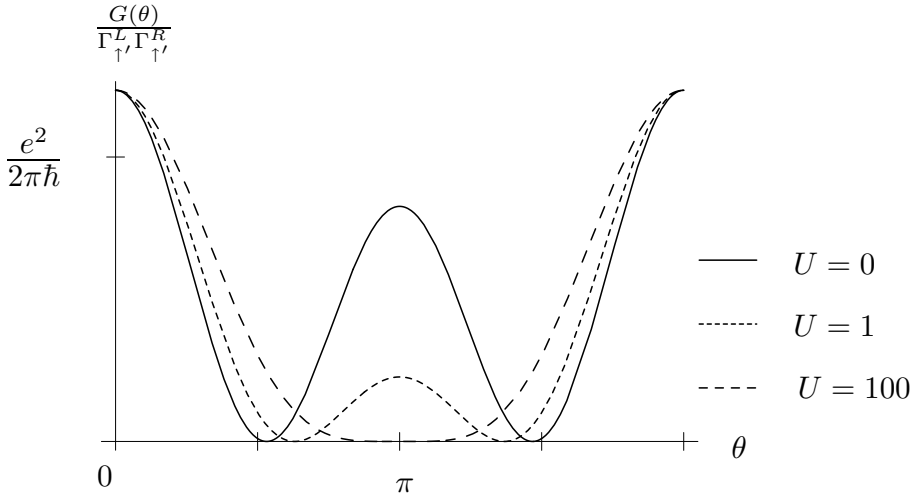

Figure 9.3: The figure shows the conductance $G(\theta)$ for $\varepsilon_d = 0.1$, $B = 1$ and $U = 0$, 1, and 100. It is seen how the anti-resonances at $\theta = \pi/2$ and $\theta = 3\pi/2$ still disappear for increasing U when the bare dot energy level is no longer fixed at the equilibrium chemical potential of the leads, but the symmetry around $\pi/2$ for $U = 0$ is broken.

So why not try to calculate the conductance to higher order in the coupling? This is a difficult task. We are looking for processes which bring an electron from one lead to the other and leave an electron in the spin-$\uparrow$ level and no in the other. This is not possible to third order in H_T, but to fourth order there are 32 possible processes! These can be reduced to 8 in the limit of $U \approx \infty$. Furthermore there is a technical problem concerning the energy denominators because intermediate states with energies equal to E_i are possible. Therefore the limit $i\varepsilon$ has to be taken correctly, and maybe higher order processes have to be included.

9.2.1 Comparison with Green's function approach

The results for the second order processes can be compared with the Green's function approach, and we start with considering the limiting cases $U = 0$ and $U \approx \infty$.

For $U = 0$ Eq. (9.24) becomes

$$G(\theta) = e^2 \frac{\Gamma^L_{\uparrow'}\Gamma^R_{\uparrow'}}{2\pi\hbar} \left[\frac{\varepsilon_d + B\cos\theta}{B^2 - \varepsilon_d^2}\right]^2, \tag{9.25}$$

and if we furthermore assume that ε_d is zero the conductance becomes

$$G(\theta) = e^2 \frac{\Gamma^L_{\uparrow'}\Gamma^R_{\uparrow'}}{2\pi\hbar} \frac{\cos^2\theta}{B^2}. \tag{9.26}$$

For $U = 0$ the equations of motion for the dot Green's functions could be solved exactly (see Chap. 4). In linear response with zero temperature, $\varepsilon_d = 0$ and fully polarized leads the conductance was for proportionate couplings

$$G_{\text{exact}}(\theta) = e^2 \frac{\Gamma^L_{\uparrow'}\Gamma^R_{\uparrow'}}{2\pi\hbar} \frac{4\cos^2\theta}{4B^2 + \Gamma^2_{\uparrow'}\cos^2\theta}, \quad \Gamma_{\uparrow'} = \Gamma^L_{\uparrow'} + \Gamma^R_{\uparrow'}. \tag{9.27}$$

In the limit where the co-tunnelling result is supposed to be valid $\Gamma_{\uparrow'} \ll B$, so we obtain

$$G_{\text{exact}}(\theta) = e^2 \frac{\Gamma^L_{\uparrow'}\Gamma^R_{\uparrow'}}{2\pi\hbar} \frac{\cos^2\theta}{B^2}, \tag{9.28}$$

which is identical to the co-tunnelling result. An interpretation for of the result for $U = 0$ was already given in Chap. 4, but note that in Eq. (9.24) is the addition of the tunnelling amplitudes for the two paths in Fig. 9.1 clearly seen.
The result in Eq. (9.28) could also be obtained directly from the Green's function approach. In weak coupling limit $\Gamma_{\uparrow'} \ll B$ the Green's function for the dot is almost equal to the Green's function for the isolated dot, see Eqs. (4.20) and (4.21). If we insert the expression for $\mathbf{G}^R_0$ in the current formula Eq. (4.22) we get an expression for the current to lowest order in the coupling and obtain Eq. (9.28).

In the limit of infinite U the second term in Eq. (9.24) vanishes and we get

$$G(\theta) = e^2 \frac{\Gamma^L_{\uparrow'}\Gamma^R_{\uparrow'}}{2\pi\hbar} \frac{\cos^4\frac{\theta}{2}}{\varepsilon^2_{\uparrow}}. \tag{9.29}$$

The disappearance of the anti-resonance is caused by the blocking of the conducting channel through the $\downarrow$-level because of the infinite energy of the intermediate step (see Fig. 9.1). In this case no destructive interference is possible. Instead, the angular dependence is similar to a spin valve geometry, where electrons tunnel between materials with different magnetizations. At $\theta = \pi$ the conduction vanishes because the spin-$\uparrow$ channel is closed due to spin blockade (see Fig. 4.2).
The limit is also named the correlated regime, because the electrons have to tunnel through the structure one by one due to the infinite energy of the doubled occupied state.

In Fig. 9.2 the results are plotted for various values of the Coulomb energy U and the bare dot energy $\varepsilon_d = \mu = 0$. It is seen how the anti-resonances existing at $\theta = \pi/2$ and $3\pi/2$ disappear and the resonances moves towards each other when U is increased. At infinite U only a single dip is seen.
For $\varepsilon_d \neq \mu$ the same behavior is seen, but the curve is no longer symmetric around $\theta = \frac{\pi}{2}$ for $U = 0$.

The U dependence was what we hoped to study with the Green's function approach because it contains tunnelling events to all orders, and not only second order as the cotunnelling result. However, we have shown that the two methods agree in the weak coupling limit for noninteracting electrons on the dot.

9.3 Applied to the FAB model (antiparallel geometry)

The analysis for obtaining the cotunnelling result for antiparallel magnetizations of the leads is identical to the parallel case presented in Sec. 9.2.
Again we calculate $\Gamma^{(2)}_{LR}$ and find the same two contributing process as showed in Fig. 9.1, and the only difference is when calculating the matrix elements M_A and M_B defined in Eqs. (9.8) and (9.9). After inserting the coupling matrix elements $V_{k\eta\sigma,\mu}$ for the antiparallel case we arrive at

$$M_A = -\frac{V^*_{k'L\uparrow',\uparrow}V_{kR\downarrow',\uparrow}}{\varepsilon_\uparrow - \varepsilon_{k_1R}}\langle\nu_L,\nu_R,\uparrow|c^\dagger_{k'L\uparrow'}c_{k'L\uparrow'}\left(1-c^\dagger_{kR\downarrow'}c_{kR\downarrow}\right)|\nu_L,\nu_R,\uparrow\rangle, \tag{9.30}$$

$$M_B = \frac{V^*_{k'L\uparrow',\downarrow}V_{kR\downarrow',\downarrow}}{\varepsilon_\uparrow - \varepsilon_{k_1R}}\langle\nu_L,\nu_R,\uparrow|c^\dagger_{k'L\uparrow'}c_{k'L\uparrow'}\left(1-c^\dagger_{kR\downarrow'}c_{kR\downarrow}\right)|\nu_L,\nu_R,\uparrow\rangle. \tag{9.31}$$

Continuing as in Sec. 9.2, the conductance can be found after inserting the definition of $V_{k\eta\sigma,\mu}$ and the result is

$$G(\theta) = e^2\frac{\Gamma^L_{\uparrow'}\Gamma^R_{\downarrow'}}{2\pi\hbar}\left[\frac{-\cos\frac{\theta}{2}\sin\frac{\theta}{2}}{\varepsilon_\uparrow} + \frac{\cos\frac{\theta}{2}\sin\frac{\theta}{2}}{\varepsilon_\downarrow + U}\right]^2. \tag{9.32}$$

Inserting the values for the energy levels gives

$$G(\theta) = e^2\frac{\Gamma^L_{\uparrow'}\Gamma^R_{\downarrow'}}{2\pi\hbar}\left[\frac{2B+U}{2(\varepsilon_d - B)(\varepsilon_d + B + U)}\right]^2\sin^2\theta. \tag{9.33}$$

For $\varepsilon_d = U = 0$ we get

$$G(\theta) = e^2\frac{\Gamma^L_{\uparrow'}\Gamma^R_{\downarrow'}}{2\pi\hbar}\frac{\sin^2\theta}{B^2}. \tag{9.34}$$

This can be compared with the Green's function result in the limit $B \gg \Gamma^L_{\uparrow'}, \Gamma^R_{\downarrow'}$ where the cotunnelling result is supposed to hold. From Eq. (5.19) we get in the cotunnelling limit

$$G_{\text{exact}}(\theta) = e^2\frac{\Gamma^L_{\uparrow'}\Gamma^R_{\downarrow'}}{2\pi\hbar}\frac{\sin^2\theta}{B^2}, \tag{9.35}$$

which is identical to the cotunnelling result in Eq. (9.34).[vii]

In the limit $U \approx \infty$ the second term in Eq. (9.32) vanishes because the conductance channel through the spin-$\downarrow$ level requires infinite energy, and we get

$$G(\theta) = e^2\frac{\Gamma^L_{\uparrow'}\Gamma^R_{\downarrow'}}{2\pi\hbar}\frac{\sin^2\theta}{4\varepsilon^2_\uparrow}. \tag{9.36}$$

The interesting point is that the angular dependence is similar to the $U = 0$ behaviour when $\varepsilon_d = 0$. This is very different from the case of parallel magnetizations of the leads where a dramatic change of the angular dependence was seen in the two limits.

[vii] The same calculation can be done for $\varepsilon_d \neq 0$ and the same conclusion is reached.

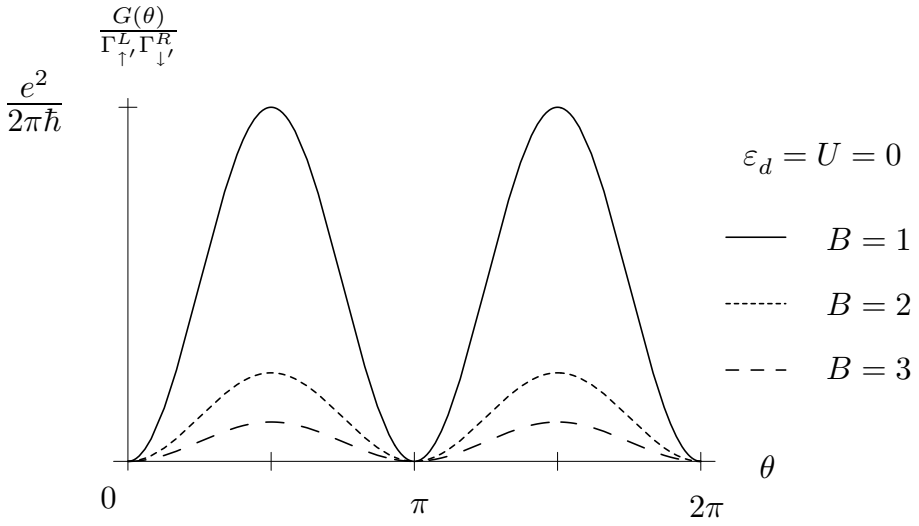

Figure 9.4: The cotunnelling results plotted for $\varepsilon_d = U = 0$ with different values for the magnetic field strength B. See Eq. (9.34).

9.4 Final remarks

The scattering formalism used in this section have given simple and intuitive analytical results for both the parallel and the antiparallel geometry. We only considered scattering processes to second order in the coupling, so we have to assume weak coupling. Moreover, the results are also only valid when the temperature and the bias voltage is much smaller than the distance between the chemical potentials of the leads and the energy levels of the dot.

For the parallel geometry, the main point is the existence of a cross-over from a resonant behavior in case of noninteracting electrons on the dot to a spin-valve effect in presence of large interactions on the dot. Both limits have been explained.
For the antiparallel geometry no significant change in the angular dependence is observed when the interactions on the dot are increased.

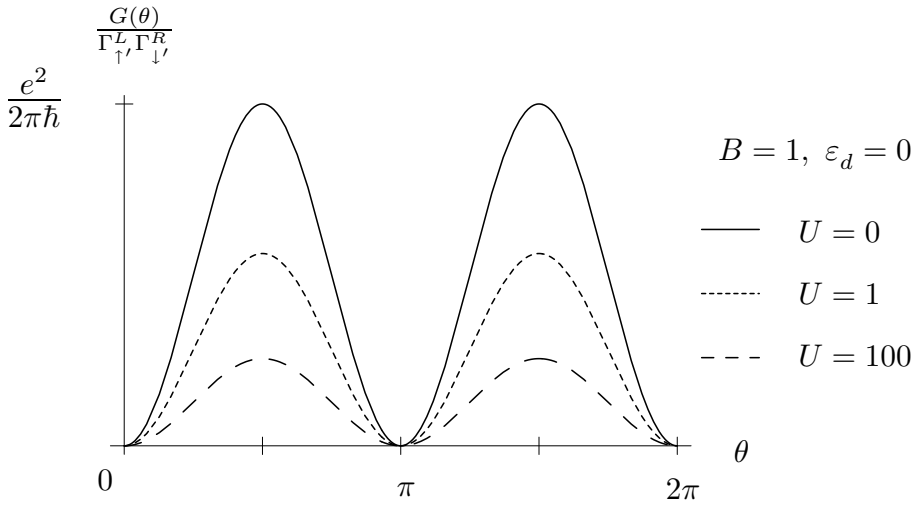

Figure 9.5: The cotunnelling results plotted for $\varepsilon_d = 0$ and $B = 1$ with different values for the Coulomb repulsion U (see Eq. (9.33)). Note how the conductance tends to $\frac{1}{4}$ of the U=0 value when $U \gg B$.

Chapter 10

Summary and outlook

We have studied the quantum transport through a small nanomagnetic device consisting of a quantum dot contacted to two ferromagnetic leads. An applied magnetic field could interact with the spin of the electrons on the quantum dot. To model the system an extended Anderson model was used and to calculate the conductance three different analytical tools were applied.

First a brief introduction to the field of nonequilibrium Green's functions was given. It is considered a strong tool for dealing with quantum transport because it incorporates tunnelling events to all orders, but technically it is difficult to work with in case of a non-quadratic Hamiltonian. For that reason an approximation scheme was applied which gave an expression for the retarded Green's function in presence of interactions. The solution for the current is restricted to the limit of weak and proportionate couplings, and it requires that the eigenstates of the central region are known. However, for noninteracting electrons on the dot exact analytical results could be obtained for fully polarized leads and low temperature.

Then the method of quantum rate equations was presented. They form an extension to (Pauli) master equations where the non-diagonal elements of the density matrix are also included. These terms describes the superposition of different quantum state and are important when the coupling between the states are strong. That is the case in the FAB model due to the large non-quadratic terms in the dot Hamiltonian. Quantum rate equations include tunnelling only to lowest order in the coupling and are often only valid in the large bias limit or for high temperatures, but sometimes it offers a quick way to obtain a result.

An attempt to derive a set of quantum rate equations for the FAB model based on an article by Bing Dong *et al.* was presented [4]. The derivation was based on the nonequilibrium Green's function formalism and the resulting set of equations were claimed to be valid for all bias voltages and temperatures. After having corrected a number of points in the derivation, we have shown that they are in fact also only valid in the large bias limit or for high temperatures. Consequently they cannot be applied to the FAB model in the linear response limit where the results could be compared with the other methods presented.

Method	**Conditions**
Green's functions, $U = 0$	None. Analytic results for $T = 0$.
Green's functions, unified description	Parallel geometry, $\Gamma \ll B$, pseudo-equilibrium
Quantum rate equations	Γ small (no broadning of levels). $\max(k_b T, eV) \gg B, U$ or $\rho_{\mu\mu'} \approx \delta_{\mu\mu'}\rho_{\mu\mu}$ $(B \gg \Gamma)$
Scattering formalism (to second order in Γ)	$k_B T, eV, \Gamma \ll B$

Table 10.1: The table shows when the different approaches can be applied when dealing with the FAB model. ($\varepsilon_d = 0$, i.e. $\varepsilon_\mu = \pm B$ and $\varepsilon_2 = U$.).

Finally, the conductance was calculated using a scattering formalism to second order in the tunnelling Hamiltonian, where an electron is passed from one lead to the other via a virtual transition. For the FAB model the conductance could only be calculated in the limit where one state is always occupied and the other always empty, and it is difficult to include higher order scattering processes. Nevertheless, for all values of the interaction it offered an intuitive picture of the processes giving rise to the anti-resonances in the conductance. For noninteracting electrons on the dot the results coincided with the exact Green's function results in the relevant limit.

The conditions for applying the methods to the FAB model is summarized in Table (10.1). It is clearly seen that in case of interacting electrons on the dot no method is available when the coupling is comparable to the other energies.

The exact results obtained with the Green's function method for noninteracting electrons on the dot have already been described in [5]. Under the condition of a bare dot energy at resonance, fully polarized leads, low temperature and parallel magnetizations of the leads anti-resonances in the conductance appear when $\theta = \frac{\pi}{2}$ and $\theta = \frac{3\pi}{2}$.[i]
When interactions are included the scattering formalism showed a cross-over to a simple spin-valve behaviour with no anti-resonances. It could be explained as the blocking of one of the conduction channels. The Green's function approach gave no clear results for strong interactions. Whether this is due to numerical problems or difficulties related to the applied approximation scheme has not been sorted out.
In case of noninteracting electrons on the dot an exact result could be obtained with the Green's function method for antiparallel magnetizations of the leads, and with the scattering formalism the conductance was found in presence of Coulomb repulsion on the dot. The interesting point is that no qualitative difference in the angular dependence between the noninteracting and the strongly correlated regime is observed. This is in contrast to the parallel geometry where a clear difference between the two regimes occurred.

[i] θ is the angle between the magnetizations of the leads and the applied magnetic field.

In the previous chapters only parallel magnetizations and fully polarized leads were considered. The effects described above remain in case of a mixture of spins in the leads but are gradually washed out. The same will happen if temperature is increased.

Through out this thesis we have used assumptions which made it possible to perform the calculations, but what is the relevance for an experiment? 1 Tesla gives a Zeeman splitting of the energy levels corresponding to a temperature of 1 Kelvin, roughly speaking, so the assumption of temperature being 200 times smaller than the magnetic field is obviously not reasonable, and the approximation of fully polarized leads can also be questioned. Nevertheless, the predicted angular dependence should persist even for higher temperatures and non-ideal leads, even though it gets smeared somewhat. Hopefully some experimental group will find it interesting to verify the predictions which are currently being written in the form of a research paper.

In conclusion, we have shown three different ways of dealing with quantum transport and the difficulties and advantageous of the methods have been discussed via the application on a relevant physical system. The inherent problem of treating the interactions between electrons on the dot properly has shown to be a technically difficult task and even more complicated models and sofisticated analytical tools are considered by other groups.[ii]
The complicated interplay between magnetism, coherence and interactions which exists in nanostructures is a delicate problem, but are "unfortunately" highly relevant for possible applications.

[ii] See [20], [21] and [22].

Appendix A

Details

A.1 Nonequilibrium Green's functions

A.1.1 Heisenberg operators as time-ordered exponentials

We show how operators in the Heisenberg picture can be transformed to a time-ordered exponential along a contour times the operator in the interaction picture.
To shorten the notation we write the Hamiltonian as

$$\mathcal{H}(t) = \tilde{H} + \tilde{V}(t) \tag{A.1}$$

where in our case $\tilde{V}(t) = H^i + V(t)$ and $\tilde{H} = H^0$.

Now consider the operator $A_{\mathcal{H}}(t)$. According to the Eqs. (3.14) and (3.17) it can we written as

$$A_{\mathcal{H}}(t) = v^{\dagger}_{\tilde{H}}(t, t_0) A_{\tilde{H}}(t) v_{\tilde{H}}(t, t_0), \tag{A.2}$$

where

$$v_{\tilde{H}}(t, t_0) = T_t e^{-i \int_{t_0}^{t} dt' \tilde{V}_{\tilde{H}}(t')}. \tag{A.3}$$

We want to show that $A_{\mathcal{H}}(t)$ can be transformed into

$$A_{\mathcal{H}}(t) = T_{C_t}[e^{-i \int_{C_t} d\tau \tilde{V}_{\tilde{H}}(\tau)} A_{\tilde{H}}(t)], \tag{A.4}$$

with C_t being the contour shown in Fig. 3.2, and proceed by transforming the right-hand side into the left-hand side.

From the definition of the time-ordered exponential we obtain

$$T_{C_t}[e^{-i \int_{C_t} d\tau \tilde{V}_{\tilde{H}}(\tau)} A_{\tilde{H}}(t)] = \sum_n \frac{(-i)^n}{n!} \int_{C_t} d\tau_1 \cdots \int_{C_t} d\tau_n T_{C_t} \left[V_{\tilde{H}}(\tau_1) \cdots V_{\tilde{H}}(\tau_n) A_{\tilde{H}}(t) \right] \tag{A.5}$$

First we consider nth order term. We split up the curve into two branches $C_t = C_{\rightarrow} + C_{\leftarrow}$, where $C_{\rightarrow}$ ($C_{\leftarrow}$) runs from t_0 (t) to t (t_0). Using the same notation we write the integral as $\int_{C_t} = \int\limits_{\rightarrow} + \int\limits_{\leftarrow}$ and get

$$\begin{aligned}\int_{C_t} d\tau_1 \cdots \int_{C_t} d\tau_n T_{C_t}\left[V_{\tilde{H}}(\tau_1)\cdots V_{\tilde{H}}(\tau_n) A_{\tilde{H}}(t)\right] \\ = \left(\int\limits_{\rightarrow} + \int\limits_{\leftarrow} d\tau_1\right) \cdots \left(\int\limits_{\rightarrow} + \int\limits_{\leftarrow} d\tau_n\right) T_{C_t}\left[V_{\tilde{H}}(\tau_1)\cdots V_{\tilde{H}}(\tau_n) A_{\tilde{H}}(t)\right].\end{aligned} \tag{A.6}$$

Expanding the expression in Eq. (A.6) gives 2^n terms, each containing n integrals. Now consider a term where m of the integrals are of the type $\int\limits_{\leftarrow}$, with $0 < m < n$. After introducing contour-ordering operators on each branch this term can be written as

$$\begin{aligned}&\left(\int\limits_{\leftarrow} d\tau_1 \cdots \int\limits_{\leftarrow} \tau_m\right)\left(\int\limits_{\rightarrow} d\tau_{m+1} \cdots \int\limits_{\rightarrow} \tau_n\right) T_{C_t}\left[V_{\tilde{H}}(\tau_1)\cdots V_{\tilde{H}}(\tau_n) A_{\tilde{H}}(t)\right] \\ &= \left(\int\limits_{\leftarrow} d\tau_1 \cdots \int\limits_{\leftarrow} \tau_m T^{\leftarrow}_{C_t}\left[V_{\tilde{H}}(\tau_1)\cdots V_{\tilde{H}}(\tau_m)\right]\right) A_{\tilde{H}}(t) \\ &\qquad \left(\int\limits_{\rightarrow} d\tau_{m+1} \cdots \int\limits_{\rightarrow} \tau_n T^{\rightarrow}_{C_t}\left[V_{\tilde{H}}(\tau_{m+1})\cdots V_{\tilde{H}}(\tau_n)\right]\right)\end{aligned} \tag{A.7}$$

where we have used that in the contour sense all times on the branch $C_{\rightarrow}$ are before the times on $C_{\leftarrow}$, and the time t is right in between.
Among the 2^n terms in Eq. (A.6) there are $\frac{n!}{m!(n-m)!}$ terms with m integrals of the type $\int\limits_{\leftarrow}$. They all give the same value because it is the same integral, with the only difference being the time labels.
If we introduce $k = n - m$ we can write the nth order term from Eq. (A.6) as

$$\begin{aligned}\int_{C_t} d\tau_1 \cdots \int_{C_t} d\tau_n T_{C_t}\left[V_{\tilde{H}}(\tau_1)\cdots V_{\tilde{H}}(\tau_n) A_{\tilde{H}}(t)\right] \\ = \sum_{m=0}^{\infty}\sum_{k=0}^{\infty} \frac{n!}{m!k!}\delta_{n,k+m}\left(\int\limits_{\leftarrow} d\tau_1 \cdots \int\limits_{\leftarrow} \tau_m T^{\leftarrow}_{C_t}\left[V_{\tilde{H}}(\tau_1)\cdots V_{\tilde{H}}(\tau_m)\right]\right) A_{\tilde{H}}(t) \\ \left(\int\limits_{\rightarrow} d\tau_1 \cdots \int\limits_{\rightarrow} \tau_k T^{\rightarrow}_{C_t}\left[V_{\tilde{H}}(\tau_1)\cdots V_{\tilde{H}}(\tau_k)\right]\right)\end{aligned} \tag{A.8}$$

and when we insert it in Eq. (A.5) we obtain

$$\begin{aligned} T_{C_t}[e^{-i\int_{C_t} d\tau \tilde{V}_{\tilde{H}}(\tau)} A_{\tilde{H}}(t)] \\ = \left(\sum_m \frac{(-i)^m}{m!} \int_{\leftarrow} d\tau_1 \cdots \int_{\leftarrow} \tau_m T_{C_t}^{\leftarrow} \left[V_{\tilde{H}}(\tau_1) \cdots V_{\tilde{H}}(\tau_m) \right] \right) A_{\tilde{H}}(t) \\ \left(\sum_k \frac{(-i)^k}{k!} \int_{\rightarrow} d\tau_1 \cdots \int_{\rightarrow} \tau_k T_{C_t}^{\rightarrow} \left[V_{\tilde{H}}(\tau_1) \cdots V_{\tilde{H}}(\tau_k) \right] \right) \end{aligned} \tag{A.9}$$

It is easy to see that the k-sum can be written as

$$\begin{aligned} \sum_k \frac{(-i)^k}{k!} \int_{\rightarrow} d\tau_1 \cdots \int_{\rightarrow} \tau_k T_{C_t}^{\rightarrow} \left[V_{\tilde{H}}(\tau_1) \cdots V_{\tilde{H}}(\tau_k) \right] \\ = T_t e^{-i\int_{t_0}^{t} dt' V_{\tilde{H}}(t')} = v_{\tilde{H}}(t, t_0), \end{aligned} \tag{A.10}$$

because the time-ordering operator $T_{C_t}^{\rightarrow}$ is equal to T_t on the interval $[t_0, t]$.
The m-sum is more difficult. We first note that the time-ordering operator $T_{C_t}^{\leftarrow} = \tilde{T}_t$ on $[t_0, t]$, where $\tilde{T}_t$ is the anti-time-ordering operator on the real axis.
For the time-ordering operators hold

$$\left(T_t[A(t)B(t')]\right)^\dagger = \tilde{T}_t[A^\dagger(t)B^\dagger(t')] \tag{A.11}$$

which follows from their definitions. Now the m-sum can be written as

$$\begin{aligned} &\sum_m \frac{(-i)^m}{m!} \int_{\leftarrow} d\tau_1 \cdots \int_{\leftarrow} \tau_m T_{C_t}^{\leftarrow} \left[V_{\tilde{H}}(\tau_1) \cdots V_{\tilde{H}}(\tau_m) \right] \\ &= \sum_m \frac{(-i)^m}{m!} \int_t^{t_0} dt_1' \cdots \int_t^{t_0} dt_m' \tilde{T}_t \left[V_{\tilde{H}}(t_1') \cdots V_{\tilde{H}}(t_m') \right] \\ &= \left(\sum_m \frac{i^m}{m!} \int_t^{t_0} dt_1' \cdots \int_t^{t_0} dt_m' T_t \left[\tilde{V}_{\tilde{H}}^\dagger(t_1') \cdots \tilde{V}_{\tilde{H}}^\dagger(t_m') \right] \right)^\dagger \\ &= \left(\sum_m \frac{(-i)^m}{m!} \int_{t_0}^{t} dt_1' \cdots \int_{t_0}^{t} dt_m' T_t \left[V_{\tilde{H}}(t_1') \cdots V_{\tilde{H}}(t_m') \right] \right)^\dagger \\ &= \left(T_t \left[e^{-i\int_{t_0}^{t} dt' V_{\tilde{H}}(t')} \right] \right)^\dagger = v_{\tilde{H}}^\dagger(t, t_0), \end{aligned} \tag{A.12}$$

where the integrals on the contour branch $C_\leftarrow$ have been changed to normal integrals along the real axis, and it has been used that $V_{\tilde{H}}(t)$ is a hermitian operator.
Finally we have proven Eq. (A.4).

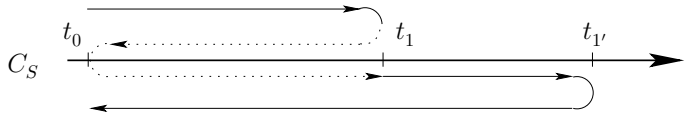

Figure A.1: The "snake" contour C_S. Like the other contours it runs on the real axis but is for clarity drawn away from it. The piece drawn above the real axis is equal to C_{t_1} and the lower is equal to $C_{t_{1'}}$, so we have $C_S = C_{t_1} + C_{t_{1'}}$.

A.1.2 Composition of operators

We show how a product of two contour-ordered operators can be gathered into a single contour-ordered operator. As in Sec. A.1.1 we use the Hamiltonian $\mathcal{H} = \tilde{H} + \tilde{V}$ defined in Eq. (A.1).

We consider the contour-ordered operators $\langle T_C[A_{\mathcal{H}}(t_1)B_{\mathcal{H}}(t_{1'})]\rangle$ on the contour C, shown at the upper figure in Fig. 3.1. We have chosen $t_1 <_C t_{1'}$, but the analysis and the result are identical for $t_1 >_C t_{1'}$.
Using the result from Eq. (A.4) we get

$$\begin{aligned}\langle T_C[A_{\mathcal{H}}(t_1)B_{\mathcal{H}}(t_{1'})]\rangle &= \langle B_{\mathcal{H}}(t_{1'})A_{\mathcal{H}}(t_1)\rangle \\ &= \left\langle T_{C_{t_{1'}}}[e^{-i\int_{C_{t_{1'}}} d\tau V_{\tilde{H}}(\tau)} B_{\tilde{H}}(t_{1'})] T_{C_{t_1}}[e^{-i\int_{C_{t_1}} d\tau V_{\tilde{H}}(\tau)]} A_{\tilde{H}}(t_1)\right\rangle .\end{aligned} \tag{A.13}$$

where the contours C_{t_1} and $C_{t_{1'}}$ are on the form shown in Fig. 3.2.
Now we introduce the "snake" contour $C_S = C_{t_1} + C_{t_{1'}}$ with the direction shown in Fig. A.1. We also introduce a contour-ordering operator T_{C_S} on C_S, and it is identical to $T_{C_{t_1}}$ and $T_{C_{t_{1'}}}$ on the common parts. With the new contour we can write

$$\langle T_C[A_{\mathcal{H}}(t_1)B_{\mathcal{H}}(t_{1'})]\rangle = \left\langle T_{C_S}[e^{-i\int_{C_S} d\tau V_{\tilde{H}}(\tau)} A_{\tilde{H}}(t_1)B_{\tilde{H}}(t_{1'})]\right\rangle , \tag{A.14}$$

where the two exponentials have been joined. The integral along the dotted piece of C_S in Fig. A.1 vanishes, because the dotted contour is an integral back an forth on the interval $[t_0, t]$ with no operators on it. Therefore we can replace the contour C_S in Eq. (A.14) with the contour C from Fig. 3.1.
Doing the same for $t_1 >_C t_{1'}$ we finally arrive at

$$\langle T_C[A_{\mathcal{H}}(t_1)B_{\mathcal{H}}(t_{1'})]\rangle = \left\langle T_C[e^{-i\int_C d\tau V_{\tilde{H}}(\tau)} A_{\tilde{H}}(t_1)B_{\tilde{H}}(t_{1'})]\right\rangle . \tag{A.15}$$

A.1.3 Partial integration for current Green's functions

We start from Eq. (3.67). Multiplication with the lead Green's function $g^t_{k\eta}(t', t_1)$ and integration over t' on both sides gives

$$\begin{aligned}\int dt'[-i\partial_{t'}G^t_{n,k\eta}(t,t')]g^t_{k\eta}(t',t_1) = \int dt'\varepsilon_{k\eta}G^t_{n,k\eta}(t,t')g^t_{k\eta}(t',t_1) \\ + \sum_m \int dt'\ V^*_{k\eta,m}G^t_{nm}(t,t')g^t_{k\eta}(t',t_1).\end{aligned} \tag{A.16}$$

Now we integrate by parts on the left-hand side and find

$$\begin{aligned}\int dt'[-i\partial_{t'}G^t_{n,k\eta}(t,t')]g^t_{k\eta}(t',t_1) = -i\left[G^t_{n,k\eta}(t,t')]g^t_{k\eta}(t',t_1)\right]^{t'=\infty}_{t'=-\infty} \\ + \int dt_1 G^t_{n,k\eta}(t,t')[i\partial_{t'}g^t_{k\eta}(t',t_1)]\end{aligned} \tag{A.17}$$

The first term vanishes.[i] Inserting Eq. (A.17) in Eq. (A.16) leads to

$$\int dt' G^t_{n,k\eta}(t,t')[i\partial_{t'} - \varepsilon_{k\eta}]g^t_{k\eta}(t',t_1) = \sum_m \int dt' V^*_{k\eta,m}G^t_{nm}(t,t')g^t_{k\eta}(t',t_1). \tag{A.18}$$

Using $(i\partial_{t'} - \varepsilon_{k\eta})g^t_{k\eta}(t',t_1) = \delta(t_1 - t')$ and carrying out the integral on the left-hand side gives

$$G^t_{n,k\eta}(t,t_1) = \sum_m \int dt'\ V^*_{k\eta,m}G^t_{nm}(t,t')g^t_{k\eta}(t',t_1). \tag{A.19}$$

After renaming the arguments, $t' \leftrightarrow t_1$, Eq. (3.69) have been obtained.

A.1.4 Convolution theorem for Fourier transforms

The first term in Eq. (3.71) is equal to

$$\int dt_1 G^R(t-t_1)g^<(t_1-t') \tag{A.20}$$

where the indices on the Green's functions have been suppressed.
The convolution theorem for Fourier transforms reads

$$\int d\tilde{t} f(\tilde{t})g(x-\tilde{t}) = \int \frac{d\omega}{2\pi} f(\omega)g(\omega)e^{i\omega x} \tag{A.21}$$

so if we in Eq. (A.22) set $x = t - t'$ we obtain

$$\int dt_1 G^R(t-t_1)g^<(t_1-t') = \int dt_1 G^R(\omega)g^<(\omega)e^{i\omega(t-t')}. \tag{A.22}$$

Doing the same for the other term we obtain

$$G^<_{n,k\eta}(t,t') = \sum_m \int \frac{d\omega}{2\pi} V^*_{k\eta,m}\left[G^R_{nm}(\omega)g^<_{k\eta}(\omega) + G^<_{nm}(\omega)g^a_{k\eta}(\omega)\right]e^{i\omega(t-t')}. \tag{A.23}$$

[i] It is difficult to give a short argument, but it can be taken as a boundary condition that the Green's functions vanish when the difference between the time-arguments becomes infinite. Otherwise correlations on infinite time-scales would exist, which is clearly unphysical.

A.1.5 Current formula

The starting point is

$$J_L = \frac{2e}{\hbar}\sum_{nmk}\int\frac{d\omega}{2\pi}\mathrm{Re}\left\{V^*_{kL,m}V_{kL,n}\left[G^R_{nm}(\omega)g^<_{kL}(\omega)+G^<_{nm}(\omega)g^a_{kL}(\omega)\right]\right\}. \tag{A.24}$$

Changing the k-sum to an integral we can write J_L as

$$J_L = \frac{2e}{\hbar}\sum_{nm}\int\frac{d\omega}{2\pi}\int\frac{d\varepsilon_{kL}}{2\pi}\mathrm{Re}\left\{\Gamma^L_{mn}(\varepsilon_{kL})\left[G^R_{nm}(\omega)g^<_{kL}(\omega)+G^<_{nm}(\omega)g^a_{kL}(\omega)\right]\right\}, \tag{A.25}$$

where the level-width function is defined in Eq. (3.74).
The lead Green's functions are defined as

$$g^<_{k\eta}(t,t') \equiv i\left\langle c^\dagger_{k\eta}(t')c_{k\eta}(t)\right\rangle, \tag{A.26}$$

$$g^A_{k\eta}(t,t') \equiv i\theta(t'-t)\left\langle\left\{c_{k\eta}(t),c^\dagger_{k\eta}(t')\right\}\right\rangle. \tag{A.27}$$

and because they are Green's function for the isolated leads, the time-evolution and average value are with respect to first part of the Hamiltonian, $H_C = \sum_{k\eta}\varepsilon_{k\eta}c^\dagger_{k\eta}c_{k\eta}$. The Fourier transforms of the Green's functions are easily found

$$g^<_{k\eta}(\omega) = 2\pi i f_L(\varepsilon_{k\eta})\delta(\omega-\varepsilon_{k\eta}), \tag{A.28}$$

$$g^A_{k\eta}(\omega) = \frac{1}{\omega-\varepsilon_{k\eta}-i0^+} = \frac{\mathcal{P}}{\omega-\varepsilon_{k\eta}} + i\pi\delta(\omega-\varepsilon_{k\eta}), \tag{A.29}$$

where $\mathcal{P}$ means the principal part of the integral.
We obtain for the first term in Eq. (A.25) that

$$\begin{aligned}\int\frac{d\varepsilon_{kL}}{2\pi}&\mathrm{Re}\left\{\Gamma^L_{mn}(\varepsilon_k)G^R_{nm}(\omega)g^<_{kL}(\omega)\right\}\\ &= f_L(\omega)\mathrm{Re}\left\{i\Gamma^L_{mn}(\omega)G^R_{nm}(\omega)\right\}\\ &= -f_L(\omega)\mathrm{Im}\left\{\Gamma^L_{mn}(\omega)G^R_{nm}(\omega)\right\}\\ &= \frac{i}{2}f_L(\omega)\left\{\Gamma^L_{mn}(\omega)G^R_{nm}(\omega)-[\Gamma^L_{mn}(\omega)]^*[G^R_{nm}(\omega)]^*\right\},\end{aligned} \tag{A.30}$$

where we have an implicit sum over n and m.
Using $[\Gamma^L_{mn}(\omega)]^* = \Gamma^L_{nm}(\omega)$ and the general property for Green's functions $[G^R_{nm}(\omega)]^* = G^A_{mn}(\omega)$ we obtain

$$\int\frac{d\varepsilon_{kL}}{2\pi}\mathrm{Re}\left\{\Gamma^L_{mn}(\varepsilon_k)G^R_{nm}(\omega)g^<_{kL}(\omega)\right\} = \frac{i}{2}f_L(\omega)\Gamma^L_{mn}(\omega)\left\{G^R_{nm}(\omega)-(\omega)G^A_{nm}(\omega)\right\}, \tag{A.31}$$

where we in the last term have exchanged the sum indices $n\leftrightarrow m$.

The second term in Eq. (A.25) is more difficult. First we note the property of the dot Green's function $[G^<_{nm}(t,t')]^* = -G^<_{mn}(t,t')$ and consequently $[G^<_{nm}(\omega)]^* = -G^<_{mn}(\omega)$, where we have assumed that $G^<_{nm}(t,t')$ only depend on the difference between the time arguments. Now we get

$$\begin{aligned}\int \frac{d\varepsilon_{kL}}{2\pi}\mathrm{Re}\left\{\Gamma^L_{mn}(\varepsilon_{kL})\left[G^<_{nm}(\omega)g^a_{kL}(\omega)\right]\right\} \\ = \int \frac{d\varepsilon_{kL}}{2\pi}\mathrm{Re}\left\{\Gamma^L_{mn}(\varepsilon_{kL})\left[\mathcal{P}\frac{G^<_{nm}(\omega)}{\omega-\varepsilon_{kL}} + i\pi G^<_{nm}(\omega)\delta(\omega-\varepsilon_{kL})\right]\right\}\end{aligned} \tag{A.32}$$

Note that $(\omega-\varepsilon_{kL})^{-1}$ is real, and consider $\mathrm{Re}[\Gamma^L_{mn}(\varepsilon_{kL})G^<_{nm}(\omega)]$, which can be written as

$$\begin{aligned}\mathrm{Re}\{\Gamma^L_{mn}(\varepsilon_{kL})G^<_{nm}(\omega)\} &= \frac{1}{2}\{\Gamma^L_{mn}(\varepsilon_{kL})G^<_{nm}(\omega) + [\Gamma^L_{mn}(\varepsilon_{kL})]^*[G^<_{nm}(\omega)]\} \\ &= \frac{1}{2}\{\Gamma^L_{mn}(\varepsilon_{kL})G^<_{nm}(\omega) - \Gamma^L_{nm}(\varepsilon_{kL})G^<_{mn}(\omega)]\} \\ &= 0,\end{aligned} \tag{A.33}$$

where we have used the implicit sum over n and m.

The second term in Eq. (A.32) gives

$$\begin{aligned}\int \frac{d\varepsilon_{kL}}{2\pi}\mathrm{Re}\left\{i\pi\Gamma^L_{mn}(\varepsilon_{kL})G^<_{nm}(\omega)\delta(\omega-\varepsilon_{kL})\right\} \\ = \frac{i}{4}\left\{\Gamma^L_{mn}(\omega)G^<_{nm}(\omega) - [\Gamma^L_{mn}(\omega)]^*[G^<_{nm}(\omega)]^*\right\} \\ = \frac{i}{2}\left\{\Gamma^L_{mn}(\omega)G^<_{nm}(\omega)\right\},\end{aligned} \tag{A.34}$$

where we in the last line again have used that the sum indices can be exchanged.

If we gather the pieces we find

$$J_L = \frac{ie}{\hbar}\sum_{nm}\int\frac{d\omega}{2\pi}\Gamma^L_{mn}(\omega)\left\{G^<_{nm}(\omega) + f_L(\omega)\left[G^R_{nm}(\omega) - (\omega)G^A_{nm}(\omega)\right]\right\}, \tag{A.35}$$

and put on matrix form we have the final expression for the current

$$J_L = \frac{ie}{\hbar}\int\frac{d\omega}{2\pi}\mathrm{Tr}\left(\mathbf{\Gamma}^L(\omega)\left\{\mathbf{G}^<(\omega) + f_L(\omega)\left[\mathbf{G}^R(\omega) - (\omega)\mathbf{G}^A(\omega)\right]\right\}\right), \tag{A.36}$$

where the matrices are in the dot indices m, n.

A.2 The FAB model for U=0 (parallel geometry)

With the assumptions introduced in Sec. 4.1 the Green's function $\mathbf{G}^R(0)$ for noninteracting electrons on the dot simplifies to (see Eq. (4.20))

$$\mathbf{G}^R(0) = \frac{-1}{B^2 + i/2\Gamma_{\uparrow'}B\cos\theta}\begin{pmatrix} B - i/2\Gamma_{\uparrow'}\sin^2\frac{\theta}{2} & i/4\Gamma_{\uparrow'}\sin\theta \\ i/4\Gamma_{\uparrow'}\sin\theta & -B - i/2\Gamma_{\uparrow'}\cos^2\frac{\theta}{2}\end{pmatrix}, \tag{A.37}$$

where $\Gamma_{\uparrow'} = \Gamma^L_{\uparrow'} + \Gamma^R_{\uparrow'}$ and $\varepsilon_d = 0$.
Using the property $\mathbf{G}^A(\omega) = [\mathbf{G}^R(\omega)]^\dagger$ we obtain

$$\mathbf{G}^R(0) - \mathbf{G}^A(0) = \frac{-2i\Gamma_{\uparrow'}}{4B^2 + \Gamma^2_{\uparrow'}\cos^2\theta} \begin{pmatrix} 1+\cos\theta & -\sin\theta \\ -\sin\theta & 1-\cos\theta \end{pmatrix}. \tag{A.38}$$

In the lead spin basis the coupling matrix $\mathbf{\Gamma}$ is

$$\mathbf{\Gamma} = \begin{pmatrix} \Gamma_{\uparrow'} & 0 \\ 0 & 0 \end{pmatrix}, \tag{A.39}$$

and in the dot spin basis it is

$$\tilde{\mathbf{\Gamma}} = \mathbf{R}^{-1}\mathbf{\Gamma}\mathbf{R} = \Gamma_{\uparrow'} \begin{pmatrix} \cos^2\frac{\theta}{2} & \cos\frac{\theta}{2}\sin\frac{\theta}{2} \\ \cos\frac{\theta}{2}\sin\frac{\theta}{2} & \sin^2\frac{\theta}{2} \end{pmatrix}, \tag{A.40}$$

where $\mathbf{R}$ is the change-of-basis matrix defined in Eq. (2.7).
Inserting the expression in the current formula Eq. (4.24) and carrying out the trace gives after some trigonometric manipulations

$$J = e^2V \frac{\Gamma^L_{\uparrow'}\Gamma^R_{\uparrow'}}{2\pi\hbar} \frac{4\cos^2\theta}{4B^2 + \Gamma^2_{\uparrow'}\cos^2\theta}, \qquad \Gamma_{\uparrow'} = \Gamma^L_{\uparrow'} + \Gamma^R_{\uparrow'}. \tag{A.41}$$

This is the linear response result for the current in case of noninteracting electrons on the dot, $\varepsilon_d = 0$, zero temperature and fully polarized leads with the same direction of magnetization.

For $\varepsilon_d \neq 0$ we obtain

$$G(\theta) = e^2V \frac{\Gamma^L_{\uparrow'}\Gamma^R_{\uparrow'}}{2\pi\hbar} \frac{4(\varepsilon_d + B\cos\theta)^2}{\Gamma^2_{\uparrow'}(\varepsilon_d + B\cos\theta)^2 + 4(B^2 - \varepsilon_d^2)^2}, \qquad \Gamma_{\uparrow'} = \Gamma^L_{\uparrow'} + \Gamma^R_{\uparrow'}. \tag{A.42}$$

A.3 Unified description (derivation of EOM for E^R)

The function E^R from Sec. 6.2 is defined as

$$E^R_{k\eta,\nu\beta\alpha'\beta'}(t) = -i\theta(t) \left\langle \left\{ \left(c_{k\eta}|\nu\rangle\langle\beta| \right)(t), |\beta'\rangle\langle\alpha'| \right\} \right\rangle. \tag{A.43}$$

The commutator $[H_T, c_{k\eta}|\nu\rangle\langle\beta|]$ gives

$$\begin{aligned} [H_T, c_{k\eta}|\nu\rangle\langle\beta|] = \sum_{nk'\eta'\alpha''\beta''} t^*_{k'\eta'n} \Big(& c^\dagger_{k'\eta'}|\alpha''\rangle\langle\beta| c_{k\eta} F_{\alpha''\beta'',n}\delta_{\beta''\nu} \\ & - c_{k\eta}c^\dagger_{k'\eta'}|\nu\rangle\langle\beta''|F_{\alpha''\beta'',n}\delta_{\beta\alpha''}\Big) \\ & + t_{k'\eta'n}\Big(|\beta''\rangle\langle\beta| F^*_{\alpha''\beta'',n} c_{k'\eta}c_{k\eta}\delta_{\alpha''\nu} \\ & - c_{k\eta}|\nu\rangle\langle\alpha''|F^*_{\alpha''\beta'',n}c_{k'\eta'}\delta_{\beta\beta''}\Big). \end{aligned} \tag{A.44}$$

Invoking the same approximations as for D^R and keeping track of the type of the dot operators involved, it can be written as

$$[H_T, c_{k\eta}|\nu\rangle\langle\beta|] \approx -\sum_{n\nu'} \Big(t^*_{k\eta n} f_\eta(\xi_{k\eta}) |\nu'\rangle\langle\beta| F_{\nu'\nu,n} + [1 - f_\eta(\xi_{k\eta})] |\nu\rangle\langle\nu'| F_{\beta\nu',n} \Big). \tag{A.45}$$

The commutators with $H_{\rm dot}$ and H_C are simple, and in after a Fourier transformation we finally obtain

$$\begin{aligned} E^R_{k\eta,\nu\beta\alpha'\beta'}(\omega) = \frac{-1}{\omega - \xi_{k\eta} + E_{\nu\beta} + i0^+} \sum_{\nu' n'} \Big(& t^*_{k\eta n'} F_{\beta\nu',n'} [1 - f_\eta(\xi_{k\eta})] G^R_{\nu\nu'\alpha'\beta'}(\omega) \\ & + t^*_{k\eta n'} F^*_{\nu'\nu,n'} f_\eta(\xi_{k\eta}) G^R_{\nu'\beta\alpha'\beta'}(\omega) \Big). \end{aligned} \tag{A.46}$$

A.4 Solving the FAB model with interactions

A.4.1 Fermi function integral

We show how to calculate the integral

$$\int \frac{d\varepsilon}{2\pi} \frac{f(\varepsilon)}{\omega - \varepsilon + i0^+} \tag{A.47}$$

from Sec. 7.2.1.
Consider the function[ii]

$$\psi(\omega) = \mathcal{P} \int d\varepsilon f(\varepsilon) \left[\frac{1}{\omega - \varepsilon} + \frac{1}{\varepsilon} \right] \tag{A.48}$$

We fix the the chemical potential at $\mu = 0$ and assume that the energy band is symmetric around it with energies from $-D$ to D. If $D \gg |\omega|$ we can write the first term in $\psi(\varepsilon)$ as

$$\begin{aligned} & \mathcal{P} \int_{-D}^{D} d\varepsilon \left[\frac{f(\varepsilon) - f(\omega)}{\omega - \varepsilon} + \frac{f(\omega)}{\omega - \varepsilon} \right] \\ & \approx -\mathcal{P} \int_0^D d\varepsilon \frac{f(\varepsilon + \omega) - f(\varepsilon - \omega)}{\varepsilon} + \mathcal{P} \int_0^D d\varepsilon \frac{1}{\varepsilon} \end{aligned} \tag{A.49}$$

Using $f(-x) = 1 - f(x)$, the second term in Eq. (A.48) is

$$\mathcal{P} \int_{-D}^{D} d\varepsilon \frac{f(\varepsilon)}{\varepsilon} = -\mathcal{P} \int_0^D d\varepsilon \frac{1}{\varepsilon} + 2\mathcal{P} \int_0^D d\varepsilon \frac{f(\varepsilon)}{\varepsilon}, \tag{A.50}$$

which gives

$$\psi(\omega) = \int_0^D d\varepsilon \frac{2f(\varepsilon) - f(\varepsilon + \omega) - f(\varepsilon - \omega)}{\varepsilon}. \tag{A.51}$$

The $\mathcal{P}$ has been dropped because the integrand is not divergent in any point (which can be seen with standard function analysis) and the integral can be computed numerically.

[ii] f is the Fermi function.

Notice that $\psi(\omega) = \psi(-\omega)$.
We still need the the integral

$$\varphi_D = \mathcal{P} \int_{-D}^{D} d\varepsilon \frac{f(\varepsilon)}{\varepsilon} \tag{A.52}$$

to calculate the integral in Eq. (A.47). For $D \gg k_B T$ holds $\varphi_D \approx \ln \frac{k_B T}{D}$.

A.4.2 Residues

As mentioned in Sec. 7.3, the function $\frac{\partial f(z)}{\partial z}$ has a pole of order 2 at $ik_n = i\frac{(2n+1)\pi}{\beta}$. The residues for $[\mathbf{G}(z) - \mathbf{G}_0(z)] \frac{\partial f(z)}{\partial z} = \tilde{\mathbf{G}}(z) \frac{\partial f(z)}{\partial z}$ at the poles ik_n are

$$\begin{aligned} \operatorname{Res}\left[\tilde{\mathbf{G}}(z)\frac{\partial f(z)}{\partial z}; ik_n\right] &= \lim_{z \to ik_n} \frac{d}{dz}\left[(z - ik_n)^2 \tilde{\mathbf{G}}(z) \frac{\partial f(z)}{\partial z}\right] \\ &= \lim_{z \to ik_n} \frac{d}{dz}\left[(z - ik_n)^2 \tilde{\mathbf{G}}(z) \frac{-\beta e^{\beta z}}{(e^{\beta z}+1)^2}\right] \\ &= \lim_{\delta \to 0} \frac{d}{d\delta}\left[\delta^2 \tilde{\mathbf{G}}(ik_n + \delta) \frac{\beta e^{\beta\delta}}{(1 - e^{\beta\delta})^2}\right], \end{aligned} \tag{A.53}$$

where $\delta = z - ik_n$ and it has been used that $e^{ik_n} = -1$.
Introducing $x = \beta\delta$ and performing the differentiation gives

$$\begin{aligned} &= \operatorname{Res}\left[\tilde{\mathbf{G}}(z)\frac{\partial f(z)}{\partial z}; ik_n\right] \\ &= \lim_{x \to 0} \frac{d}{dx}\left[x^2 \tilde{\mathbf{G}}\left(ik_n + \frac{x}{\beta}\right) \frac{e^x}{(1-e^x)^2}\right] \\ &= \lim_{x \to 0}\left[\frac{1}{\beta}\tilde{\mathbf{G}}'\left(ik_n + \frac{x}{\beta}\right) \frac{x^2 e^x}{(1-e^x)^2} + \tilde{\mathbf{G}}\left(ik_n + \frac{x}{\beta}\right) \frac{x e^x \left(e^x(x-2) + x + 2\right)}{(1-e^x)^3}\right] \end{aligned} \tag{A.54}$$

By expanding the exponentials around $x = 0$ it is easy to see that the first term becomes

$$\lim_{x \to 0}\left[\frac{1}{\beta}\tilde{\mathbf{G}}'\left(ik_n + \frac{x}{\beta}\right) \frac{x^2 e^x}{(1-e^x)^2}\right] = \frac{1}{\beta}\tilde{\mathbf{G}}'\left(ik_n\right). \tag{A.55}$$

The second term vanishes. Expanding the nominator around $x = 0$ gives

$$\begin{aligned} x e^x \left(e^x(x-2) + x + 2\right) &= x e^x \left(\left(\left(1 + x + \frac{1}{2}x^2 + \frac{1}{6}x^3 + \ldots\right)(x-2) + x + 2\right)\right) \\ &= x e^x \left(\frac{1}{6}x^3 + \mathcal{O}\left(x^4\right)\right) \\ &= \frac{1}{6}x^4 + \mathcal{O}\left(x^5\right). \end{aligned} \tag{A.56}$$

After expanding the denominator around $x = 0$ the second term in Eq. (A.54) is

$$\begin{aligned}\lim_{x\to 0}\left[\tilde{\mathbf{G}}\left(ik_n+\frac{x}{\beta}\right)\frac{xe^x\left(e^x(x-2)+x+2\right)}{(1-e^x)^3}\right] &= \lim_{x\to 0}\left[\tilde{\mathbf{G}}\left(ik_n+\frac{x}{\beta}\right)\frac{\frac{1}{6}x^4+\mathcal{O}\left(x^5\right)}{x^3+\mathcal{O}\left(x^4\right)}\right]\\ &= \lim_{x\to 0}\left[\tilde{\mathbf{G}}\left(ik_n+\frac{x}{\beta}\right)\frac{1}{6}\,\frac{x+\mathcal{O}\left(x^2\right)}{1+\mathcal{O}\left(x\right)}\right]\\ &= 0.\end{aligned} \tag{A.57}$$

Now we have obtained that

$$\mathrm{Res}\left[\left(\mathbf{G}(z)-\mathbf{G}_0(z)\right)\frac{\partial f(z)}{\partial z};ik_n\right] = \frac{1}{\beta}\left(\mathbf{G}'(ik_n)-\mathbf{G}_0'(ik_n)\right). \tag{A.58}$$

A.4.3 Explicit form of $[\mathbf{M}_0^R]^{-1}$

$$\left[\mathbf{M}_0^R(\omega)\right]^{-1} = \begin{pmatrix} \omega+E_{0\uparrow}+i0^+ & 0 & 0 & 0\\ 0 & \omega+E_{0\downarrow}+i0^+ & 0 & 0\\ 0 & 0 & \omega+E_{\downarrow 2}+i0^+ & 0\\ 0 & 0 & 0 & \omega+E_{\uparrow 2}+i0^+ \end{pmatrix}, \tag{A.59}$$

with $E_{\alpha\beta} = \varepsilon_\alpha - \varepsilon_\beta$.

A.4.4 Occupancies

In this section the derivation of the equations (7.18)-(7.21) is presented. It is assumed that the dot is in thermal equilibrium with the leads and therefore the equilibrium relations hold.

For the diagonal Green's functions the following relations hold [1]

$$iG_{aa}^<(\omega) = 2\mathrm{Im}G_{aa}^R(\omega)f(\omega), \tag{A.60}$$

which gives

$$\begin{aligned}\langle n_a\rangle &= -iG_{aa}^<(t=0)\\ &= -2\mathrm{Im}\int_{-\infty}^{\infty}\frac{d\omega}{2\pi}G_{aa}^R(\omega)f(\omega).\end{aligned} \tag{A.61}$$

where $a = \uparrow, \downarrow$.

The non-diagonal occupations are more cumbersome. The following relations can be established with use of the Lehmann representation[iii]

$$\left(G_{ab}^R(\omega)\right)^* = G_{ba}^A(\omega) \tag{A.62}$$

$$G_{ab}^<(\omega) = -\left[G_{ab}^R(\omega)-G_{ab}^A(\omega)\right]f(\omega), \tag{A.63}$$

[iii] The derivation also holds for the diagonal occupation numbers.

where $a, b = \uparrow, \downarrow$.
Using these relations we obtain

$$\begin{aligned}\langle n_{ab}\rangle &= \left\langle c_a^\dagger c_b \right\rangle \\ &= -iG_{ba}^<(t=0) \\ &= -i\int_{-\infty}^{\infty}\frac{d\omega}{2\pi}G_{ba}^<(\omega) \\ &= i\int_{-\infty}^{\infty}\frac{d\omega}{2\pi}\left[G_{ba}^R(\omega) - \left(G_{ab}^R(\omega)\right)^*\right] f(\omega).\end{aligned} \tag{A.64}$$

A.4.5 Interacting electrons, more results

The following figures are plotted for $\Gamma_{\uparrow'}^L = \Gamma_{\uparrow'}^L = 0.1$ and the band width is fixed at $D = 50$, where the energy unit is 200 $k_B T$. A discussion of the figures are given in Sec. 7.4.2.

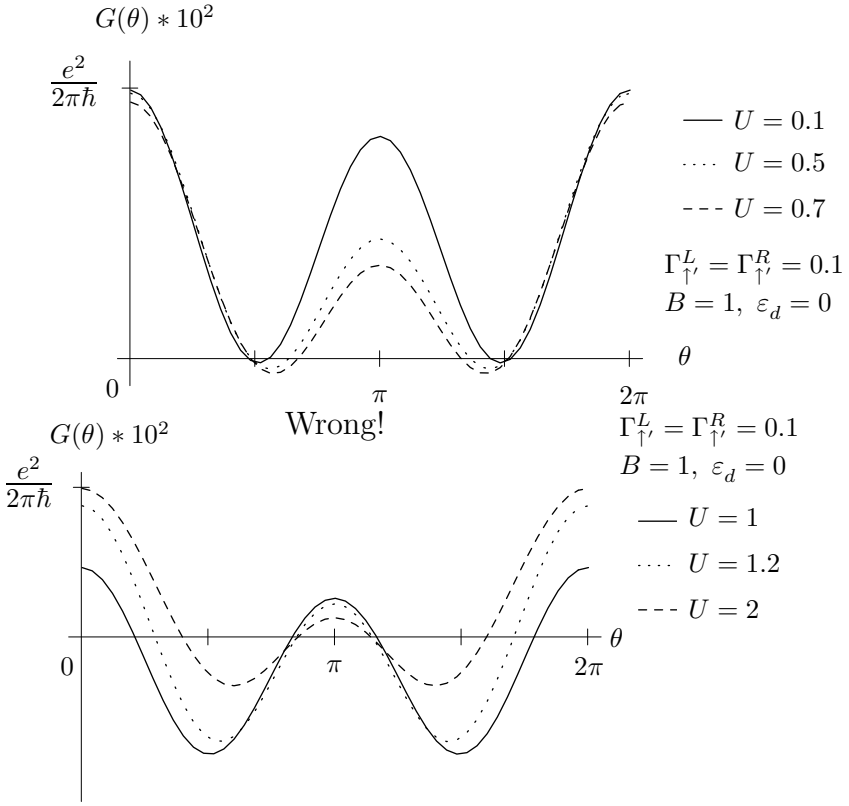

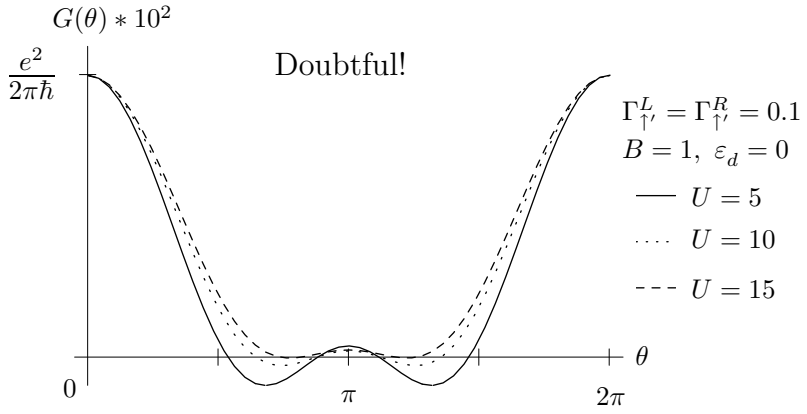

A.5 Current Green's functions for the rate equations

The current Green's functions in Eqs. (8.14)-(8.17) can be calculated in the same way as when deriving the current formula in Sec. 3.5. In this section we show that the current Green's functions presented in [4] are not exact, because they have neglected a term.
As an example we choose $G^<_{0\sigma,\eta k\sigma'}(t,t')$ from Eq. (8.15), and as in Sec. 3.5 we start from the time-ordered Green's function

$$G^t_{0\sigma,\eta k\sigma'}(t,t') = -i\left\langle T_t\left[(|0\rangle\langle\sigma|)(t)c^\dagger_{\eta k\sigma'}(t')\right]\right\rangle. \tag{A.65}$$

The time-derivative with respect to t' is found

$$-i\partial_{t'}G^t_{0\sigma,\eta k\sigma'}(t,t') = -i\left\langle T_t\left[(|0\rangle\langle\sigma|)(t)\{-i\partial_{t'}c^\dagger_{\eta k\sigma'}(t')\}\right]\right\rangle, \tag{A.66}$$

and again we use the Heisenberg equation of motion to obtain

$$-i\partial_{t'}c^\dagger_{\eta k\sigma'}(t') = [H, c^\dagger_{\eta k\sigma'}](t'), \tag{A.67}$$

where H is the full Hamiltonian (see Eq. (8.10)).
Calculating the commutator and inserting the result in Eq. (A.66) gives

$$\left[-i\partial_{t'} - \varepsilon_{\eta k\sigma'}\right]G^t_{0\sigma,\eta k\sigma'}(t,t') = V^*_{\eta\sigma'}\left(G^t_{0\sigma\sigma'}(t,t') + \sigma' G^t_{0\sigma,\bar{\sigma'}2}(t,t')\right). \tag{A.68}$$

The Green's functions on the right-side are

$$G^t_{0\sigma\sigma'}(t,t') = -i\left\langle T_t\left[(|0\rangle\langle\sigma|)(t)|0\rangle\langle\sigma'|(t')\right]\right\rangle, \tag{A.69}$$
$$G^t_{0\sigma,\bar{\sigma'}2}(t,t') = -i\left\langle T_t\left[(|0\rangle\langle\sigma|)(t)|2\rangle\langle\bar{\sigma'}|(t')\right]\right\rangle. \tag{A.70}$$

To derive the current Green's function correctly requires that we keep the Green's function $G^t_{0\sigma,\bar{\sigma'}2}(t,t')$ in Eq. (A.66) when we proceed as in Sec. 3.5. However, later on we make the assumption that the Green's functions in presence of tunnelling are on the same form as the decoupled Green's functions (see Sec. 8.2), and the Green's function $G^t_{0\sigma,\bar{\sigma'}2}(t,t')$ is zero in absence of tunnelling. For $t > t'$ it corresponds to creating a doubled occupied

state at time t' and leaving the dot empty at time t. This can only happen if the electrons can tunnel out from the dot. The same argument holds for $t' > t$. Therefore $G^t_{0\sigma,\bar{\sigma'}2}(t,t')$ can be neglected in the in expression for the current Green's function in case of weak coupling between the leads and the dot. This is not stated in [4].
The rest of the calculation when deriving the expressions for the current Green's functions in Eqs. (8.14)-(8.17) is identical to the procedure in Sec. 3.5. We end up with the Green's functions in Eqs. (8.33)-(8.36) when we neglect the dot Green's functions which vanish in absence of tunnelling.

Appendix B

List of abbreviations and symbols

Some of the most important abbreviations and symbols.

NGF: Nonequilibrium Green's function.
WBL: Wide Band Limit.
EOM: equation of motion
k_B: Boltzmann's constant.
T: temperature
$\beta = \frac{1}{k_B T}$.
θ: angle between the magnetic field and the magnetizations of the leads.
$\theta(t)$: the unit step function ($\theta(t) = 0$ for $t < 0$ and 1 elsewhere.)
B: strength of the magnetic field.
$\mathbf{A}$: a matrix.
$\bar{A}$: a vector.
$[A, B] = AB - BA$: the commutator.
$\{A, B\} = AB + BA$: the anti-commutator.
$\int$: with no limits assigned it means from $-\infty$ to ∞.
μ: the equilibrium chemical potential of the leads (the zero point on the energy scale).
μ_η: the chemical potential of the lead $\eta = L, R$.
Γ^η_σ: the coupling constant between the lead η and the dot for lead electrons with spin-σ.[i]
ε_d: the energy of the dot levels in absence of an applied magnetic field.
ε_μ: the energy of the dot level with spin-μ.
ε_2: the energy of the doubled occupied state.
$\varepsilon_{\eta k\sigma}$: energy of lead electron in lead η with spin-σ and other quantum numbers k.
$\mathbf{G}^R$: retarded Green's function.
$\mathbf{G}^A$: advanced Green's function.

[i] $\eta = L, R$ for the left and right lead, respectively. Not to be confused with R on the Green's functions meaning retarded.

Bibliography

[1] H. Bruus and K. Flensberg, "Introduction to Many-body quantum theory in condensed matter physics", rsted Lab., NBI, MIC, DTU, 2002.

[2] Jonas R. Hauptmann, "Spin-Transport in Carbon Nanotubes", M.Sc. thesis, rsted Laboratory, NBIfAPG, University of Copenhagen (2003).

[3] J.R. Petta, S.K. Slater and D.C. Ralph, condmat/0404740.

[4] B. Dong, H. I. Cui, X.L. Lei, Phys. Rev. B 69, 035324, (2004).

[5] Jesper Qvist Thomassen, "Mesoscopic transport in magnetically contacted quantum dots", cand.scient thesis, rsted Laboratory, NBIfAPG, University of Copenhagen (2003).

[6] K. Flensberg, unpublished.

[7] H. Haug and A.P. Jauho, "Quantum Kinetics in Transport and Optics of Semiconductors", Springer, Berlin, (1996).

[8] Y. Meir, N.S. Wingreen and P.A. Lee, Phys. Rev. Lett. 66, 3048, (1991).

[9] K. Flensberg, Phys. Rev. B 68,205323, (2003).

[10] S.A. Gurvitz and Ya.S. Prager, Phys. Rev. B 53, 15932, (1996).

[11] T.H. Stoof and Yu.V. Nazarov, Phys. Rev. B 53, 1050, (1996).

[12] Yu.V. Nazarov, Physica B 189, 57-69, (1993).

[13] J. Rammer, "Uligevgt i supraledere". MSc Thesis, University of Copenhagen (in Danish), (1981).

[14] J. Rammer and H. Smith, Rev. Mod. Phys. 58, 323, (1986).

[15] D.C. Langreth, in "Linear an Nonlinear Electron Transport in Solids", ed. by J.T. Devreese and E. van Doren, Plenum, New York, (1976).

[16] Y. Meir and N.S. Wingreen, Phys. Rev. Lett. 68, 2512, (1992).

[17] Z. Zou and P.W. Anderson, Phys. Rev. B 37, 627, (1998).

[18] C. Lacroix, J. Phys. F 11, 2389, (1981).

[19] J.R. Schrieffer and P.A. Wolff, Phys. Rev. 149, 491, (1966).

[20] J. Martinek, Y. Utsumi, H. Imamura, J. Barnaś, S. Maekawa, J. Knig and G. Schn, Phys. Rev. Lett. 91, 127203, (2003).

[21] J. Martinek, M. Sindel, L. Borda, J. Barnaś, J. Knig, G. Schn and J. von Delft, Phys. Rev. Lett. 91, 247202, (2003).

[22] J. Knig, J. Martinek, J. Barnaś and G. Schn, condmat/0404509 (2004). To be published in "Lecture Notes in Physics".

[23] C. Cohen-Tannoudji, J. Dupont-Roc and G. Grynberg, "Processus d'interaction entre photons et atomes", EDP Sciences/CNRS ditions, (in French), (2001).

[24] Richard L. Liboff, "Introductory Quantum Mechanics", 3rd Ed., Addison-Wesley, (1997).

[25] J.J. Sakurai, "Modern Quantum Mechanics", Rev. Ed., Addison-Wesley, (1994).